UNIVERSITÀ DEGLI STUDI DI MILANO-BICOCCA

Facoltà di Scienze Matematiche, Fisiche e Naturali

Dottorato di Ricerca in Biologia

DEVELOPMENT OF A FLUOROPOLYMER BASED BIOSENSOR FOR THE OPTICAL DETECTION OF BIOMOLECULAR INTERACTIONS

Tutor: Prof. Paolo TORTORA

Matteo SALINA

Matr. 030429

Anno Accademico 2008/2009

UNIVERSITY OF MILAN-BICOCCA

Faculty of Mathematics, Physics and Natural Science

Doctorate in Biological Research

DEVELOPMENT OF A FLUOROPOLYMER BASED BIOSENSOR FOR THE OPTICAL DETECTION OF BIOMOLECULAR INTERACTIONS

Tutor: Prof. Paolo TORTORA

Matteo SALINA

Matr. 030429

Academic year 2008/2009

1 ABSTRACT

The last two decades have witnessed remarkable progress in the development of devices enabling the detection of biomolecules in solution and the measurement of their interactions. These devices, generally named "biosensors", are based on various detection principles, all enabling to transduce a localized quantity of specific molecules into a detectable signal. Most standard laboratory assays used to characterize the presence and the interactions of biomolecules require the labeling of the analyte with fluorescent or radioactive groups. However, the development of a label-based method requires additional time and cost allocation, a component of which is not required for true label-free assays, which typically rely on the direct measurement of the quantity of analyte (molecules) interacting with a specific ligand. Novel methods to realize label-free biosensors are still emerging and they are the object of increasing research efforts, since they represent an attractive alternative to the standard labelled assays to report interactions between bio-molecules.

The aim of this thesis is to develop and test a new label-free method for the optical detection of molecular interactions taking place on the surface of a polymeric material with peculiar optical and chemical properties. The method proposed in this thesis is based on a simple optical phenomenon, still unexplored in biosensors applications: the intensity of light reflected from an interface between two materials with similar refractive index increases significantly when a thin molecular layer with different refractive index is placed at the interface. In particular, the method is based on the variation of the low intensity signal reflected from a surface of perfluoropolymer material isorefractive to water, as ligand and receptors are absorbed or immobilized on the surface. This phenomenon can be monitored simply illuminating the interface with a LASER or a LED and detecting the reflection with a photodiode or a CCD camera. Since the reflection from a film depends on this thickness, we can follow the gradual adsorption of several molecular layers onto the surface.

The sensor is based on a Hyflon®AD perfluoropolymer produced by Solvay-Solexis in Bollate (MI), featuring peculiar properties: (i) its refraction index matches that of water, (ii) it is hydrophobic and slightly charged negatively, a combination that makes on it certain kind of proteins to spontaneously adsorb; (iii) it is transparent and (iv) inert to most chemical substances. These characteristics make Hyflon®AD an attractive substrate for developing a biosensor.

The protein Avidin with positive net charge under physiological conditions spontaneously adsorbs on Hyflon AD, thus allowing a general strategy for immobilization of biotin-labeled receptors. In this way, the method can be used for the detection of biologically relevant molecules interacting with other receptors previously adsorbed on the sensor surface.

Several stages of design, realization and test of the prototypes have been made. The activity has been mainly devoted to a large variety of tests aimed to optimize the hardware and protocols of the method, to assess the quality of the measurements and to treat the surface with functional linkers. A great effort has been devoted to the design, realization and characterization of the measuring cell, in particular for what concerns the transport of biomolecules into the fluidic system.

One of the instrumental realization includes an interferometric, real-time measurement of the concentration of analyte in contact to the active surface. This innovation is based on the small change of refractive index present in the cell. This set-up is required to perform accurate kinetic measurements for which fully characterized fluidics is necessary.

The final sensors has performances similar to other label-free optical biosensors recently developed. The limit of detection (30 pg/mm^2) is comparable to most commercial biosensors. The sensitivity of the method might be further improved by reduction of stray light and electronic noise.

Numerous biological experiments have been carried out using the method here developed. Antigen-antibody interaction has been tested with BSA conjugated with biotin and anti-BSA in solution; a peptide-protein interaction has been characterized with an immobilized phosphorylated peptide and a fragment of SRC with the SH2 domain. Moreover, test experiments aimed at the measurement of the concentration in solution of an antigen of biomedical

relevance (PSA) have been also using three different strategies of surface immobilization. Measurements of the kinetics of interaction have been carried out between BSA and its antibody and between protein A and human IgG.
The simultaneous measurement of different interactions has also been tested. An instrumental set-up based on the detection of the reflection image of the active surface has been developed. In this way, the reflectivity increase of multiple spots is measured simultaneously, thus allowing the detection of multiple interactions with a single cell. This device represents a proof of concept for a protein array based on optical label-free detection.

This work was carried out at the Complex Fluids and Molecular Biophysics laboratory under the supervision of Prof. T. Bellini; Department of Chemistry, Biochemistry and Medicine Biotechnology LITA - University of Milan.

SUMMARY

2 LABEL-FREE BIOSENSORS

2.1 Overview

The term biosensor was introduced around 1960s, relating to exploration of transducer principles for the direct detection of biomolecules at surfaces. According to International Union of Pure and Applied Chemistry (IUPAC), biosensors *"are analytical devices comprised of a biological element (tissue, microorganism, organelle, cell receptor, enzyme, antibody) and a physicochemical transducer. Specific interaction between the target analyte and the biological material produces a physico-chemical change detected by the transducer. The transducer then yields an analog electronic signal proportional to the amount (concentration) of a specific analyte or group of analytes"* (http://www.iupac.org/).

Some argued that all small devices capable of reporting parameters of the human body were biosensors (ion-sensitive field-effect transistors measuring pH). According to the present definition, in biosensors the recognition element ligand of the sensor or the analyte should originate from a biological source. Currently the most prominent example of a biosensor is the glucose sensor, reporting glucose concentration as an electronic signal, based on a selective, enzymatic process (Clark et al. 1962).

A large number of basic biosensors, all combining a biological recognition element and a transducer, were subsequently developed. Currently, the trend is toward more complex integrated multi-analyte sensors capable of more comprehensive analyses. In the literature and in practice, there are numerous types of biosensors, and the choice of a suitable system for a particular application is complex, based on many factors such as the nature of the application, the label molecule (if used), the sensitivity required, the number of channels (or area), cost, technical expertise, and the speed of detection needed.

A useful categorization of biosensors is to divide them into two groups: direct recognition sensors, in which the biological interaction is directly measured, and indirect detection sensors, which rely on secondary elements for

detection. Figure 2.1 shows a schematic of the two groups of biosensors. In each group, there are several types of transducers including optical, electrochemical, and mechanical.

Direct detection biosensors utilize direct measurement of the biological interaction. Such detectors typically measure physical changes (e.g., changes in optical, mechanical, or electrical properties) induced by the biological interaction, and they do not require labeling of molecules (label free). Direct biosensors can also be used in an indirect mode, typically to increase their sensitivity. Direct detection systems include optical-based systems (most common being surface plasmon resonance - SPR) and mechanical systems such as quartz crystal resonators.

Indirect detection sensors rely on secondary elements (labels) for detection. Examples of such secondary elements are enzymes (e.g., alkaline phosphatase or glucose oxidase) and fluorescently tagged antibodies that enhance detection of a sandwich complex.

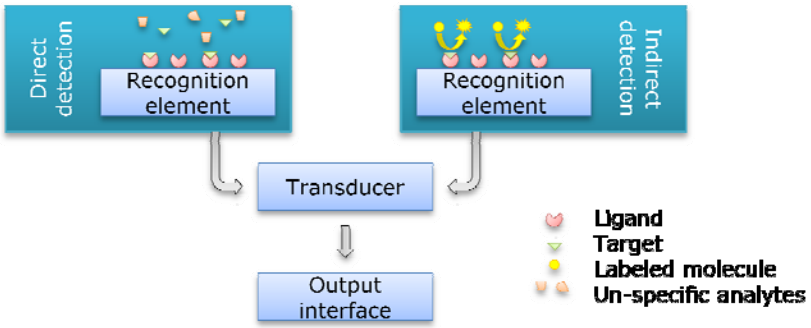

Figure 2.1 General schematic of biosensors: direct detection biosensors where the recognition element is label free; indirect detection biosensors using a "sandwich" assay where the analyte is detected by labeled molecule.

For all of these technologies, the recognition ligand plays a major role. Although the most commonly used ligands are antibodies, other ligands are being developed including aptamers (protein-binding nucleic acids) and peptides. Ligands are recognition molecules that bind specifically with the target molecule to be detected. The most important characteristics for ligands are affinity and specificity. Various types of ligands are used in biosensors. Biosensors that use antibodies as recognition elements (immunosensors) are common because antibodies are highly specific, versatile, and bind strongly

and stably to the antigen. Several limitations of antibodies are long-term stability, and manufacturing costs, especially for multi-target biosensor applications where many ligands are needed.

2.1.1 The key strengths of biosensors

Applications of biosensors include medical, environmental, public security, and food safety areas. Medical applications include clinical, pharmaceutical and device manufacturing, and research. Biosensor-based diagnostics might facilitate disease screening and improve the rates of earlier detection and attendant improved prognosis. Biosensors allow multi-target analyses, automation,
and reduced costs of testing.
The key strengths of biosensors are the following:
Fast or real-time analysis: Fast or real-time detection provides almost immediate interactive information about the sample tested, enabling users to take corrective measures before infection or contamination can spread.
Point-of-care detection: Biosensors can be used for point-of-care or on-site testing where state-of-the-art molecular analysis is carried out without requiring a state of-the-art laboratory.
Continuous flow analysis: Many biosensor technologies can be configured to allow continuous flow analysis. This is beneficial in food production, air quality, and water supply monitoring.
Miniaturization: Biosensors can be miniaturized so that they can be integrated into powerful lab-on-a-chip tools that are very capable while minimizing cost of use.
Control and automation: Biosensors can be integrated with on-line process monitoring schemes to provide real-time information about multiple parameters at each production step or at multiple time points during a process.
Highthroughput screening (HTS): Many biosensor technologies can use robotics, data processing and control software, liquid handling devices, and sensitive detectors to perform a lot of biochemical, genetic or pharmacological tests in a very short time.

2.1.2 Label vs. label-free

From the earliest days of screening and molecular profiling in drug discovery, assay development has exploited a variety of labeled assays to report an interaction of a drug candidate with a receptor or cell. These include ELISAs, radio-labeled pull-down assays, scintillation proximity assays and an ever-expanding suite of intensity and time-resolved fluorescence assays [-intensity, - lifetime, -polarization, -fluorescence resonance energy transfer (FRET) and so on]. Such assays are used extensively in most stages of preclinical drug discovery and form the basis for dedicated HTS instrumentation developed by the major technology suppliers to the pharmaceutical industry.

Label-free techniques use biological or chemical receptors to detect analytes (molecules) in a sample. They give detailed information on the selectivity, affinity, and, in many cases, also the binding kinetics and thermodynamics of an interaction. Although they can be powerful tools in the hands of a skilled user, there is often a lack of knowledge of the best methods for using label-free assays to screen for biologically active molecules and accurately and precisely characterize molecular recognition events.

The development of a label-based biosensor requires additional time and cost allocation, a component of which is not required for true label-free assays. Following a decade of major investment in compound generation, storage and characterization, and the industrialization of assay development, implementation and data handling, major pharma companies can now run several major screening campaigns each quarter, with each encompassing over a million drug candidates (Cooper M. A. et al. 2006).

Unfortunately, most HTS platforms still give high hit rates and do not always discriminate causal perturbation of a biological pathway from non-specific or concomitant activation of non-relevant cellular processes. More importantly, the label can, in some cases, interfere with the molecular interaction by occluding a binding site, leading to false negatives. For many fluorescent and chemiluminescent reporter compounds, background binding can be a significant problem, leading to false positives. There are also a large number of other artifacts inherent with label-based assays that originate from the screened compounds themselves in particular, auto-fluorescence. These

artifacts can be offset by the use of multicomponent fitting (e.g. fluorescence lifetime and fluorescence intensity) and other proprietary software algorithms; however, these approaches all add to the complexity of the screening assay (Comley et al. 2003).

2.1.3 Label-free for research

Although labeled assays require significant initial effort to develop the assay platform, it is important to note that the end user is only exposed to these additional R&D requirements through higher instrumentation pricing. The technology supplier usually carries out the development work that provides the foundation for most assay platforms. In other words, many tools companies put a lot of effort into developing robust assays tailored specifically to a particular assay class, a signaling event or a specific cellular process. According to M. A. Cooper survey (data of December 2006) most respondents perceived label-free 'as a promising analytical tool that needs to mature' (Figure 2.2a), with most respondents having no access, or limited access, to label-free instrumentation (Figure 2.2b). Aside from the intrinsic benefits outlined above, most respondents felt that the real-time readout and ability to measure interaction kinetics was a principal benefit (Figure 2.2c), a view most likely predicated by the capabilities of the dominant player in the market today: Biacore.

Biacore, a Swedish company spun out from Pharmacia Biotech in the 1990s, is the pioneer of commercial label-free systems and currently dominates the biosensor market in the life sciences. The late 1990s and early 2000s witnessed the demise of several emergent competitors, which slowed wider market penetration for label-free platforms. In addition, the rapid development of 1536-, 2080- and 3456-well plates has driven down screening consumable costs and potentially 'priced out' label-free technology for HTS.

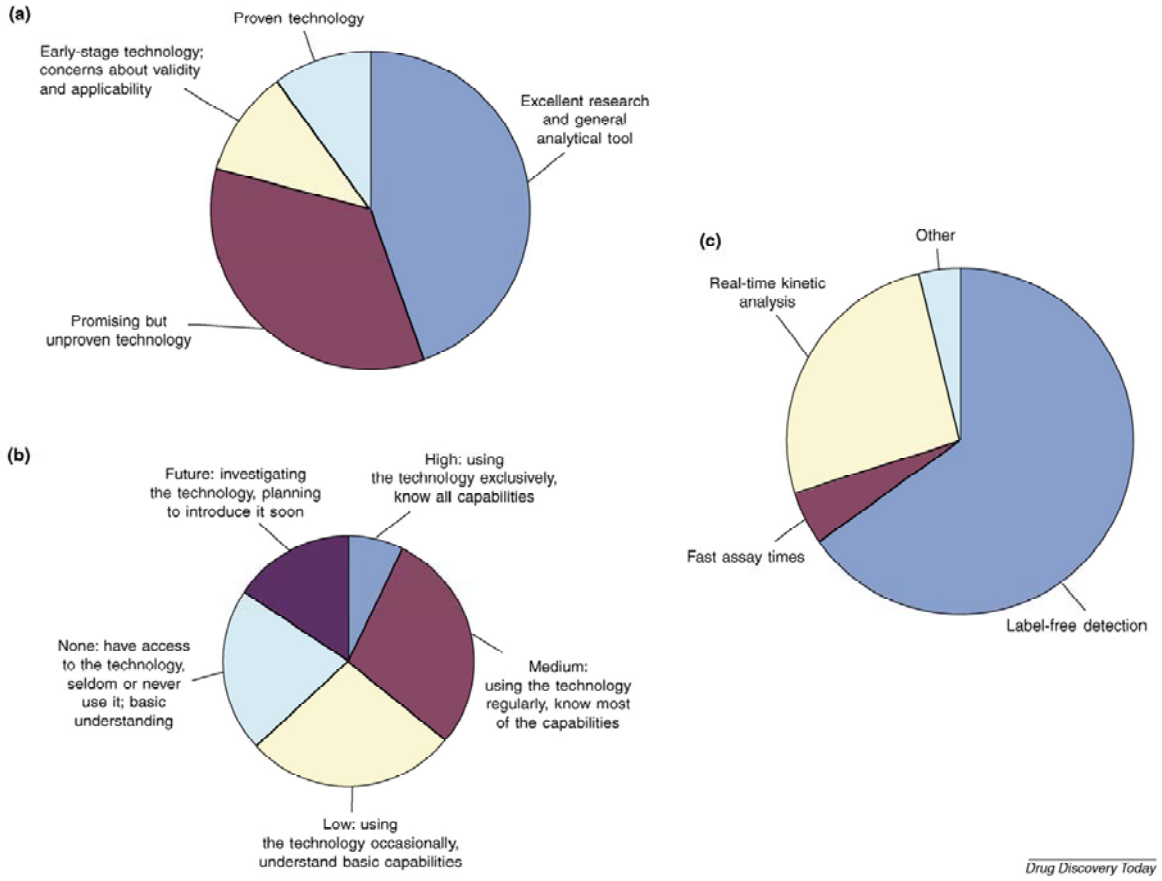

Figure 2.2 Market perceptions of label-free technologies survey of December 2006. (a) Current perception of label-free detection; (b) current uptake of label-free detection; and (c) biggest perceived benefit of label-free detection

Emergent competitors also suffered from competing project and technology investment cycles in large pharma companies. Following a sustained period of technology spend in the 1990s, many pharmaceutical companies then reduced technology evaluation and acquisition budgets in favor of increased of project and product-based expenditure. There has also been an element of 'novel platform fatigue', and young technologies seeking to ride on the back of the HTS and combinatorial chemistry 'wave' have found senior management more reluctant to invest significant time and money into less established discovery tools than was the case in the 1990s. However, in recent years there has been the emergence of several new players in the label-free development arena that are bringing new products to the market, and that will stimulate the development of new products from existing players (Comley 2005) (Fan et al. 2008).

This section wants to give a general introduction to Label-Free technology already on market or in advanced state of development. In the following I will select the instruments that represent the majority of sensor techniques. In particular, I will describe the surface plasmon resonance (SPR), the most diffuse label-free instrument. However most of the applications and technological considerations can be extended to the other sensors. Without the aim to fully cover the fast-moving field of biosensing, this work presents some of the many types of biosensors to give the reader a sense of the enormous potential for these devices.

2.2 Surface Plasmon Resonance

Since the first observation by Wood (Wood R.W. 1902), the physical phenomenon of SPR has found its way into practical applications in sensitive detectors, capable of detecting sub-monomolecular coverage. Wood observed a pattern of ‘‘anomalous’’ dark and light bands in the reflected light, when he shone polarized light on a mirror with a diffraction grating on its surface. The physical interpretation of the phenomenon was initiated by Lord Rayleigh (Rayleigh 1907), but a complete explanation was not possible until 1970s. Application of SPR-based sensors to biomolecular interaction was first demonstrated in 1983 (Liedberg et al. 1983). To understand the excitation of surface plasmons consider the experimental set-up depicted in Figure 2.3. When polarized light is shone through a prism on a sensor chip with a thin metal film on top, the light will be reflected by the metal film acting as a mirror. Up on changing the angle of incidence, and monitoring the intensity of the reflected light, the intensity of the reflected light passes through a minimum (Figure 2.3, line A). At this angle of incidence, the light will excite surface plasmons, inducing surface plasmon resonance, causing a dip in the intensity of the reflected light. Photons can interact with the free electrons of the metal layer, inducing a wave-like oscillation of the free electrons and thereby reducing the reflected light intensity.

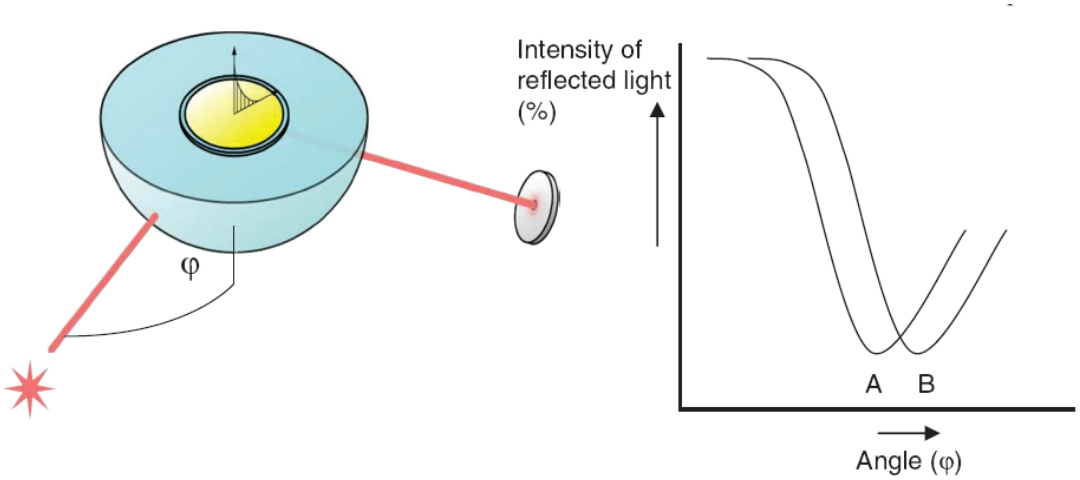

Figure 2.3 Schematic experimental set-up of surface plasmon resonance excitation. A sensor chip with a gold coating is placed on a hemisphere (or prism). Polarized light shines from the light source (star) on the sensor chip. Reflected light intensity is measured in the detector (disk). At a certain angle of incidence (j), excitation of surface plasmons occurs, resulting in a dip in the intensity of the reflected light (A). A change in refractive index at the surface of the gold film will cause an angle shift from A to B.

The angle at which the maximum loss of the reflected light intensity occurs is called resonance angle or SPR angle. The SPR angle is dependent on the optical characteristics of the system: on the refractive indices of the media at both sides of the metal, usually gold. While the refractive index at the prism side is not changing, the refractive index in the immediate vicinity of the metal surface will change when accumulated mass (e.g. proteins) adsorb on it, hence changing the surface plasmon resonance conditions. The measure of shift of the SPR angle can be suited to provide information on the kinetics of molecule adsorption on the surface.

2.2.1 From Dip to Real-time Measurement

Surface plasmon resonance is an excellent method to monitor changes of the refractive index in the near vicinity of the metal surface. When the refractive index changes, the angle at which the intensity minimum is observed will shift as indicated in Figure 2.3, where (A) depicts the original plot of reflected light intensity vs. incident angle and (B) indicates the plot after the change in refractive index. Surface plasmon resonance is not only suited to measure the difference between these two states, but can also monitor the change in time, of the shift of the resonance angle at which the dip is observed.

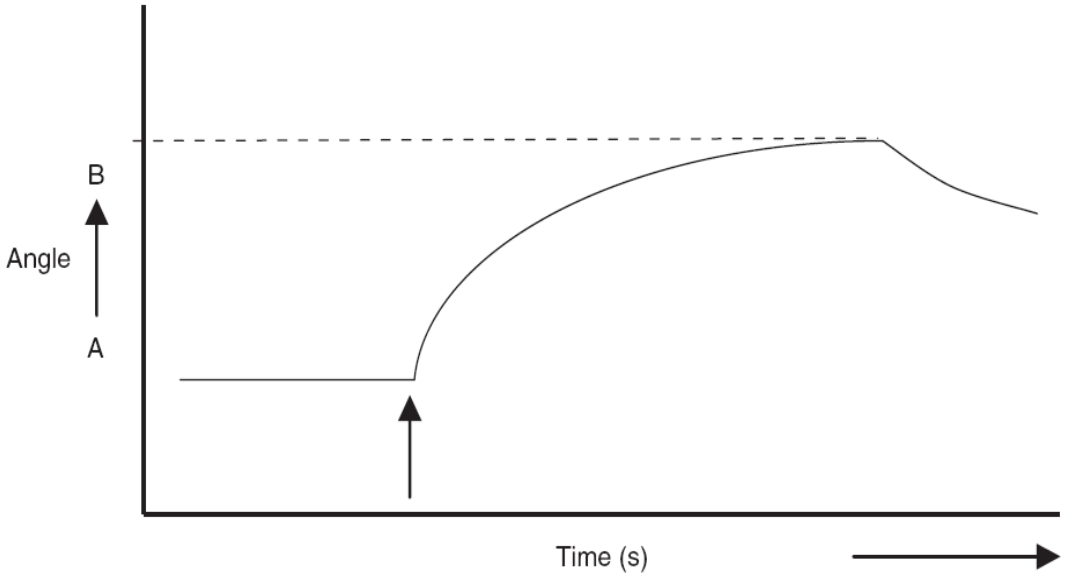

Figure 2.4 A sensorgram: the angle at which the dip is observed vs. time. First, no change occurs at the sensor and a baseline is measured with the dip at SPR angle (A). After injection of the sample (arrow) biomolecules will adsorb on the surface resulting in a change in refractive index and a shift of the SPR angle to position B. The adsorption–desorption process can be followed in real time and the amount of adsorbed species can be determined.

Figure 2.4 depicts the shift of the dip is a function of time, the so-called sensorgram. If this change is due to a biomolecular interaction, the kinetics of the interaction can be studied in real time.

SPR sensors investigate only a very limited vicinity or fixed volume at the metal surface. The penetration depth of the electromagnetic field (so-called evanescent field) at which a signal is observed typically does not exceed a few hundred nanometers, decaying exponentially with the distance from the metal layer at the sensor surface. The penetration depth of the evanescent field is a function of the wavelength of the incident light.

SPR sensors lack intrinsic selectivity: all refractive index changes in the evanescent field will be reflected in a change of the signal. These changes can be due to refractive index difference of the medium, e.g. a change in the buffer composition or concentration; also, adsorption of material on the sensor surface can cause refractive index changes. The amount of adsorbed species can be determined after injection of the original baseline buffer, as shown in Figure 2.4. To allow selective detection at an SPR sensor, its surface needs to be modified with ligands suited for selective capturing of the target

compounds but which are not prone to adsorbing any other components present in the sample or buffer media.

2.2.2 Basics of Instrumentation

SPR-based instruments use an optical method to measure the refractive index near a sensor surface (within 200 nm to the surface). SPR instruments comprise three essential units integrated in one system: optical unit, liquid handling unit and the sensor surface. The features of the sensor chip have a vital influence on the quality of the interaction measurement. The sensor chip forms a physical barrier between the optical unit (dry section) and the flow cell (wet section). SPR instrumentation can be configured in various ways to measure the shift of the SPR-dip. In general, three different optical systems are used to excite surface plasmons: systems with prisms, gratings and optical waveguides.

Most widespread are instruments with a prism coupler. In this configuration, which is shown in Figure 2.3, a prism couples polarized light into the sensor coated with a thin metal film. The light is reflected on a detector (a photodiode or a camera), which measuring its intensity. In instruments with a grating coupler, light is reflected at the lower refractive index substrate. All configurations share the same intrinsic phenomenon: the direct, label-free and real-time measurement of refractive index changes at the sensor surface. SPR sensors offer the capability of measuring low levels of chemical and biological compounds near the sensor surface. Sensing of a biomolecular binding event occurs when biomolecules accumulate at the sensor surface and change the refractive index by replacing the background electrolyte.

For instance protein molecules have a higher refractive index than water molecules ($\Delta n \approx 0{,}1$). The sensitivity of most SPR instruments is in the range $\Delta n \approx 10^{-5}$ or 1 pg/mm^{-2} (1 RU: Resonant unit) of proteinous material the new product sell in the last years improve the sensibility to 0,1 pg/mm^{-2} (a definition of this parameter can be found in section 5).

2.2.3 Flow cells

BIAcore (http://www.biacore.com/) is the first and the most advanced of commercial label-free systems and currently dominates the biosensor market in SPR. In BIAcore and in many othersystems, interactions occur in flow cells on a sensor surface. Interacting partners in solution are delivered to flow cells, formed when a microfluidic flow system is brought into contact with a sensor surface on which another interacting partner is immobilized. Several flow system designs have evolved.

In the configuration showing in figure 2.5, sample is injected through the flow cells, which can be opened and closed by a system of valves. Interactions may be analyzed in up to four flow cells, according to the system design. Selected flow cells may be used as on-line reference cells, allowing blank subtracted data to be presented directly on the screen during analysis.

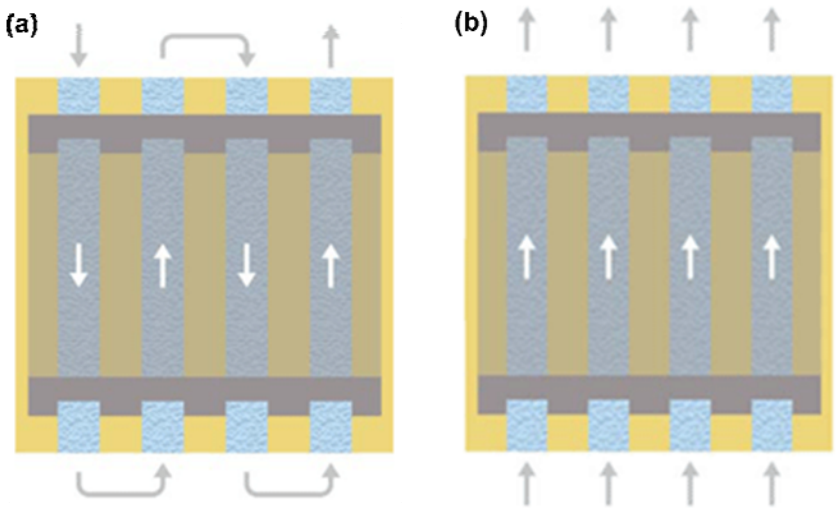

Figure 2.5 The serial flow cell configuration. Software-controlled valves at each outlet and at the entry to each flow cell enable the user to select a combination of active flow cells during the experiment.

Hydrodynamic addressing (figure 2.6) is another configuration, a process by which multiple interactants may be immobilized on detection spots in a single flow cell, allowing simultaneous analysis of interactions. As there is no lag time between interactions, highly accurate reference subtraction allows the measurement of very rapid kinetics. Further, by immobilizing several interactants in one flow cell, comparative binding properties may be directly examined under optimal experimental conditions.

By adjusting the relative flow at the two inlets (one for the immobilized partner and the other for buffer), liquid can be directed to different addressable detection spots. The flow cell design allows rapid and efficient switching of flow between buffer and sample solutions and the transverse arrangement of the detection spots ensures that access of sample to all spots is simultaneous. Although the detection spots are addressed separately during immobilization, the injected sample flows over all spots simultaneously.

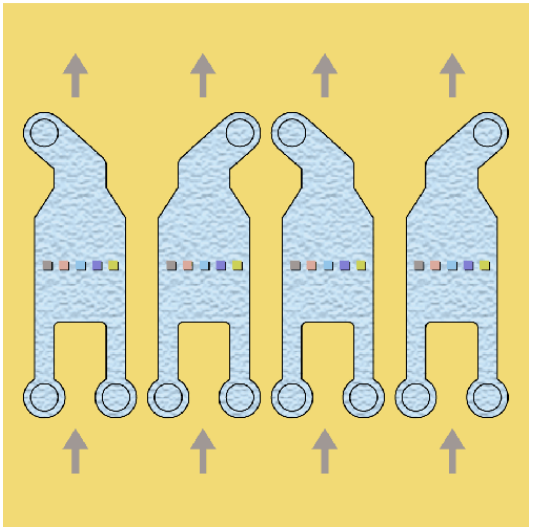

2.6 Hydrodynamic addressing, multi-spot flow cell system

The design of this flow cell is a single broad channel through which sample is injected, interacting simultaneously with all spots on an array. After the sensor surface is spotted according to user specifications, a gasketed window with an inlet and an outlet valve is then positioned and hermetically sealed over the array to form the flow cell, which is then inserted into a Biacore Flexchip system. This system is expanding by a variant of SPR known as grating-coupled SPR, in which incident light from above directly strikes the entire array, generating data from up to 400 interactions simultaneously.

2.2.4 SPR imaging technology

GenOptics (http://www.genoptics.com/) has adapted SPR imaging (SPRi) technology for the rapid quantification and monitoring of biomolecular interactions in the laboratory.

The SPRi technology developed by GenOptics is a label-free sensitive method of visualization of the whole biochip area thanks to a video CCD camera. All

molecular interactions are monitored dynamically and information is transformed into quantitative data. This feature allows the functionalization of biochips in array format and the collection of data from all the different spots. Perturbations at the surface of the biochip, such as an interaction between probes immobilized on the chip and targets, induce a modification of resonance conditions which can be measured.

Briefly, a broad monochromatic polarized light (at a specific wavelength) illuminates the whole functionalized area of the SPRi-Biochip™ which is combined with a detection chamber. A CCD video camera gives access to array format (up to 1000 spots) by image capture of all local changes at the surface of the SPRi-Biochip™ (Figure 2.7).

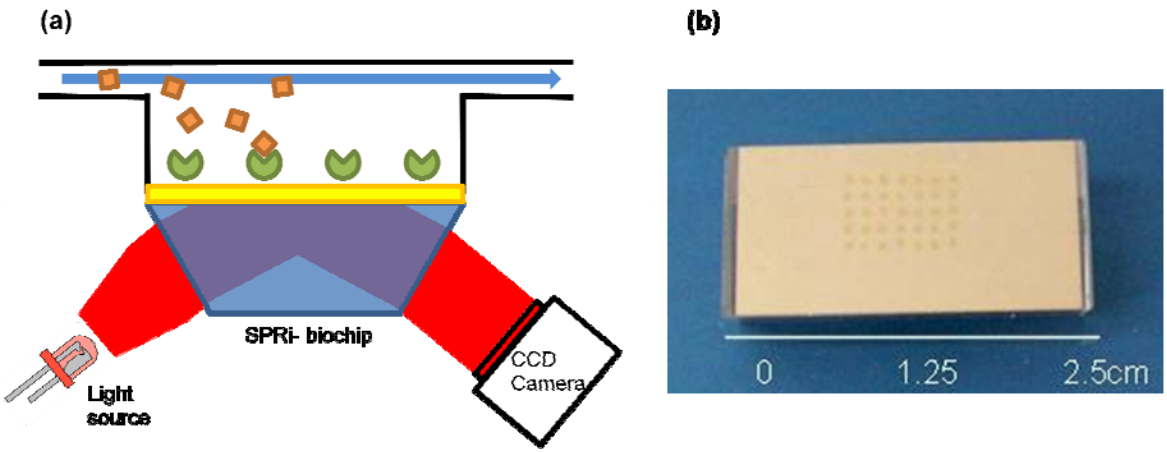

Figure 2.7 (a) The flow cell based on a led illumination (b) The GenOptics sensor chip

The chips are made of a high refractive index glass prism coated with a thin gold film specially developed for imaging purposes. To detect biomolecular interactions, probes are first grafted (spotted) onto the chip surface. Depending on the diameter of the spots, up to 1000 spots (100µm), 300 spots (200µm) or 64 spots (500µm) can be deposited on the 1 cm^2 sensitive surface of the biochip.

With the appropriate regeneration procedure, spotted SPRi-Biochips™ are re-usable at least 30 times. (Cherif et al. 2006). Spotting can be performed by means of users according to their requirements. Genoptics also offers the possibility of performing electrodeposition with an automatic SPRi-Arrayer.

Compared to other optical techniques in high-throughput label-free detection, SPRi is no doubt the most attractive and has been undergoing intensive development (Xiaobo Yu et al. 2006)

2.2.5 Gradient measure

SensíQ (made to ICx Nomadics http://www.discoversensiq.com/) is a semi-automated SPR system which utilizes advanced microfluidics (figure 2.8). This company has a patent for an innovative measure of association and dissociation constants (Patent number: WO2009025680A1). The analyte gradient is flowed through the flow cell from a low to high concentration: this special process allows the kinetic analysis without requiring multiple discrete injections to archive a range of concentration; this operation is obtained with a detailed knowledge of the instrument fluidics, a fine injection system and a mixer system (Patent number: WO2009014553A1).

Figure 2.8 Pioneer introduces full automation in a high performance platform

2.2.6 Applications for SPR

This section outlines the applications for which SPR is particularly well suited. Also described are some applications. Of course, future technical improvements are likely to extend the range of applications for which the SPR is useful.

What SPR is good for

Evaluation of macromolecules. Most laboratories studying biological problems at the molecular or cellular level need to produce recombinant proteins. It is important to be able to show that the recombinant protein has the same structure as its native counterpart. With the possible exception of enzymes, this is most easily done by confirming that the protein binds its natural ligands. Because such interactions involve multiple residues, which are usually far apart in the primary amino acid sequence, they require a correctly folded protein. In the absence of natural ligands monoclonal antibodies (mAbs) that are known to bind to the native protein are an excellent means of assessing the structural integrity of the recombinant protein. The SPR is particularly well suited to evaluate the binding of recombinant proteins to natural ligands and mAbs. Setting up an assay for any particular protein is very fast, and the data provided are highly informative.

Equilibrium measurements (affinity and enthalpy). Equilibrium analysis requires multiple sequential injections of analyte at different concentrations (and at different temperatures). Because this is very time-consuming it is only practical to perform equilibrium analysis on interactions that attain equilibrium within about 30 min. The time it takes to reach equilibrium is determined primarily by the dissociation rate constant, k_{off}. High affinity interactions (K_D < 10 nM) usually have very slow k_{off} values and are therefore unsuitable for equilibrium analysis. Conversely, very weak interactions (K_D >100 μM) are easily studied. The small sample volumes required for instrument injections (<20 μL) make it feasible to inject the very high concentrations (>500 μM) of protein required to saturate low affinity interactions.

Equilibrium affinity measurements on the SPR are highly reproducible. This feature and the very precise temperature control makes it possible to estimate binding enthalpy by van't Hoff analysis . This involves measuring the (often small) change in affinity with temperature. Although not as rigorous as calorimetry, much less protein is required.

Kinetic measurements. The fact that the SPR generates real-time binding data makes it well suited to the analysis of binding kinetics. There are, however, important limitations to kinetic analysis. Largely because of mass transport

limitations it is difficult to measure accurately k_{on} values faster than about 10^6 $M^{-1}s^{-1}$. This upper limit is dependent on the size of the analyte. Faster k_{on} values can be measured with analytes with a greater molecular mass. This is because the larger signal produced by a large analyte allows the experiment to be performed at lower ligand densities, and lower ligand densities require lower rates of mass transport. For different reasons measuring k_{off} values slower than 10^{-5} s^{-1} or faster than ~1 s^{-1} is difficult. Because the SPR is easy to use and the analysis software is user-friendly, it is deceptively easy to generate kinetic data. However obtaining accurate kinetic data is a very demanding and time-consuming task, and requires a thorough understanding of binding kinetics and of the potential sources of artefact.

Analysis of mutant proteins. It is possible using SPR to visualise the capture of proteins from crude mixtures onto the sensor surface. This is very convenient for analysing mutants generated by site-directed mutagenesis. Mutants can be expressed as tagged proteins by transient transfection and then captured from crude tissue culture supernatant using an antibody for the tag, thus effectively purifying the mutant protein on the sensor surface. It is then simple to evaluate the effect of the mutation on the binding properties (affinity, kinetics, and even thermodynamics) of the immobilised protein. This provides the only practical way of quantifying the effect of mutations on the thermodynamics and kinetics of weak protein/ligand interactions.

What SPR is not good for

High throughput assays. The fact the BIAcore can only few sample can be analysed at a time, with each analysis taking 5-15 min, means that it is neither practical nor efficient for high throughput assays. Automation does not solve this problem because the sensor surface deteriorates over time and with re-use. Blockages or air bubbles in the microfluidic system are also common in long experiments, especially when many samples are injected.

Concentration assays. the BIAcore is also unsuitable for concentration measurements, because these require the analysis of many samples in parallel, including the standard curve. A second problem is that, for optimal sensitivity, concentration assays require long equilibration periods.

Studying small analytes. Because the SPR measures the mass of material binding to the sensor surface, very small analytes (M_r <1000) give very small responses. The recent improvements in signal to noise ratio have made it possible to measure binding of such small analytes. However a very high surface concentration of active immobilized ligand (~1 mM) is needed, and this is difficult to achieve. Furthermore, at such high ligand densities accurate kinetic analysis is not possible because of mass-transport limitations and re-binding . Thus only equilibrium analysis is possible with very small analytes, and then only under optimal conditions. This assessment may need to be revised as and when future improvements are made in the signal to noise ratio.

2.3 Other commercial label-free biosensor

2.3.1 Spectral reflectance

Interferometry makes use of the superposition principle to combine separate waves together in a way that will cause the result of their combination to have some meaningful property that is diagnostic of the original waves state.

In 2006, ForteBio (http://www.fortebio.com/) released the Octet system, based on a proprietary technique called BioLayer Interferometry (BLI). The Octet system uses disposable sensors with an optical coating layer at the tip of each sensor (Figure 2.9). This optical surface is coated with a biocompatible matrix that can interact with molecules from a surrounding solution. A minimum sample volume of 80 µL should be used in low-volume microplate wells to make accurate measurements because smaller volumes than this can generate measurement artefacts due to internal reflections during measurement. To overcome the effects of diffusion on kinetic measurements, the sample plate is subject to orbital motion relative to the biosensor. Experiments can be performed with static samples (for binding steps), or with motion ranging from 100 to 1500 rpm.

The Octet instrument then shines white light down the biosensor and collects the light reflected back. Interference patterns in the reflected light are captured by a spectrometer as a characteristic profile of wavelength peaks and

troughs. When biological molecules bind to the biosensor surface, its thickness increases and the binding can be monitored by analysing changes in the interference pattern at the spectrometer. The white incident light and the reflected beams are collected by a optical fiber which simplify the measure system and allow a disposable probe for immersion measure (Patent number US005804453A). The HTS use 8 probes in parallel. Unbound molecules do not change the interference pattern, which enables the use of crude cell lysates or periplasmic samples.

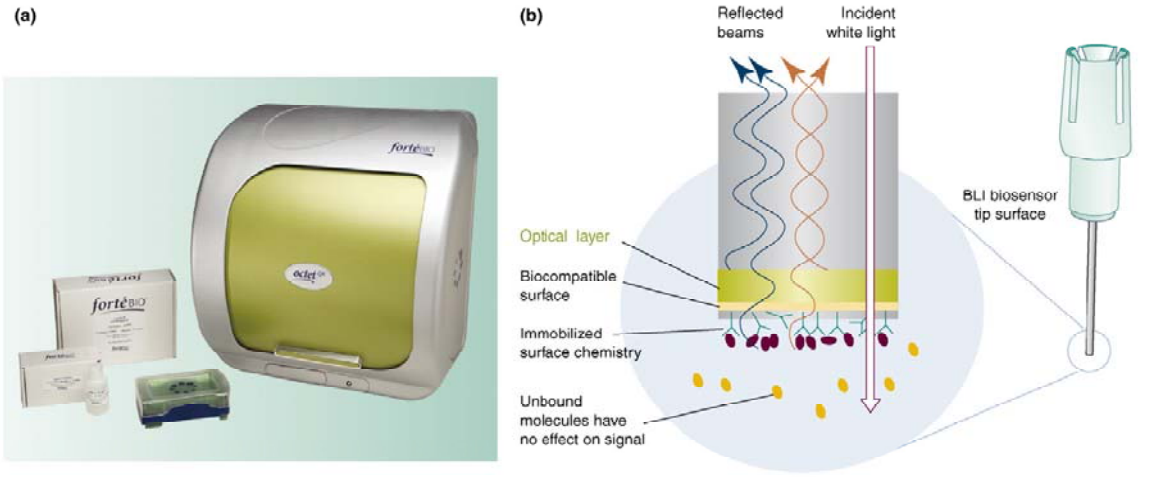

Figure 2.9 The ForteBio Octect system: (a) the reader with integrated sensor tip handling for application to 96 well plates; and (b) a schematic of a disposable fiber optic biosensor tip with capture antibodies.

2.3.2 Dual Polarisation Interferometer

Another instrument based on interferometry technique (Young Interferometer) is currently available from Fairfield Scientific (http://www.farfield-group.com/). The commercial product has 4 waveguides able to flux the analytes. Three waveguides (sensor arms) are functionalized with different antibodies and one waveguide (reference arm) is non-functionalized. When antigens bind, they interact with the evanescent wave at the surface of the waveguide, changing the refractive index. The optical output of the arms combines to form interference fringes on a detector screen, which is a CCD camera, adsorption of biomolecules on the sensing waveguide surface results in a shift in the interference fringe pattern that can be quantified and recorded. The sensor demonstrates a response time of just a few minutes. Using information from measurements of the sensor arms and reference arm

modes, accurate values for both thickness and refractive index of the adsorbed layer can be obtain. Information about the density of an adsorbed protein monolayer can be used, for example, to detect changes in the conformation (i.e., folding) of the protein. The instrument are shown in figure 2.10.

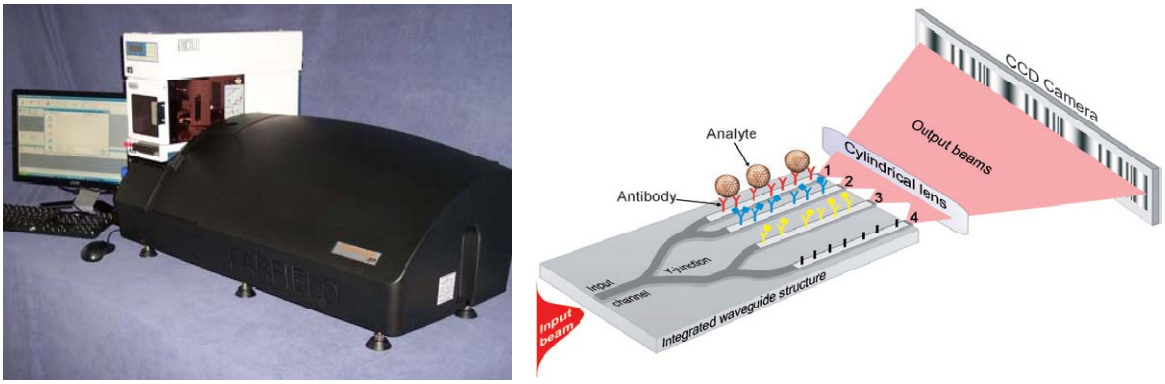

Figure 2.10 (a) The AnaLight® 4D (b) Four-Arm interferometer . the arm 1, 2, and 3 are the sensor channels which are functionalized with antibody capture probes and 4 is the reference channel.

2.3.3 Waveguide grating

Corning has developed a label-free detection platform that utilizes resonant waveguide grating (RWG) sensors. The Corning Epic™ system consists of a standard 384-well micro-plate with RWG (figure 2.11).

When illuminated with broadband light, the RWG plate reflect only specific wavelengths, that is a sensitive function of the index of refraction close to the sensor surface. The sensors are chemically modified with a surface layer that enables covalent attachment of protein targets via a primary amine group. The surface chemistry provides a high-binding-capacity surface, with low levels of nonspecific binding; users can choose to immobilize proteins, peptides, small molecules or DNA. After a target is immobilized, the reader obtains a baseline measurement. During the subsequent binding assay, if analyte molecules bind to the immobilized target, a change in the local refractive index is induced, and this results in a shift in the wavelength of light that is reflected from the sensor. The magnitude of this wavelength shift is proportional to the amount of analyte that binds to the immobilized target. The Epic™ system determines the binding signal strength by subtracting a reference signal from the sample signal to determine the net response, measured in pedometers of wavelength shift. The platform has a sensitivity of 5 pg/mm^2. Although not exceptional,

but microplate reader are capable of reading up to 40 000 wells in an eight-hour period.

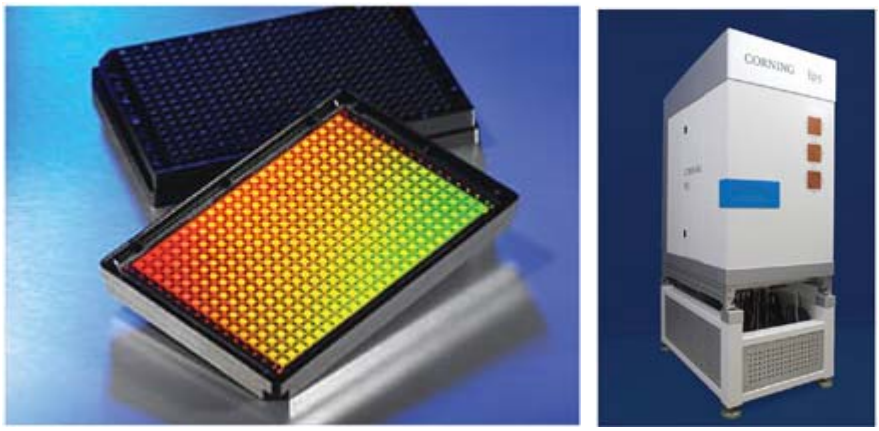

Figure 2.11 A disposable 384-well microplate and an optical reader of Corning EpicTM system

2.3.4 Isothermal Titration Calorimetry

Isothermal Titration Calorimetry (ITC) simultaneously determines all binding parameters in a single experiment information that cannot be obtained from any other method. This is a true in-solution technique: no immobilization or labeling required and no buffer restrictions.

When substances bind, heat is either generated or absorbed. ITC is a thermodynamic technique that directly measures the heat released or absorbed during a biomolecular binding event. Measurement of this heat allows accurate determination of binding constants (K_D), reaction stoichiometry (n), enthalpy (ΔH) and entropy (ΔS), thereby providing a complete thermodynamic profile of the molecular interaction in a single experiment. Because ITC goes beyond binding affinities and can elucidate the mechanism of the molecular interaction, it has become the method of choice for characterizing biomolecular interactions.

MicroCal's (http://www.microcal.com/) ultrasensitive ITC systems use a cell feedback network to differentially measure and compensate for heat produced or absorbed between the sample and reference cell (O'Brien et al. 2000). Twin coin-shaped cells are mounted in a cylindrical adiabatic environment, and connect to the outside through narrow access tubes (Figure 1). A thermoelectric device measures the

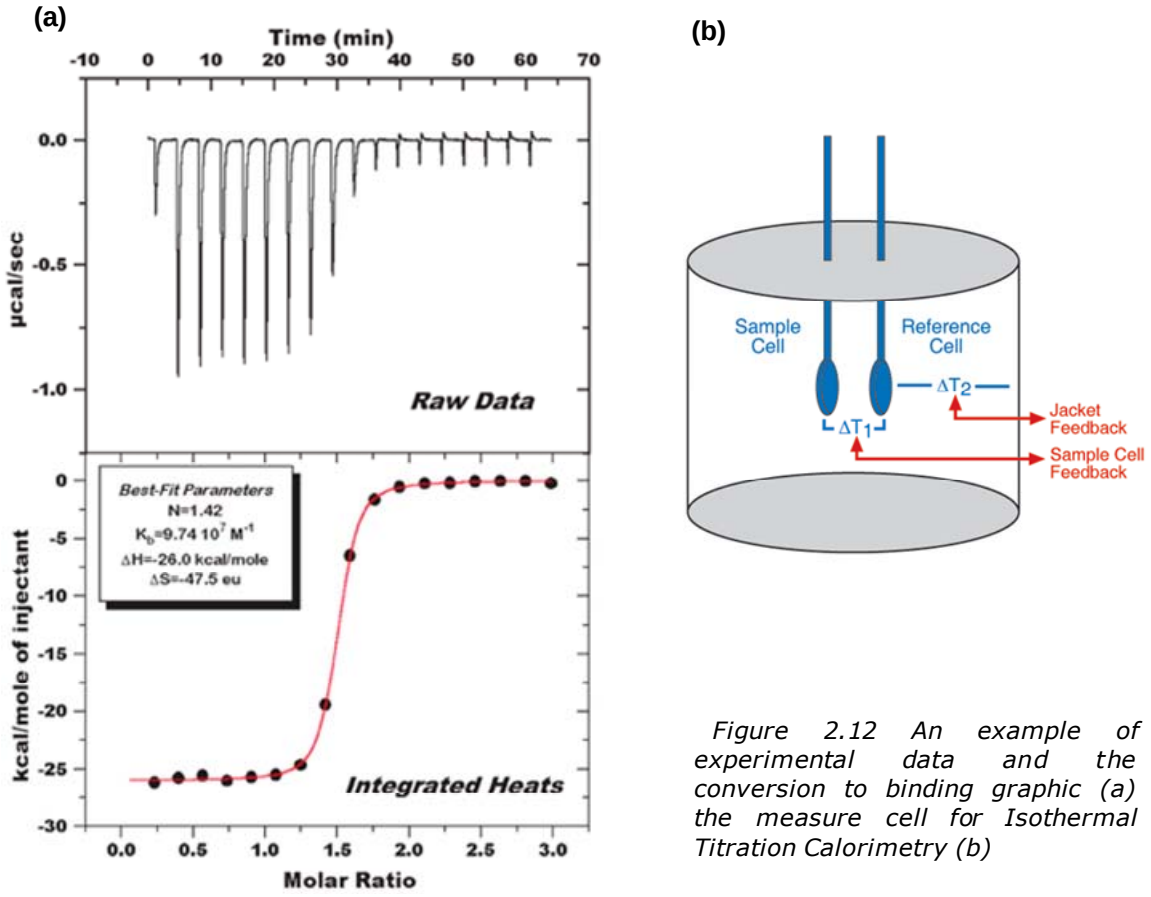

Figure 2.12 An example of experimental data and the conversion to binding graphic (a) the measure cell for Isothermal Titration Calorimetry (b)

temperature difference between the two cells and a second device measures the temperature difference between the cells and the jacket. As chemical reactions occur in the sample cell, heat is generated or absorbed. The temperature difference between the sample and reference cells (ΔT1) is kept at a constant value (i.e. baseline) by the addition or removal of heat to the sample cell, as appropriate, using the cell feedback system. The integral of the power required to maintain ΔT1 = constant over time is a measure of total heat resulting from the process being studied. Figure 2.12b is a schematic drawing of the ITC cells and syringe.

In a typical ITC experiment, a solution of one biomolecule ("ligand" such as.a drug, protein, DNA molecule, etc) is titrated into a solution of its binding partner. The heat released upon their interaction (ΔH) is monitored over time (Figure 2.12a). Each peak represents a heat change associated with the injection of a small volume of sample into the ITC reaction cell. As successive

amounts of the ligand are titrated into the ITC cell, the quantity of heat absorbed or released is in direct proportion to the amount of binding. As the system reaches saturation, the heat signal diminishes until only heats of dilution are observed. A binding curve is then obtained from a plot of the heats from each injection against the ratio of ligand and binding partner in the cell (Figure 2.12a). The binding curve is analyzed with the appropriate binding model to determine K_B, n and ΔH.

A wide range of applications can be accomplished with the ITC including: characterization of molecular interactions of small molecules, proteins, antibodies, nucleic acids, lipids and other biomolecules, enzyme kinetics and the effects of molecular structure changes on binding mechanism. GE Healthcare has developed some product as Auto iTC_{200} for analysis with 75 sample.

Figure 2.13 MicroCal develops and manufactures microcalorimeters in combination of GE Healthcare's (Auto iTC200™ is s show in this picture) that provide detailed information on the binding properties

2.3.5 Resonant acoustic sensor

The piezoelectric effect was discovered by the Curie Brothers in 1880, who observed that a mechanical stress applied to the surfaces of various crystals caused a corresponding electrical potential across the crystal, whose magnitude was proportional to the applied stress. The Curies also verified the converse piezoelectric effect in which application of a voltage across these crystals caused a corresponding mechanical strain. Application of an alternating electric field across the crystal substrate results in an alternating

strain field. This causes a vibrational, or oscillatory, motion in the crystal, resulting in the generation of acoustic standing waves. Depending on the crystal type, the oscillator vibrates at a characteristic resonant frequency.

Piezoelectric materials are often composed of crystals without a center of symmetry, for example, potassium sodium tartrate (Rochelle's salt), lithium niobate and, most frequently encountered, quartz (SiO_2). Next to their chemical composition, piezoelectric sensors can be distinguished by their mode of operation: thickness shear mode sensors and surface acoustic wave devices being the most prominent. Thickness shear mode sensors consist of a thin, circular quartz plate with electrodes (often made of gold) on both sides.

Between the two electrodes, a standing acoustic wave is generated. It has been shown that a mass deposition on the surface only changes the thickness of the resonator and thus its resonance frequency (Szostak et al. 1990), while all its other mechanical properties remain constant. Mass sensitivity decreases monotonically along the plate radius, then becoming negligible at and beyond the electrode boundary.

Piezoelectric sensors have become a versatile tool in biosensing to study protein–protein and protein–small molecule interactions. Akubio (http://www.akubio.com/) is developing a highly sensitive, real time, label-free molecular interaction analysis system based on this technology.

Called Resonant Acoustic Profiling (RAP™) (figure 2.14), the technique measures the changes in oscillation of quartz crystal resonators to give information about the specificity, affinity, kinetics and concentration of molecular binding. Based on the same technology the electronics industry uses for timing devices in everything from cell phones to microwaves, the technology is cost-effective, robust, and very scalable.

During RAP analysis target molecules are attached to the sensor surface through direct linkage or capture. Samples containing potential binding partners are then applied to the sensor surface using either flow-based or static delivery techniques.

Frequency and resistance parameters of the crystal oscillation are then measured over time to characterize binding of sample molecules to the surface bound target. Measurement of the changes in frequency of crystal oscillation provides information about changes in mass at the sensor surface. The RAP

technique has already been employed to characterize the binding of compounds as small as a few hundred Daltons and as large as whole cells.

Figure 2.14 RAP·id 4 is a flow-based analysis system which reduces the need to purify samples and generates accurate kinetic, affinity and concentration measurements from complex mixtures, such as blood, serum, cell culture supernatants and periplasmic extracts. Typically processing an average of 400 samples per day.

The RAP analysis technique overcomes a number of problems intrinsic to optical based label-free analysis methods. Since RAP measures the change in molecular mass attached to the sensor surface, changes in fluid environment have minimal effect on binding measurements. Analyses of samples in media such as serum, as well as in organic solvents, cause little if any artefacts in binding measurements. Also due to the simplicity of the detection method RAP technology is very scalable. Both an 8-channel (RAPid) and a 96-well format instrument (RAPArray) are under development. Akubio launched the RAPid instrument in 2006 and the RAPArray system in early 2007.

2.4 From laboratory to Point of care

The technologies mentioned are only an introduction to Label-Free technology for laboratory research (like drug discovery).Tipocally they are instruments with a high cost and they need skilled users.

However, such technology may be also extremely useful for enhancing health care delivery in the community setting and to underserved populations. Environmental applications include spill clean-up, monitoring, and regulatory instances. Food safety applications include monitoring of food production, regulatory monitoring, and diagnosis of food poisoning. Biosensors have several potential advantages over other methods of biodetection, especially increase
d assay speed and flexibility. Rapid, essentially real-time analysis can provide immediate interactive information to users. This speed of detection is an advantage in essentially all applications. Biosensor-based diagnostics might facilitate disease screening and improve the rates of earlier detection and attendant improved prognosis. (Sia et al. 2008 - Yager et al. 2008 - Ligler et al 2009)

Despite a growing focus from the academic community, the field of microfluidics has yet to produce many commercial devices for point-of-care (POC) diagnostics. One of the main reason for this is the difficulty in producing low-cost, sensitive, and portable detection systems. Conventional systems, however, are costly, require careful alignment, and do not translate well to POC devices (Frank et al. 2008). Thus, a great effort is still necessary to achieve these purposes.

3 BIOMOLECULAR RECOGNITION

3.1 Receptor-ligand interactions

The formation and dissociation of specific interactions between a variety of macromolecules play a crucial role in the function of biological systems.

The terms receptor and ligand are words with a wide range of meaning. In biological systems, a "receptor" is usually a protein molecule, either embedded in the plasma membrane or present in the cytoplasm of a cell or other biological structures, to which a mobile signaling molecule may attach; the molecule which binds to a receptor is called a "ligand". In this thesis we must extend these definitions to the biosensor world. When a molecule forms a stable interaction with a surface, it is called the "receptor"; a second molecule which binds the first one is called the "ligand". However, if the second molecule interacts with another molecule (present in solution) the terms will change: the second is the "receptor" and the third is the "ligand".

The interaction of most ligands with their receptors can be characterized in terms of a binding affinity. In general, high affinity ligand binding results from greater intermolecular force between the ligand and its receptor while low affinity ligand binding involves less intermolecular force. The specific association of ligand and receptor depends on hydrogen bonds, hydrophobic interactions, electrostatic forces, and Van Der Waals forces. These are all bonds of a weak, non-covalent nature, yet some of the associations between ligand and receptor can be quite strong.

To simplify the model, a monovalent system will be introduced. Of course, ligand and receptor can be multivalent, either through multiple copies of the same epitope, or through the presence of multiple epitopes that are recognized by multiple ligands. Interactions involving multivalency can produce more stabilized complexes, however multivalency can also result in steric difficulties, thus reducing the possibility for binding, in particularly when the interactions take place on a surface.

All ligand-receptor bindings are reversible and follows the basic thermodynamic principles of any reversible bimolecular interaction:

$$A + B \rightleftharpoons AB$$

In this model, B (analyte in solution) is injected over a surface coated with A (ligand immobilized on the sensor chip surface). AB complex formation is monitored in real time to produce a binding response, R.

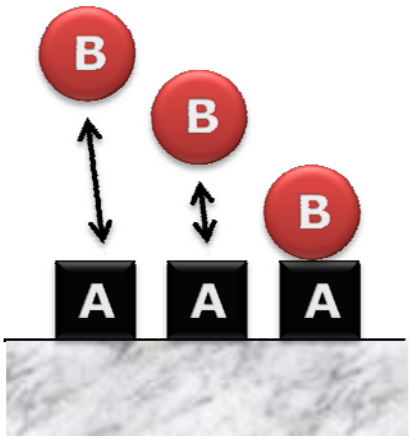

Figure 3.1 A ligand-receptor bindings on a surface

Under steady-state conditions, the equilibrium association constant, K_A, is defined as:

$$K_A = \frac{[AB]}{[A][B]} \qquad [3.1]$$

which is related to dissociation constant, K_D, by the relationship:

$$K_D = \frac{1}{K_A} \qquad [3.2]$$

The fraction of ligand binding sites occupied corresponds to $[AB]/[A_{tot}]$ and is correlated with: R/R_{max}:

$$\frac{R}{R_{max}} \cong \frac{[AB]}{[A_{tot}]} = \frac{[AB]}{[A] + [AB]} \qquad [3.3]$$

where R_{max} is the response observed when all A binding sites are occupied. Substituting $[AB] = [A][B]/K_D$, the equation can be rewritten as:

$$R = R_{max} \frac{[B]}{K_D + [B]} \qquad [3.4]$$

A plot of binding responses R versus injected analyte concentrations $[B]$ is fit to an isotherm described by this equation to yield R_{max} and K_D parameters.
Example isotherms for an equilibrium analysis, shown in figure 3.2, illustrate that as $[B]$ increases R approaches R_{max}, and the $[B]$ that generates a half-saturation response (0.5 R_{max}) corresponds to the K_D.
The bond between antibodies and antigens is a typical model of receptors-ligands interactions. For example, a standard SPR application is to analyze the association constant of monoclonal antibodies.

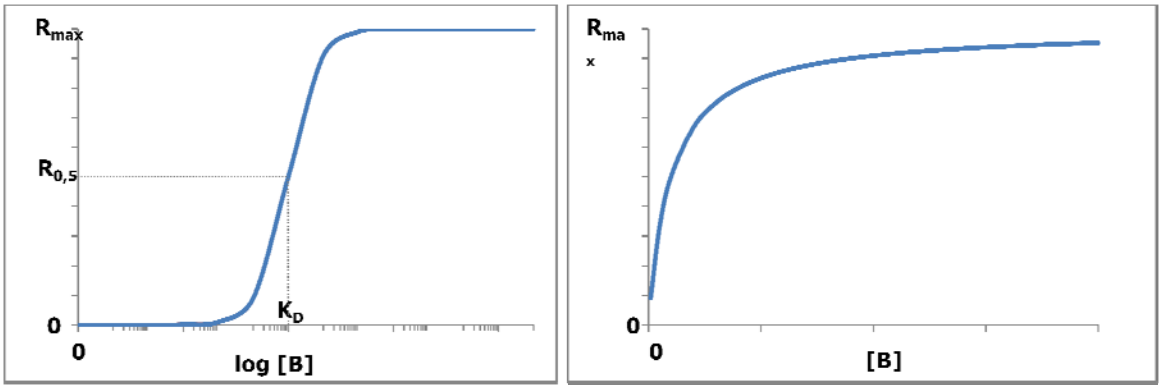

Figure 3.2 Typical binding isotherms obtained from affinity measurements of a simple single site interaction. Binding isotherm on linear and logarithmic scale: the second one is more useful to determine the dissociation constant

3.2 The protein Avidin

As previously described, our method is based on prefluorinated material, on which protein called avidin (AVD) is adsorbed.
The highly specific interaction of AVD with biotin can be a useful tool in designing purification and detection systems. The extraordinary affinity of these molecules (KA = 10^{15} M^{-1}) is the strongest known non-covalent interaction of a protein and a ligand and allows biotin-containing molecules in

a complex mixture to be discretely bound with avidin conjugates. Some applications in which the AVD-biotin interaction has been used include: ELISA; immunohistochemical staining; Western, Northern and Southern blotting; immunoprecipitation; cell-surface labeling; affinity purification.

AVD is a protein originally isolated from chicken egg white and also found in the tissues of birds. It is tetrameric with four identical subunits having a combined molecular weight of about 66-69,000 (128 amino acid residues) depending on the method of analysis and purification. It is a basic glycoprotein with an isoelectric point (pI) of approximately 9.5 (about 24 positive charge at pH 7.40). The AVD monomer contains 128 amino and 20 acid residues (Green 1962). The extent of glycosylation is very high, carbohydrate accounts for about 10% of the total mass. The heterogeneous oligosaccharide present on each subunit is a distinguishing characteristic of AVD. The carbohydrate is linked to Asparagine 17 on the subunit through one of its acetylglucosamine residue. The glycopeptide fractions of AVD range from 1.2 to 2.0 in the ratio of mannose to N-acetylglucosamine. For its carbohydrate content and basic isoelectric point, AVD has relatively high nonspecific binding (www.pierce.com).This protein is soluble in aqueous solutions and stable over wide pH and temperature ranges (Green 1963) (Green 1966) (Meir Wilchek 2006). AVD has one disulfide bridge per subunit. This bridge can be reduced only after the tetramer is dissociated into subunits. This disulfide bridge has not been identified as playing a critical role in the binding of biotin to AVD. Consequently, reducing agents do not have an impact on the interaction.

Figure 3.3 The AVD structure

AVD is resistant to denaturation in 8 M urea or 3 M guanidine hydrochloride (HCl). (Green 1963 - Green 1966). In 6 M guanidine, the tetramer is dissociated into monomers. However, AVD can regain its ability to bind biotin when the concentration of guanidine is decreased to 3 M. The combined treatment of 6 M guanidine and pH 1.5 has been reported to break the AVD - biotin interaction. Studies indicate that 8 M guanidine, pH 1.5, is required for efficient dissociation of the complex (Green 1962).

It's important to point up the exceptional stability and strength of the bond AVD-biotin. Therefore, this protein can be used for the functionalization of biosensor surface.

Biotin is a naturally occurring vitamin found in every living cell (vitamin H). Yeast and milk are also high in biotin content. Biotin is necessary for cell growth, the production of fatty acids, and the metabolism of fats and amino acids. Biotin not only assists in various metabolic reactions, but also helps to transfer carbon dioxide. It plays a role in the citric acid cycle, which is the process by which biochemical energy is generated during aerobic respiration. The chemical name for biotin is cis-hexahydro-2-oxo-1H-thieno[3,4]imidazole-4-pentanoic acid. The molecular weight of biotin is 244.31. It has very little chromophoric properties. At 250 nm, biotin has an absorbance of 0.111 for a 1 mg/ml solution. The valeric acid side chain of the biotin molecule can be

derivatized to incorporate various reactive groups that are used to attach biotin to other molecules.

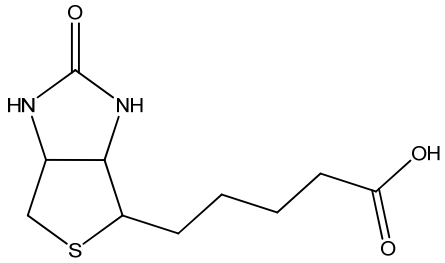

Figure 3.4 Biotin, also known as vitamin H or B7 molecular structure

In the biology laboratory, biotin is often chemically linked to a molecule or protein for biochemical assays. This process is called biotinylation (section 3.3.1). Biotin-tagged molecules can be extracted from a sample with covalently-attached AVD, and washing away the solution. For example biotinylated antibodies are used to capture AVD in the ELISA techniques. In many biosensors, like SPR, a commonly used chip presents AVD immobilizated on the surface (Cooper 2009).

3.3 The antibodies and antigens

The basic principle of any immunological detector is that a specific antibody will combine with its specific antigen to give an exclusive antibody-antigen complex.

An antibody is defined as "an immunoglobulin capable of specific combination with the antigen that caused its production in a susceptible animal." They are produced in response to the invasion of foreign molecules in the body. Most antibodies exist as one or more copies of a Y-shaped unit, composed of four polypeptide chains. Each Y contains two identical copies of a heavy chain, and two identical copies of a light chain, named as such by their relative molecular weights.

Mammalian antibodies can be divided into five classes: IgG, IgM, IgA, IgD and IgE, based on the number of Y units and the type of heavy chain. Each of these classes present a lot of species-dependent subtypes: for example, the mouse IgG have four subgroups (IgG_1, IgG_{2a} ,IgG_{2b} and IgG_3). Heavy chains of IgG, IgM, IgA, IgD, and IgE, are known as g, μ, a, d, and e, respectively. The

light chains of any antibody can be classified as either a kappa or a lambda type (based on small polypeptide structural differences); however, the heavy chain determines the subclass of each antibody.

The subclasses of antibodies differ in the number of disulfide bonds and the length of the hinge region. The most commonly used antibodies in immunochemical procedures belong to the IgG class because they are the major immunoglobulins released in serum.

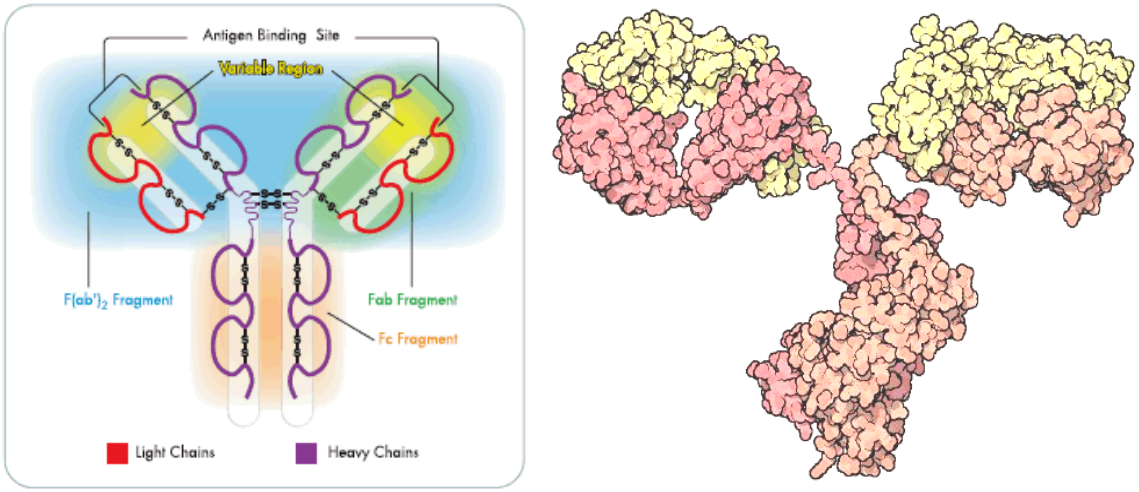

Figure 3.5 The antibody structure and an artistic structure image

The classical Y shape of IgG is composed of the two variable, antigen specific F(ab) arms, which are critical for actual antigen binding, and the constant Fc "tail" that binds immune cell Fc receptors and also serves as a useful "handle" for manipulating the antibody during most immunochemical procedures. The number of F(ab) regions on the antibody, corresponds with its subclass, and determines the valence of the antibody (loosely stated, the number of "arms" with which the antibody may bind its antigen). The Fc region also anchors the antibody to the plate in ELISA procedures and is also seen by secondary antibodies in immunoprecipitation, immunoblots and immunohistochemistry.

Immunochemical techniques capitalize upon the extreme specificity, at the molecular level, of each immunoglobulin for its antigen, even in the presence of high levels of contaminating molecules. The multi-valence of most antigens and antibodies enables them to interact to form a precipitate. Examples of experimental applications that use antibodies are Western blot, Immunohistochemistry and Immunocytochemistry, ELISA, Immunoprecipitation, Flow Cytometry and Immunobiosensor in general.

Because antigen molecules exist in space, the epitope recognized by an antibody may be dependent upon the presence of a specific three-dimensional antigenic conformation (e.g., a unique site formed by the interaction of two native protein loops or subunits), or the epitope may correspond to a simple primary sequence region. Such epitopes are described as conformational and linear, respectively. The range of possible binding sites is enormous, with each potential binding site having its own structural properties derived from covalent bonds, ionic bonds and hydrophilic and hydrophobic interactions.

For efficient interaction to occur between the antigen and the antibody, the epitope must be readily available for binding. If the target molecule is denatured, e.g., through fixation, reduction, pH changes or during preparation for gel electrophoresis, the epitope may be altered and this may affect its ability to interact with an antibody. For example, some antibodies are ineffective in Western blot but very good in immunohistochemistry because in the latter procedure, a complex antigenic site might be maintained in the tissue, whereas in the former procedure the process of sample preparation alters the protein conformation sufficiently to destroy the antigenic site and hence eliminate antibody binding. Thus, the epitope may be present in the antigen native, cellular environment, or only exposed when denatured. In their natural form they may be cytoplasmic (soluble), membrane associated, or secreted. The number, location and size of the epitopes depends on how much of the antigen is presented during the antibody making process.

3.3.1 Antibody Biotinylation

Biotinylation is widely used to enable isolation, separation, concentration and further downstream processing and analysis of biomolecules. Biotin with different spacer arm lengths reduces steric hindrances associated with AVD binding and allows for efficient capturing of biotinylated proteins. It is also provided with reactivity toward wide variety of groups and can be coupled to either primary amine, secondary amine, sulfhydryl, carboxyl or phosphate groups of proteins or peptides.

The most commune strategy of the antibody biotinylation uses the reactivity of nucleophiles which are present as lysine side chain epsilon-amines and N-

terminal α-amines (Hermanson 2008). An N-hydroxysuccinimide (NHS) ester is perhaps the most common reagents to bind group on amine. NHS reagents react with nucleophiles to form an acylating bond and NHS becoming leaving groups (figure 3.6).

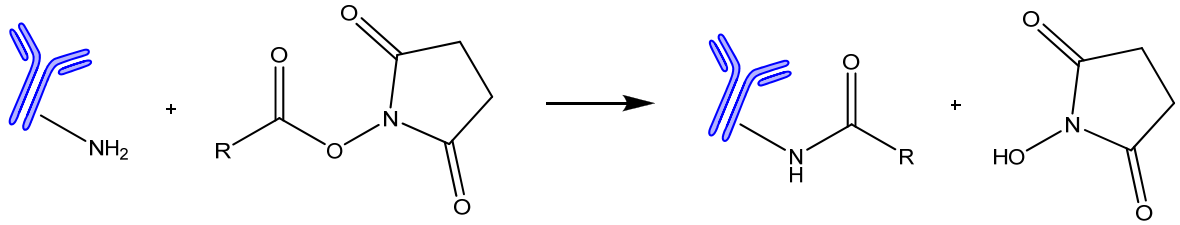

Figure 3.6 The antibody labeling: reaction NHS-derivate with a primary amine, NHS is a leaving group (byproduct) in the reaction; this leaving group as well as any nonreacted biotin reagent is removed during the final desalting step in the procedure.

Because the targets for the ester are deprotonated primary amines, the reaction is prevalent above pH 7. Hydrolysis of the NHS-ester is a major competing reaction, and the rate of hydrolysis increases with increasing pH. NHS-esters have a half-life of several hours at pH 7, but only a few minutes at pH 9. There is some flexibility in the conditions for conjugating NHS-esters to primary amines. Incubation temperatures can range from 4-37°C, pH values in the reaction range from 7-9, and incubation times range from a few minutes to 12 hours. Buffers containing amines (such as Tris or glycine) must be avoided because they compete with the reaction (http://www.pierce.com).

NHS-esters of biotin have poor solubility in aqueous solutions. For reactions in aqueous solution, they must first be dissolved in an organic solvent, then diluted into the aqueous reaction mixture.

Purification of the biotinylated antibody can be performed with a gel filtration using a desalting resin or a dialysis. For example, BSA contains 59 primary amines and 30-35 of these are on the surface and can be reacted with NHS-esters.

This strategy is easy and has a very good yield. Nevertheless it can reduce the affinity for the substrate. Amine groups are as plentiful in antibodies as they are in most proteins; the distribution of them within the tree-dimensional structure of an immunoglobulin is nearly uniform throughout the surface topology. For this reason, this strategy will link somewhat randomly to the molecule. This in turn leads to a random orientation of the antibody within the conjugate structure, often blocking the antigen binding sites against the

surface of another coupled protein or molecule. Obscuring the binding sites in this manner results in decreased antigen binding activity in the conjugate compared to that observed for the unconjugated antibody (G. T. Hermanson 2008).

3.3.2 Antibody-binding proteins

Because antibodies have predictable structure, including relatively invariant domains, it has been possible to identify certain protein ligands that are capable of binding to antibodies generally. The biotinylation of this proteins allow another strategy to link the antibodies to the avidin surface.

Protein A and Protein G are two bacterial proteins whose antibody-binding properties have been well characterized. These proteins have been produced recombinant and used routinely for affinity purification of key antibody types from a variety of species. The interaction between the various proteins and IgG is not equivalent for all species or all antibody subclasses.

Protein A is a cell wall component produced by several strains of *Staphylococcus aureus*. It consists of a single polypeptide chain (MW 46.7 kDa) and contains little or no carbohydrate (Bjork et al. 1972) Protein A binds specifically to the Fc region of immunoglobulin molecules, especially IgG. It has four high-affinity (K_a = 10^8 M^{-1}) binding sites that are capable of interacting with the Fc region of IgGs of several species. This measure was made with a radioactive binding and confirmed with a SPR technology (Lindmark et al. 1981; Andersson et al. 1999).

However, the interaction between Protein A and IgG is not equivalent for all animal sources and subclasses of IgG. For example, human IgG_1, IgG_2 and IgG_4 bind strongly to Protein A, while IgG_3 does not bind. (Goding 1978). In mice, IgG_{2a} , IgG_{2b} and IgG_3 bind strongly to Protein A, but IgG_1 (the dominant subclass in serum) binds only weakly using standard buffer conditions. Most rat IgG subclasses bind weakly or not at all to Protein A. Despite this variability, Protein A is very effective for routine affinity purification of IgG from the serum of many species. It is especially suited for purification of polyclonal antibodies from rabbits.

Protein G is a bacterial cell wall protein isolated from streptococci group. Like Protein A from *Staphylococcus aureus*, Protein G binds to most mammalian immunoglobulins primarily through their Fc regions. Protein G binds weakly to Fab fragments (Bjork et al. 1972). Sequencing of DNA that encodes native Protein G indicates that there are two binding sites for the immunoglobulins and one for the albumin (Guss et al. 1986). In the recombinant form of Protein G, this albumin binding site has been eliminated to reduce nonspecific binding when purifying immunoglobulins. With the albumin site removed, recombinant Protein G can be used to separate albumin from crude human immunoglobulin samples. Recombinant Protein G has a mass of approximately 22 kDa. However, its apparent mass by SDS-PAGE is nearly 34 kDa. Immobilized Protein G is most commonly used for the purification of mammalian monoclonal and polyclonal antibodies that do not bind well to Protein A. It has been reported that most mammalian immunoglobulins bind with greater affinity to Protein G than Protein A. There are, however, species to which Protein A has greater affinity. Protein G binds with significantly greater affinity to several immunoglobulin subclasses including human IgG_3 and rat IgG_{2a}. Unlike Protein A, Protein G does not bind to human IgM, IgD or IgA (Bjork et al. 1972). Differences in binding characteristics between Protein A and Protein G are explained by differences in the immunoglobulin binding sites of each protein. Although the tertiary structures of these proteins are similar, their amino acid compositions differ significantly.

3.4 Tumor markers

Now I want to describe some molecules with a biomedical relevance used to test the potentiality of our technique. For example, a typical application of biosensor is the detection of tumor markers. The development of microfluidic and the cost reduction have permitted the miniaturization and the diffusion of new techniques to enable high-throughput and low-cost measurements in basic research and clinical applications in this sector.

Tumor markers are substances produced by tumor cells or by other cells of the body in response to cancer or certain benign (noncancerous) conditions (http://www.cancer.gov/cancertopics/). These substances can be found in

blood, urine, tumor tissue, or in other tissues. Different tumor markers are found in different types of cancer, and levels of the same tumor marker can be altered in more than one type of cancer. In addition, tumor marker levels are not altered in all people with cancer, especially if the cancer is early stage. Some tumor marker levels can also be altered in patients with noncancerous conditions. Researchers have identified hundred substances that seem to be expressed abnormally when some types of cancer are present. Screening tests are a way of detecting cancer early, before there are any symptoms. For a screening test to be helpful, it should have high sensitivity and specificity. Sensitivity refers to the test ability to identify people who have the disease. Specificity refers to the test ability to identify people who do not have the disease.

3.4.1 Prostate-specific antigen

Prostate cancer is the most commonly diagnosed cancer in men. It is highly curable when detected early. Currently, prostate-specific antigen (PSA) is the recommended screening tool for prostate cancer resulting in earlier detection of prostate cancer (Jemal 2008). PSA is a protein produced by cells of the prostate gland, it is normally present in the blood at very low levels.

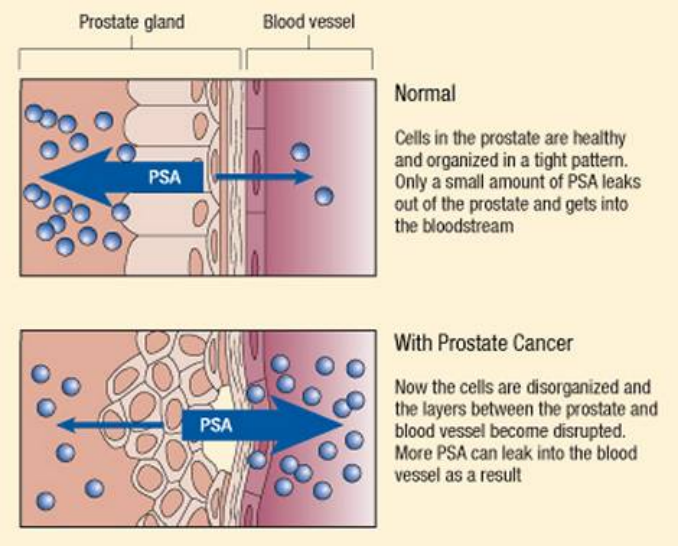

Figure 3.7 The growth of cancer cells in the prostate disrupts the structure and organisation of the tissue. PSA inside the prostate is able to leak into the nearby blood vessels more readily than it does in a healthy prostate. As a result, the amount of PSA in the blood increases, which is why measurement of PSA in a blood sample can help to diagnose prostate cancer.

The reference ranges from 0 to 4 ng/mL for the first commercial PSA test. Furthermore, evidence suggests that prostate cancer prevalence is high in men with PSA levels less than 4 - 10 ng/ml (Ankerst 2007) (figure 3.7).
The U.S. Food and Drug Administration (FDA) has approved the PSA test for annual screening of prostate cancer in men of age 50 and older. The standards test is based on the ELISA technology or other immunological methods.

3.4.2 Src family

The Src tyrosine kinases are receptor tyrosine kinases; a number of these have become key targets for both basic research and anticancer drug discovery over recent years. Src features several functional domains, including N-terminal (NT), Src homology 3 (SH3), Src homology 2 (SH2), kinase (catalytic), and the C-terminal (CT) non-catalytic domain (Nam et al 2004). Src is involved in intracellular signal transduction. Src kinases have been associated with several different cancers including colon and breast cancers for which transformed phenotypes have been correlated with Src mutations and/or over-expression of Src tyrosine kinase activities. Therefore, Src is an important target for drug discovery. SH2 domains are modules of approximately 100 amino acids that have evolved to recognize and bind specifically to tyrosyl-phosphorylated sequences located on proteins in response to extracellular signals.

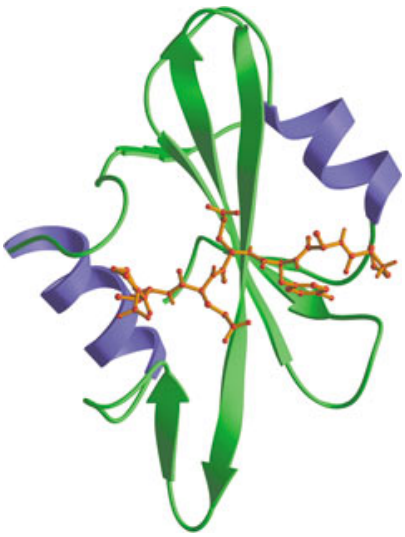

Figure 3.8 Src SH2 domain bound to phosphotyrosine peptide

The SH2 domain controls the range of proteins interacting with the Src family kinases. The Src SH2 domain preferentially binds peptides with the sequence pTyr-Glu-Glu-Ile (pYEEI) (Songyang et al 1993) with high affinity (K_D = 100 nM) (Ye et al 2005).

4 BIOSENSOR DEVELOPMENT

4.1 Introduction

The purpose of this thesis is to develop a method for the quantitative determination of ligand interactions with receptors absorbed or immobilized on the surface of a solid material with a very low reflectivity, by direct measurement of the reflected light intensity.

The intensity of reflection, from an interface between two media, depends on the difference between their refractive indexes, and therefore if the two materials are isorefractives, the reflection from their interface tends to zero. This work takes advantage of the special properties of a perfluorinated and transparent material which has a refractive index almost matched with the one of water. If a different material (e.g. a protein) adsorbs at the interface between the perfluorinated material and water, forming a thin molecular layer, the reflection increases. This phenomenon can be monitored simply illuminating the interface with a laser or LED (Light Emitting Diode) and detecting the of reflection with a photodiode or a CCD camera. Since the intensity reflected from a thin film depends on its thickness as well as on its refractive index, we can follow the gradual adsorption of several layers at the interface. In this way, the method can be used for the detection of biologically relevant molecules interacting with other receptors previously adsorbed on the sensor surface.It has been found that the protein avidin which is positively charged at physiological conditions spontaneously adsorbs on a transparent perflorinated isorefractive to water, thus allowing a general strategy for immobilization of biotin-labeled receptors.

The aims of this work are:

- to develop a sensor based on the measure of light reflection;
- to develop a strategy to functionalize the surface allowing the immobilization receptors;
- to carry out the measures of the adsorbed mass through the reflection signal;
- to test the sensor using an interaction with biomedical relevance.

4.1.1 The laws of geometrical optics

If you have ever half-submerged a straight stick into water, you have probably noticed that the stick appears bent at the point it enters the water. This optical effect is due to refraction. As light passes from one transparent medium to another, it changes speed, and bends. How much this happens depends on the refractive index of the media. The index of refraction is defined as the speed of light in vacuum divided by the speed of light in the medium. In many cases, the refractive index increases with the density of material and decreases with temperature and wavelength.

When a light ray crosses an optical system consisting of several homogeneous media in sequence, the optical path is a sequence of straight-line segments. Discontinuities in the line segments occur each time the light is reflected or refracted. The concepts of geometrical optics that describe the subsequent direction of the rays are the laws of reflection e refraction.

Law of Reflection: when a ray of light is reflected at an interface dividing two uniform media, the reflected ray remains within the plane of incidence, and the angle of reflection equals the angle of incidence. The plane of incidence includes the incident ray and the normal to the point of incidence.

Law of Refraction (Snell's Law): In 1621, a Dutch physicist named Willebrord Snell (1591-1626), derived the relationship between the different angles of light as it passes from one transperent medium to another. When a ray of light is refracted at an interface dividing two uniform media, the transmitted ray remains within the plane of incidence and the sine of the angle of refraction is directly proportional to the sine of the angle of incidence.

$$\sin\,\theta_1\;n_1 = \sin\,\theta_2\;n_2 \qquad [4.1]$$

Both laws are summarized in figure 4.1, in which an incident ray is partially reflected and partially transmitted at a plane interface separating two transparent media. The angle between the incident light ray and the normal is the angle of incidence. The angle between the refracted light ray and the normal is called the angle of refraction.

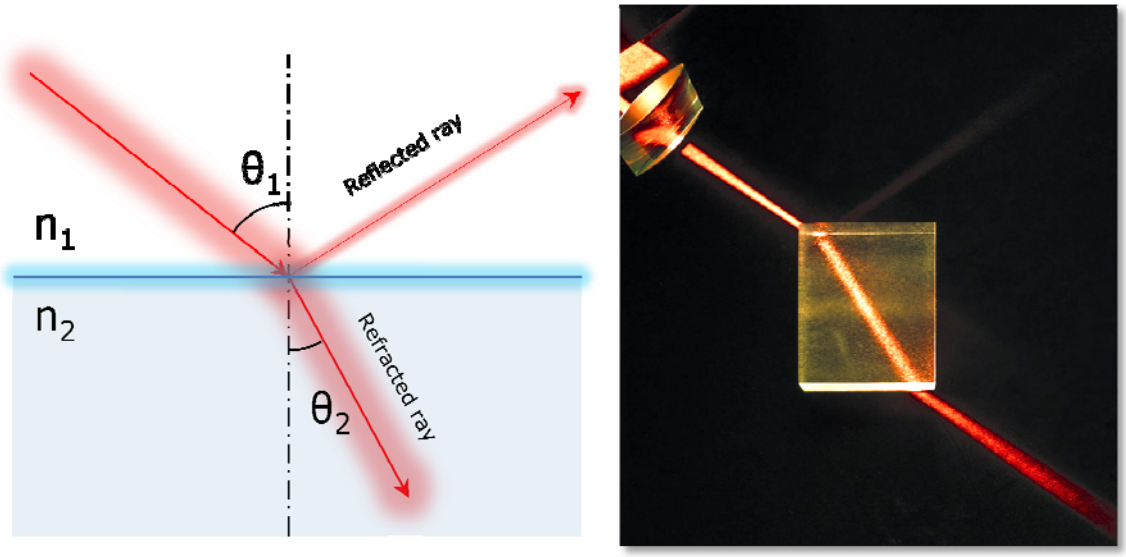

Figure 4.1 Scheme for laws of refraction and reflection(a) an example of reflection and refraction(b)

To understand the phenomenon measured in our method it is important to introduce the Fresnel laws. They describe the fraction of incident energy transmitted or reflected at a plane surface crossed by light. These quantities depend on the change in the refractive index and the angle of incidents (Pedrotti et al. 1987). For the model used in this thesis we need to consider the intensity of light refrected by a thin layer of refractive index n_l, placed between two materials with refractive index n_b and n_s. In particular, in our case, the substances can be: the buffer solution ($n_s = 1{,}332$), the thin layer of biological molecules ($n_l = 1{,}44$ – Voros et al. 2004) and the bulk (the perfluorinated material $n_b = 1{,}327$). In the case of normal incidence the intensity (I/I_0) of reflected light is given by:

$$\frac{I}{I_0} = \frac{{n_l}^2\,(n_b - n_s)^2\ cos(k\,d)^2\ +\ (n_b\,n_s - {n_l}^2)^2\ sin(k\,d)^2}{{n_l}^2\,(n_b + n_s)^2\ cos(k\,d)^2\ +\ (n_b\,n_s + {n_l}^2)^2\ sin(k\,d)^2} \qquad [4.2]$$

Where d is the thickness of the the layer, $k = 2\pi\,n_l/\lambda$ and λ is wavelength of light. With 4.2 equation, we can describe the reflection (the signal) obtained with our technique and this provides a measure of the thickness of the thin layer. Figure 4.2 reports the values of I/I_0 as a function of the thin layer thickness computed with equation 4.2 using the refractive index values defined above.

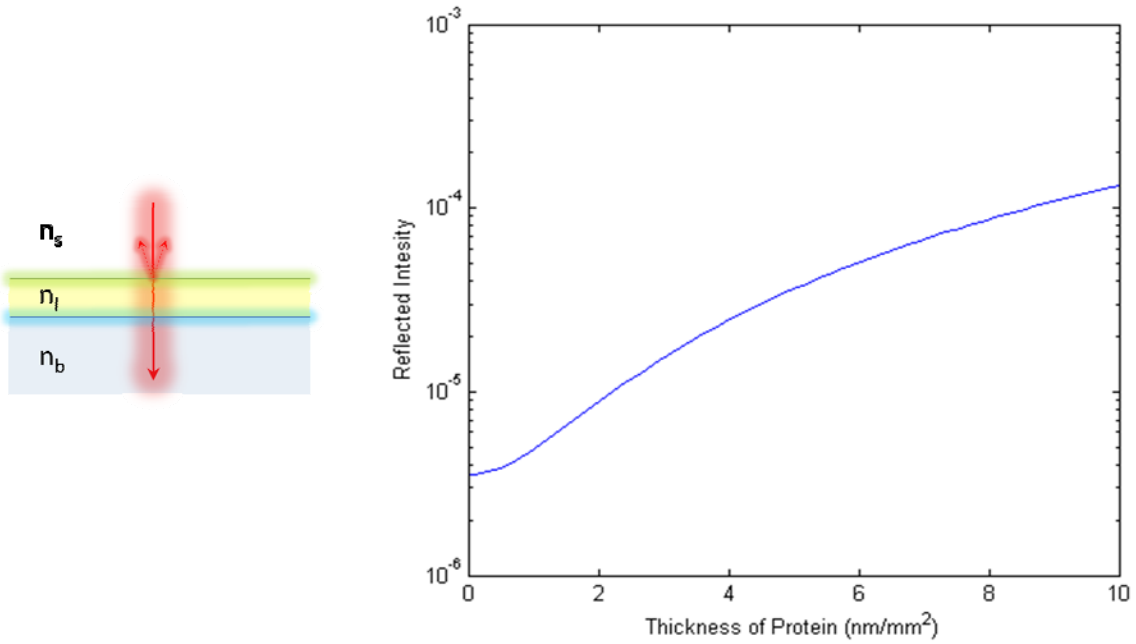

Figure 4.2 the Fresnel laws in our system

4.1.2 The perfluorinated material

In our biosensor we use a plastic surface with the refractive index close to that of water. It means that the reflection of the plastic interface and water is very low. A low signal allows to detect the formation of thin film, for example the formation of a protein layer. The plastic used is called Hyflon AD.

Hyflon AD is a family of amorphous perfluoropolymers which resemble semicrystalline materials in their performance properties. These materials are obtained from copolymers of TFE (tetrafluoroethylene) and 2,2,4-trifluoro-5 trifluoromethoxy-1,3 dioxole. This plastic is made by Solvay Solexis (Bollate, Italy).

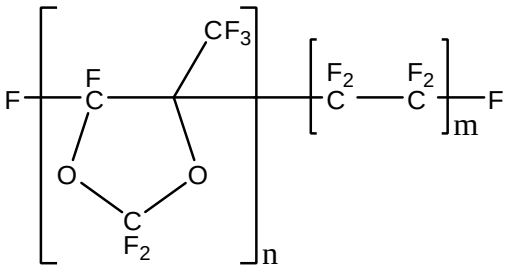

Figure 4.3 The chemical structure of Hyflon AD: poly[tetrafluoroethylene-co-(2,2,4-trifluoro-5-trifluoromethoxy-1,3-dioxole)]

The characteristics of this material family are: high temperature stability, good chemical resistance, high hydrophobicity, low dielectric constant and peculiar optical properties (i.e. high transmittance, low refractive index). The index of refraction of Hyflon AD is very close to that of water: 1,326 ± 0,003 (water: 1,333 @ 20°). This provides a very low reflectivity of the interface water/Hyflon AD.

We have tested the chemical resistance of the Hyflon AD by immersing a piece of this material into: 2 M sulfuric acid, 2 M sodium hydroxide, acetone, ethanol and other aggressive substances for one week without reporting any particular effect. The only classes of substance able to dissolve the Hyflon AD are the fluorinated solvents like Galden® (Solvay Solexis, Bollate, Italy).

When Hyflon AD is immerged in an aqueous solution there is a significant presence of negative charges. An explication for the presence of the negative charges is the residual presence of a carboxyl group made in polymerization process, notwithstanding the number and the density of the charges are not totally compatible with this theory.

There are many theories to explain the presence of negative charges on hydrophobic surfaces. Konstantin et al. (2007) reports an *ab initio* molecular dynamics simulations of hydroxide (OH^-) and hydronium (H_3O^+) ions near a hydrophobic interface, indicating that both ions behave like amphiphilic surfactants that stick to a hydrophobic hydrocarbon surface with their "hydrophobic side": this is due to the asymmetry of the molecular charge distribution: in other words, the ions can be almost compared to an amphiphilic particle. In the model, the hydroxide ions stay more time on a hydrophobic surface than the regular water molecules or the hydronium ions. This phenomenon produce a higher negative charge presence (figure 4.4).

Proteins and other biological molecules have a low adhesion to the surfaces made of fluoropolymers. Obviously, the presence of negative charges can influence the adsorption phenomena. Particularly in controlled condition, Avidin (a positive charged protein) spontaneously adsorb on a Hyflon AD, thus allowing a general strategy for immobilization of biotin-labeled receptors.

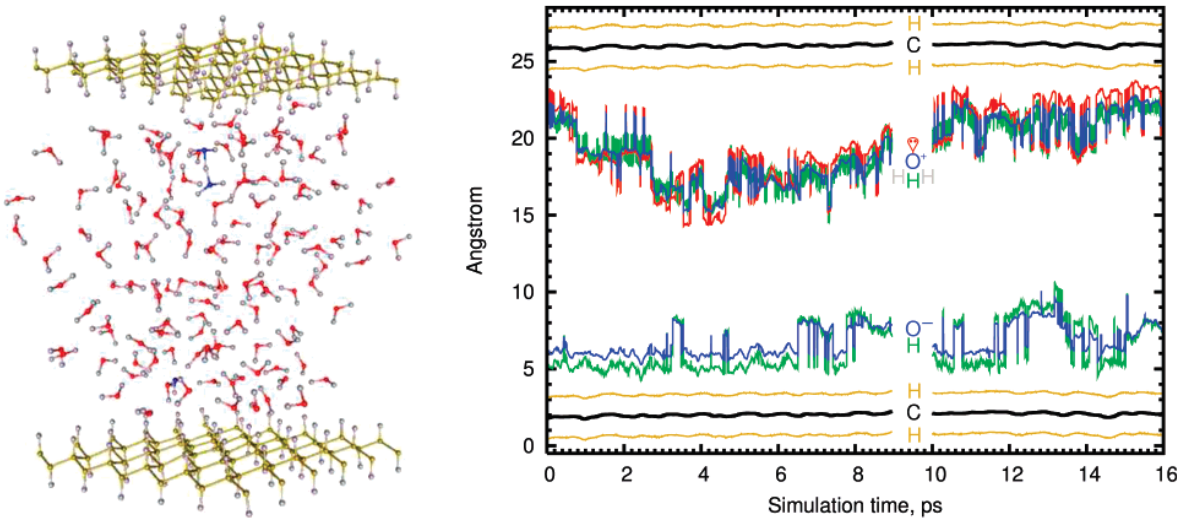

(a) (b)

Figure 4.4 (a) System layout from a snapshot of the simulation. The three-dimensional periodic simulation cell contains 127 water molecules, 1 hydronium H+, 1 hydroxide OH-, and 1 fully hydrogenated graphene sheet (72 C and 72 H atoms). (b)Simulation time evolution (blue line) of the vertical position of the hydroxide oxygen and of the hydronium oxygen The hydroxide is in the lower part of the figure; the hydronium is in the upper part. Specifically, the positions of the hydroxide hydrogen and of the most distant hydrogen covalently bonded to OH+ are shown in green. The instantaneous center of mass of the carbons is shown in black, and the instantaneous centers of mass of the hydrogens on the two opposite sides of the graphene sheet are shown in brown.

4.2 Single Reflection Biosensor

The first generation of biosensor based on Hyflon AD is based on a measure of the reflection of a single surface. This prototype has been created test the real potentiality of our methods. The purpose is to study the molecular interactions between a protein adsorbed on a water-Hyflon AD interface and its molecular partner in solution.

4.2.1 Experimental set-up

An outline of the first biosensor realized in this thesis is shown in figure 4.5. The prototype has three fundamental components: the optical system (light source, lenses and reflection detector); the fluidic system (motorized pump, syringe, and waste); the measure cell.

The experiment is carried out with a Laser. the light produced is spatially coherent, which means that the beam either is emitted in a narrow and low-divergence or can be converted into it with the help of optical components such as lenses. Light intensity measures are performed with a 50 mW HeNe

LASER (LASOS, Jena, Germany) which generates a frequency-stabilized beam with a diameter of about 2 mm, and wavelength of 632,8 nm. The interface between the water sample and the Hyflon surface generates a low intensity signal, which is collected by a photodiode (a device capable of converting light to current/voltage signal) (Thorlabs inc., Munich, Germany). Few lenses Are used for the focalization on the photodiode and stabilization of the low intensity signal reflected from the active surface.

The buffers are injected into the cell by a motorized commercial syringe pump (Kent Scientific Genie, Torrington, UK) from a glass syringes with various volumes: from 0,5 to 5 ml (Hamilton, Bonaduz, Switzerland and SGE Ringwood, Australia). By pushing the glass syringe with a worm screw, this system allows a continuous flow without pressure variations. The flow rate used in the experiments vary from 1 to 25 µl/min.

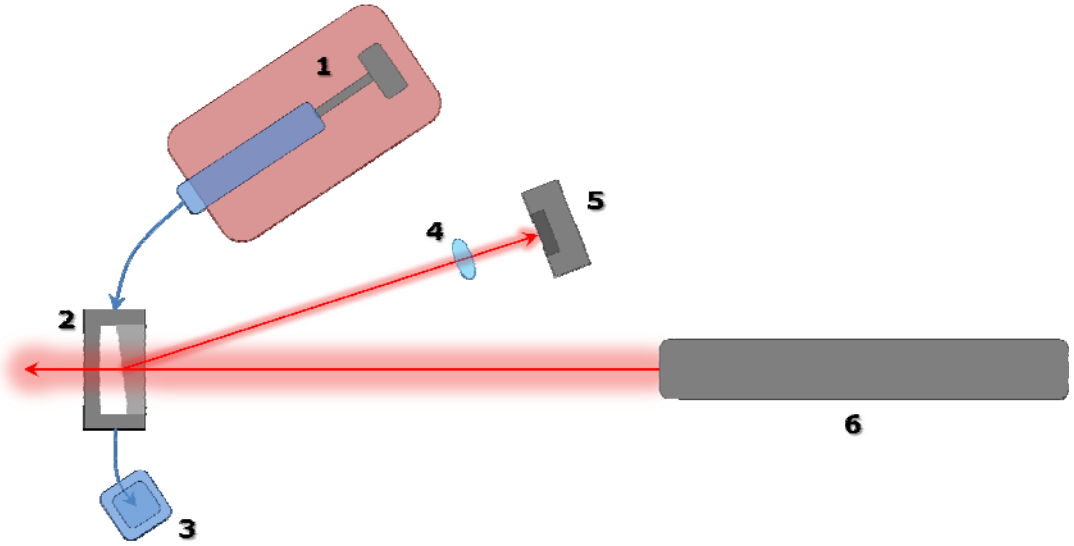

Figure 4.5 The biosensor version 1.0. The components are: motorized syringe pump (1) flow cell (2) waste for analyzed buffer (3) lens (4) photodiode (5) Laser (6)

A software has been developed to control the flow rate and to analyze the data generated from the photodiode. This program works on normal personal computers and it is made with LabVIEW 8.2 (National Instruments Corporation, Austin, USA - figure 4.6). LabVIEW is a functional programming environment used to develop graphical interface for instrument and control systems using intuitive icons and wires that resemble a flowchart. LabVIEW offers integration with all components of hardware devices present in this prototype and in the successive biosensor versions.

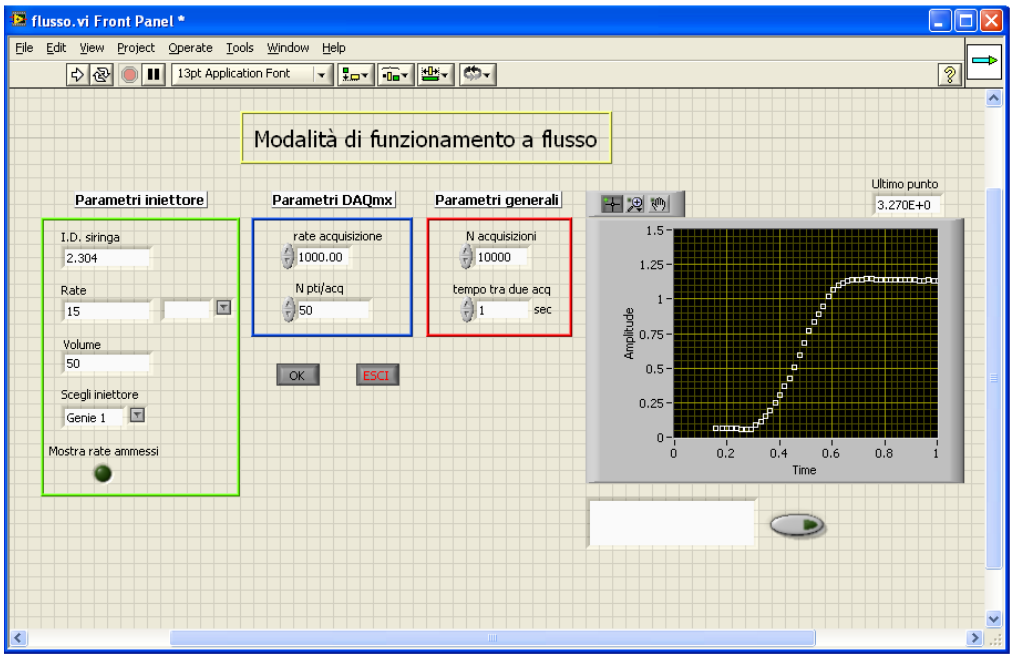

Figure 4.6 The main window of our program realized in LabVIEW 8.2

Inert materials for biosensor

All "wet-components" (syringe pumps, cell and the waste collector) are connected with Teflon and PEEK (polyetheretherketone) tubing (VICI Valco Instrument Inc.) with an outer diameter of 1/8 of inch (1,6 mm) and an inner diameters of 1/16, 1/24 and 1/32 of inch. All tubing are connected with ferrule and nut system made of PEEK (VICI Valco Instrument Inc.) In order to work at controlled concentration of sample, it is fundamental that the analytes do not interact with the tubing: the material used are notoriously inert. This material must resist during the physical chemical analysis procedures, such as the treatment for the surface regeneration. I want to introduce two particular polymers (Teflon and PEEK) used on our biosensors prototype to assemble the biosensor components. This tubing is used for all version prototypes.

Polytetrafluoroethylene (PTFE) is a synthetic fluoropolymer of tetrafluoroethylene which finds numerous applications. PTFE is most well known as the DuPont Teflon (http://www.dupont.com/brand).

Industrial products made with Teflon fluoropolymer resins have exceptional resistance to high temperatures, chemical reactions, corrosion, and stress-cracking. The properties of Teflon make it the preferred plastic for a host of industrial applications and different processing techniques.

Teflon can be tailored to have narrow solubility in selected perfluoroinated solvents but remains chemically resistant to all common solvents and chemical processes. Since the family of Teflon are fluoropolymers, the adhesion of substrates on them may be limited. Of course, the considerations about the surface charge are the same as Hyflon AD (section 4.1.2). The interface between water and PTFE in some conditions can be negatively charged.

Many of today pharmaceutical and biopharmaceutical manufacturing facilities must be flexible to produce multiple products while meeting both traditional and growing needs for product purity, wash ability, durability and low maintenance costs. Biacore and the other biosensor companies use Teflon tubing.

PEEK is an abbreviation for polyetheretherketone. PEEK offers chemical resistance and it can be used continuously to 250°C and in hot water or steam without permanent loss in physical properties. For hostile environments, PEEK is a high strength alternative to fluoropolymers. PEEK exhibits excellent resistance to a wide range of organic and inorganic chemicals. The only solvents which will attack PEEK are concentrated nitric acid and sulphuric acids. The biocompatibility of PEEK polymer has been tested (http://www.fda.gov).

Many companies use the PEEK or Teflon for the components in contact to the biosensor solution.

Six-way valve

A sample injection valve has been added to facilitate the loading of samples. This valve is derived from a six-way valve (VICI Valco Instrument Inc.) (Figure 4.7), which is in use in the majority of HPLC devices. This system comprises a stator with inlets for the sample (position 1) and the buffer flow coming from the motorized pumps (position 4), outlets leading to the cell (position 5) and to a waste collector (position 2), as well as connections for both ends of a sample loop (positions 3 and 6). Its rotor has the customary connection channels. An additional washing liquid inlet opens into the connecting channel that, in valve position A, connects the sample inlet to the outlet leading to the waste collector. With the valve in Position A, sample flows through the external loop while the buffer flows directly through to the cell. When the

valve is switched to Position B, the sample contained in the sample loop is injected onto the cell. This enables the sample inlet and the pipette or syringe located therein to be rinsed. All "wet" components (rotor, stator and loop) are made in PEEK to be protected from the chemical aggressions of buffers or wash substance.

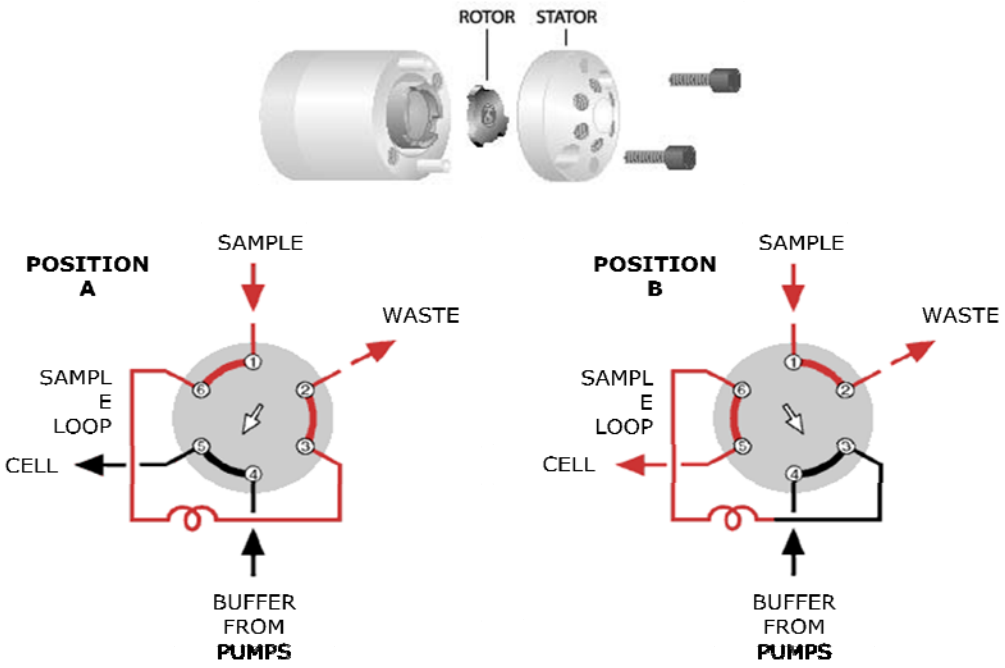

Figure 4.7 The 6-way valve used to inject the sample

The loop used in this work has a volume from 10 to 500 µL; this parameter determines the quantity of sample injected. The injection is performed by using a glass syringe (Hamilton inc, Australia) with the appropriate capacity.
To facilitate the regeneration procedure a three-way has been introduced between the motorized pumps and the six-way valve; it allows to switch off the buffer flow and to insert the syringes for the regeneration protocols without bubbles.

4.2.2 Plexiglas flow cell

The most important component of our sensor is the measure chamber, also called the "cell", where the analytes are adsorbed on the Hyflon AD surface generating the reflection signal. The realization of the first cell prototype (figure 4.8) has been the result of a complex study: and many trial cell have been tested.

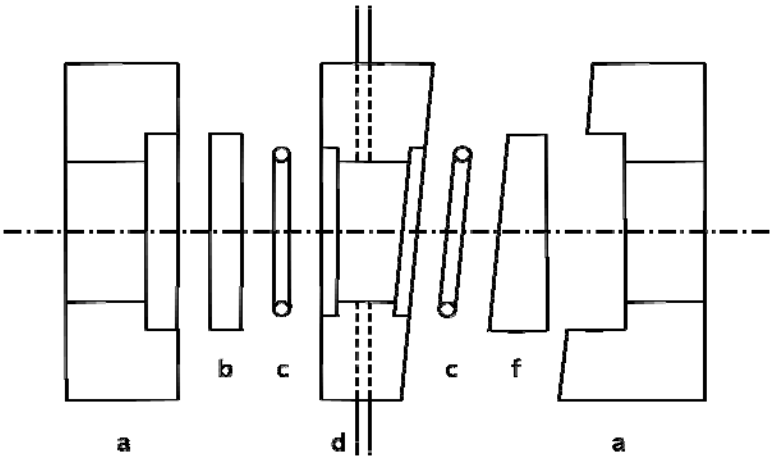

Figure 4.8 The cross-section of the cell (not in scale). The components are: (a) the Plexiglas external support; (b) the inner chamber cover made in glass; (c) the gasket made with silicon O-rings (d) the inner support made in Plexiglas with, substituted with silicon resins in the biosensor successive version there are the injection and quit tubes (f) The wedge Hyflon prism

We measure a low reflection signal, that allows to detect a low increment of signal. Since, we can detect a low level of adsorbed analytes, our device has a high sensitivity. This is an important feature of our methods.

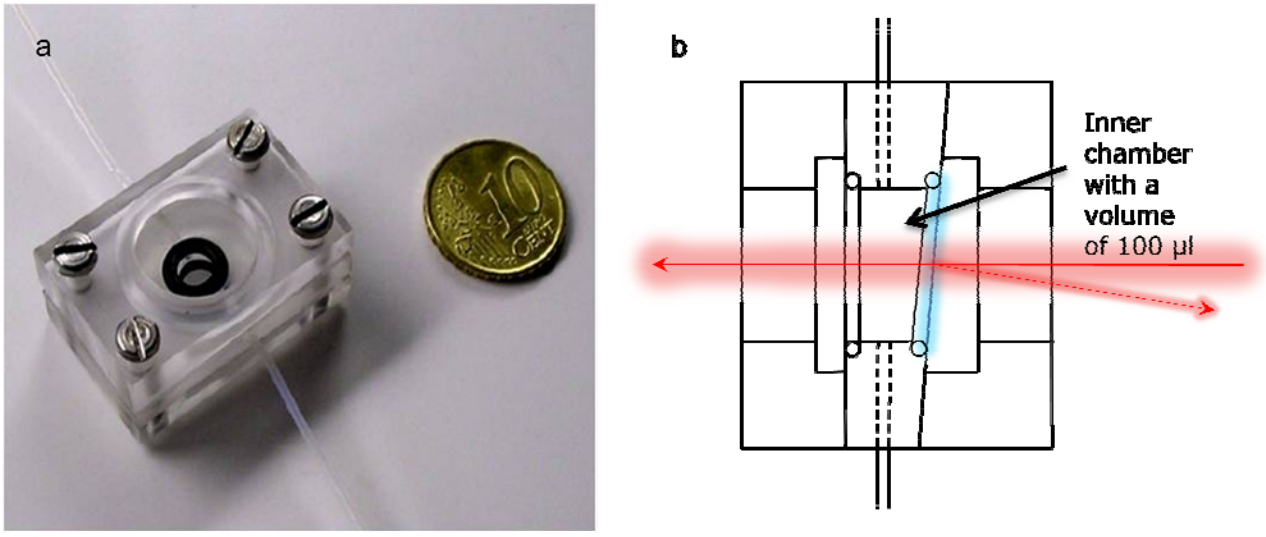

Figure 4.9 (a) A schematic picture of the assembled cell. The interface between buffer and Hyflon AD is displayed in sky blue. The laser light and the reflected beam are in red. (b) A photo of the flow cell of the biosensor 1.0

Of course, it is essential to discriminate between the reflection of the signal and the reflection of the external faces of the cell (that is interface air/Hyflon). In order to facilitate this operation, the interface between the buffer and Hyflon AD must be tilted relative to the other interface. Therefore, the signal

beam will be orientated in a distinctive direction: as shown in figure 4.9b, the interface colored in blue is the only one tilted and it generates a unique reflection. This complicates the construction of the cell but simplifies the optic set-up and avoids interference problems (figure 4.9b). The tilt of the buffer-Hyflon AD interface is 5°. This determinates an angle of 10° between the incident and the reflected beam.

In this prototype, the materials used for the inner chamber are Plexiglas, glass, Hyflon AD and two gaskets made with silicon O-rings (mechanical seals in the shape of a torus) (figure 4.9a). The volume of the inner chamber is about 100 µl.

4.2.3 Surface functionalization and biotinylated receptors immobilization

The surface is the fundamental component of all systems, including our biosensors. Receptors must be attached to some form of solid support to transduce a binding event to the sensor. During this process, receptors must retain their native conformation and binding activity, and the attachment to the sensor must be stable over the course of the assay.

The particular index of refraction (the same as water) is not the only feature of the perfluoropolymers used for the this biosensor, since the possibility to efficiently adsorb biomolecules is also very important. When Hyflon is dipped into the water it acquires negative charges (section 4.1.2) while, as shown in the previous section, the AVD is positive charged (section 3.2). Therefore, we will demonstrate that the surface can be spontaneously coated with a monomolecular layer of functional AVD thus allowing a general strategy for immobilization of biotin-labeled receptors.

In general, we can inject 50 µl of 3 µM AVD solution (it is resuspended from a lyophilized powder purchased from Sigma-Aldrich) with a pumping rate of 20 µl/minute (volume, concentration and flow can be changed for different set-ups or protocols). By monitoring the reflection in few minutes the signal growths and achieves a steady state. Successive injections of AVD solution do not generate any increase of the reflectivity which can be explained with the formation of a molecular mono-layer. This proves the correct surface fictionalization

(figure 4.10). If we use the formula 4.2, we can obtain the mass adsorbed on the active surface: we get about $1{,}65\ ng/ml$ of AVD.

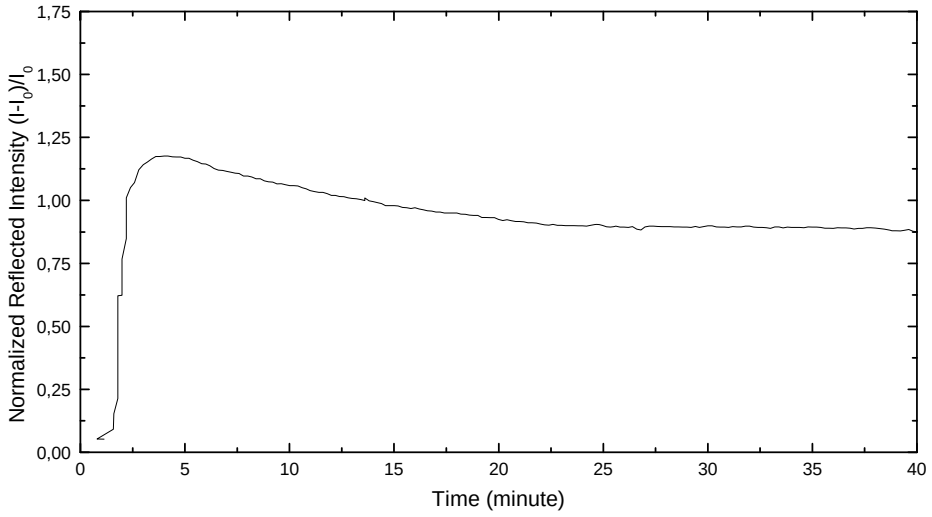

Figure 4.10 The Avidin layer formation

We can check this value. By considering the AVD diameter ($4\ nm$ - Pugliese L et. al 1993), we can assume that any single protein takes up an area of about $10{,}4\ nm$. Then, in a square millimeter, we can suppose to have $9{,}62 * 10^{10}$ molecules, corresponding to $2{,}43\ ng$. This vale is very close to our calculation.

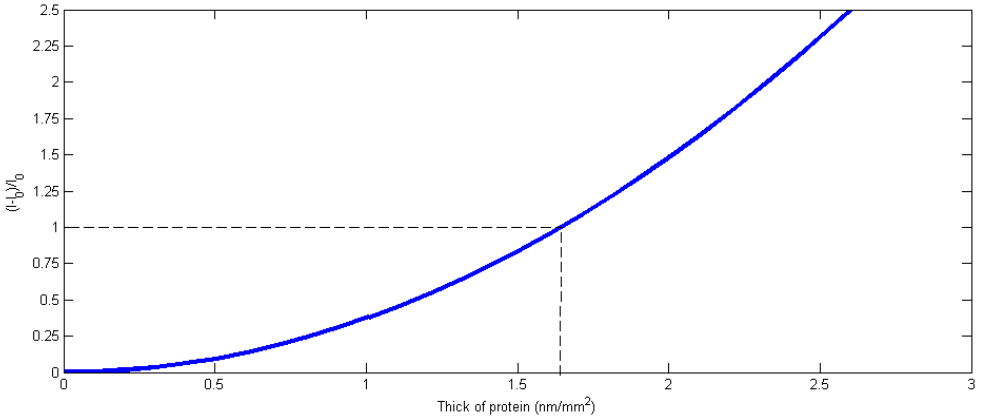

Figure 4.11 The conversion between our signal (the intensity) and the mass absorbed on the surface

To study the ligand-receptor interactions, it is necessary to prepare a second layer of biomolecules. Our "gold standard" to test the surface functionalization is the biotinylated BSA (bBSA) (Albumin, Bovine-biotin Labeled - Sigma Aldrich).

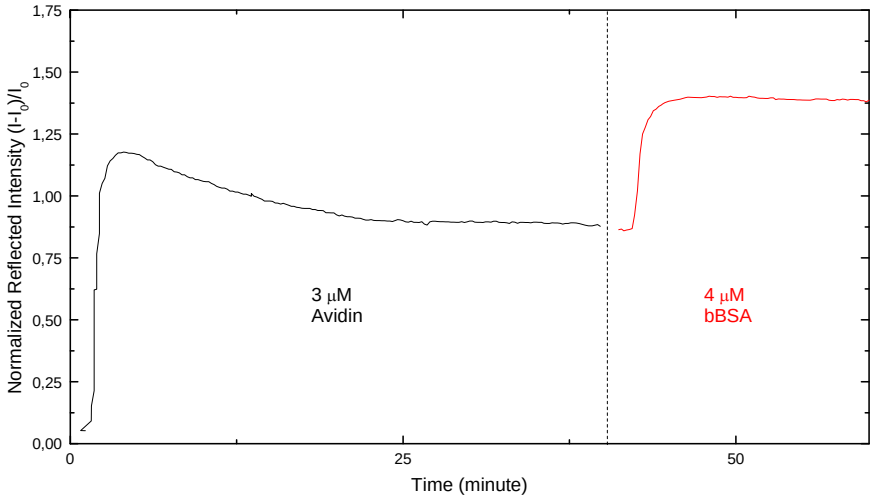

Figure 4.12 A plot of the interaction between an AVD surface and a biotinylated protein: the BSA. This data are obtained by using the six-way valve.

The figure 4.12 shows a test experiment. After the formation of a mono-layer of AVD (as previously describe), we inject the biotinylated protein. In general, it is helpful to use the six-way valve to avoid the entering of a bubble of air. We use a bBSA concentration of 4 μM and a loop volume of about 50 μl.

The behavior of bBSA is similar to the AVD: the biotinylated protein forms a single molecular layer on the AVD. The thickness is another time consistent with the absorbed mass.

Surface regeneration test

Many biosensor technologies do not allow a complete regeneration of the surface. For example, some chips made by SPR constructor permit to reuse the functionalizated surface about 5-10 times, but it is impossible to remove the immobilized substrate (like the surface receptors) and restart a functionalization procedure without impairing the surface. Regeneration conditions often depend on ligand density, and there is no guarantee that regeneration conditions optimized for one specific ligand density are valid if the ligand density is drastically changed. Otherwise, in our method the process of protein adsorption on the Hyflon AD allows a simple, "on line" and complete surface regeneration.

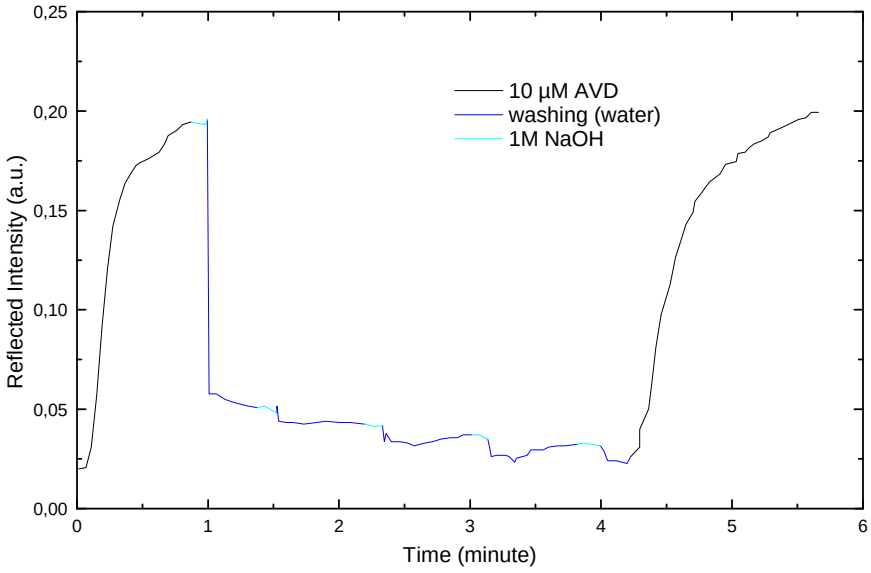

Figure 4.13 The initial washing protocol

The first strategy used is to flux 1 M sodium hydroxide for few hours (figure 4.13). The idea consists in washing the surface with the positive cations (Na^+) which compete with the proteins for the Hyflon AD negative charges; this process is similar to the chromatography elution. This procedure shows only a partial effectiveness without a true reproducibility and it requires a lot time. In many cases it is necessary to immerge the Hyflon AD surfaces in a solution of 1M NaOH overnight. This means to disassemble the cell, which is a long and complicated process. Organic solvents, like acetone, speed up the regeneration process. However the Plexiglas frame of the cell does not allow treatments with this kind of solvents. Therefore a new cell design is required.

4.2.4 Silicone flow cell

The Plexiglas flow cell has been used to test the basic of methods. However it shows some problem. The first problem is the flow cell volume: a large chamber (100 µl) needs a lot of sample and a single flow measure needs too much volume to reach the requisite concentration. The second problem is the materials used: they don't allow to flow the aggressive substances required for the regeneration of the active surface (the regeneration and washing processes are described in the next section). In order to improve the

precedent version, the intermediate frame of plexiglas (figure 4.9) is replaced with a support in silicone made up with a stamp: this design allows acetone washing and facilitates the construction of a smaller cell.

Silicone resins (Sylgard 184, Dow Corning Corp) are generally used to make microfluidic chips (S. R. Quake, et al 2000). This polymer poly-tetra (trimethylsiloxy)silane is resistant to most acid/basic or organic solutions. It is supplied in two parts: a base and a curing agent that are mixed in a ratio of 10:1 by weight. If air bubbles are still present, vacuum degassing may be required. When liquid components are thoroughly mixed, the mixture cures to a flexible elastomer.

We use Sylgard 184 to produce a wedge gasket with the connection tubes in a mold process. The inner chamber is made up by punching a silicone wedge. The O-rings has been eliminated. The cell volume obtained with this procedure is about 25 µl. (figure 4.12). This cell has been used to standardize the regeneration procedure.

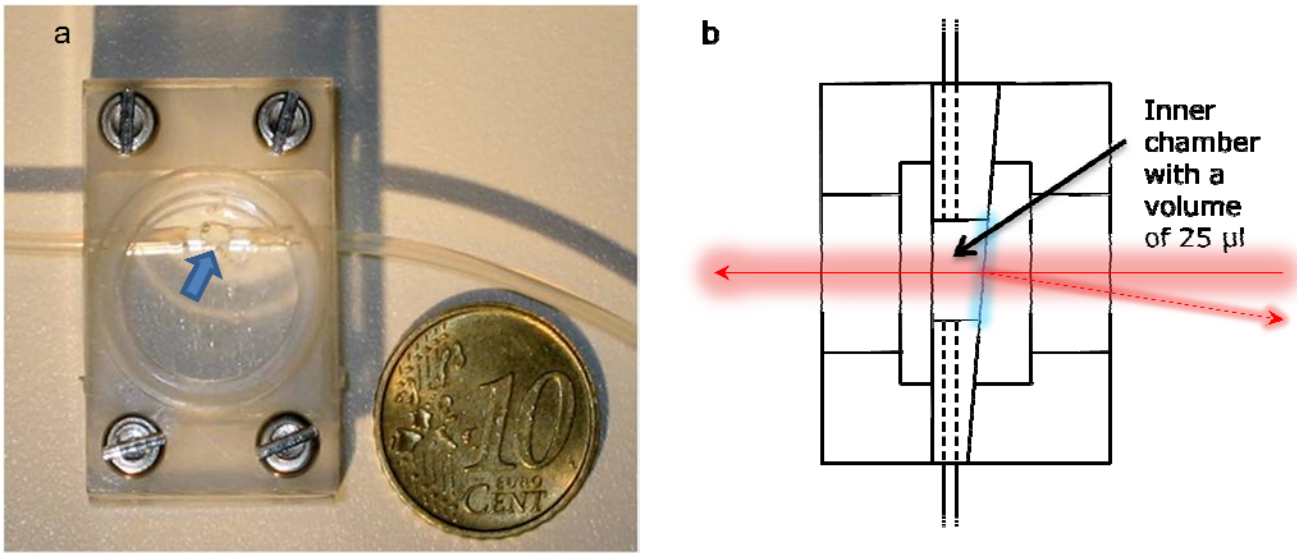

figure 4.12 (a) The cell made in Sylgard 184: the inner chamber is marked with an arrow (b) the schematic representation of the "chemical proof" cell with a small volume.

A second version of this cell has been created with a smaller volume (10 µl – Figure 4.13). The most part of experiment present in the result section, has been performed with this "small" cell.

Figure 4.13 The cell on the set-up of the single spot biosensor

4.2.5 Regeneration procedure

The AVD binding is a non covalent interaction, nevertheless the bonds are very strong. The presence of many negative charges and the typical hydrophobicity of Hyflon AD cause a strong interaction with the positive charges and the glucide residues of the proteins. The first experiments and the limitations of the regeneration protocol are described in the section 4.2.3, where we observed that the simple "chromatography-like eluition" procedure, the washing with organic solvent or the treatments with various detergent (for example SDS or tween) do not achieve the complete surface regeneration.

Thus, we tried other procedures, such as the use of Sodium hypochlorite (NaOCl), the active ingredient in household bleach. Despite its widespread utilization, little is known about its mode of action. It causes oxidation of protein and irreversible unfolding. Hypochlorous acid reacts readily with amino acids that have amino group side-chains, with the chlorine from HClO displacing a hydrogen, resulting in an organic chloramine. Chlorinated amino acids rapidly decompose, but protein chloramines are longer-lived and retain some oxidative capacity. The HClO mechanism of sulfhydryl oxidation is disimilar to that of chloramine, because, once the residual chlorine is dissipated, some sulfhydryl function can be restored. The degradation of NaClO generates NaOH and NaCl.

The oxidation and the unfolding effect on proteins, together with the presence of sodium hydroxide, make the household bleach a possible candidate for the Hyflon surface regeneration. The tests confirm this thesis: the complete effect can be reached in 10-20 minutes and the procedure proves to be repeatable. The protocol used for the regeneration is the following:

- Inject the sodium hypochlorite 4 % solution for 5 minutes
- Inject the EtOH solution for 5 minutes
- Measure the signal with the initial buffer
- If the signal is not restored repeat point 1-2

Sometimes it is necessary to wash the sensor with acetone to remove the impurity of ethanol. Furthermore, we observe that the efficiency of regeneration after a second injection with sodium hypochlorite is equal to 100%. An important note: hypochlorite and acetone must not be mixed because they form an insoluble and toxic precipitate.

4.2.6 Transport limitations

The single reflection biosensor cell made with the silicone frame, demonstrated the correct working of the basic principle of our method. However, this cell, consisting of two cylindrical crisscrossed tubes (figure 4.14), and does not allow to perform experiments with a controlled concentration since the shape of the cell does not allow a correct flow. The sample injected reaches the surface not for hydrodynamic addressing but for diffusion, and this phenomenon is influenced by gravity. A simple experiment proves this theory. By flipping the cell we measure a differ kinetics of the protein absorption. When the Hyflon surface is on the lower part the rate observed is faster. We need to design a new flow cell to allow a concentration measures.

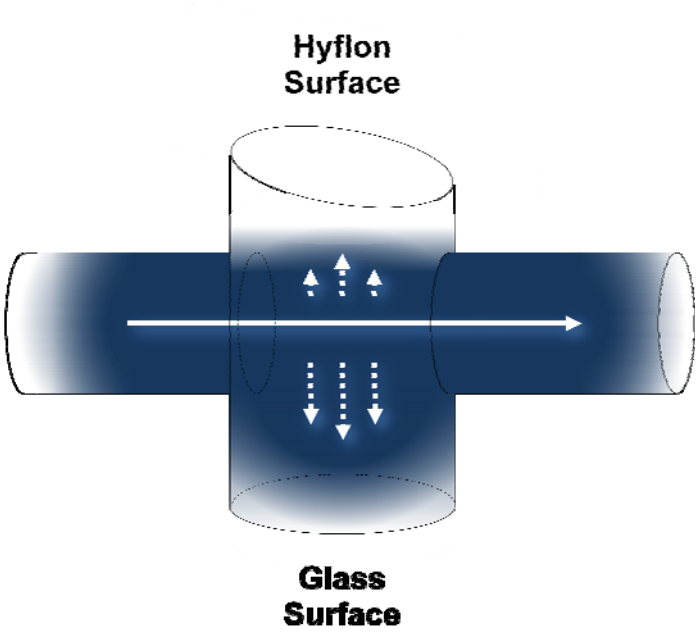

Figure 4.14 A simplify version of the fluidic in the inner cell of the single reflection biosensor, the sample injected (in blue) reaches the surface not for hydrodynamic addressing but for diffusion

4.3 Double Reflection Biosensor

4.3.1 Instrument Description

The fundamental change of this sensor is the cell. We use two complementary wedges in Hyflon AD. One of them has two holes to insert the Teflon tube (figure 4.16c). Between the two wedges, we have inserted a home-made gasket in silicone rubber (Tecnoloflon) with a rectangular channel. This gasket-channel is the "wall" of the measure chamber with the "active" Hyflon AD surfaces on the bottom and on the top (figure 4.16). The buffer with the sample comes into the cell by the Teflon tube; it flows through the two Hyflon AD surfaces and goes out by the other Teflon tube. This process happens without stagnation and it reduces the sample diffusion problems. We can control the cell volume by regulating the height of the gasket. This considerably improves the possibility to have a smaller cell.

The instrument has two propulsion buffers. The first one is 10 mM phosphate buffer (pH 6.5-8) which allows a correct AVD functionalization. After 15-20 minutes, we introduce into the cell a solution of 150 mM NaCl and 10 mM buffer phosphate (pH 6.5-8). The change of buffer is performed by loading the first solution with a manual syringe and pumping the second buffer with the motorized syringe pump.The acquisition system is a photodiode and the angle of acquisition is near to 60° (figure 4.15).

A second copy of set-up has been created on a semi-portable breadboard and has a final dimension of 30 x 60 x 25 cm (figure 4.17). The volume of the cell is 25 µl (figure 4.18). This prototype is commissioned from the Solvay-Solexis Pharma division, our partner in this project.

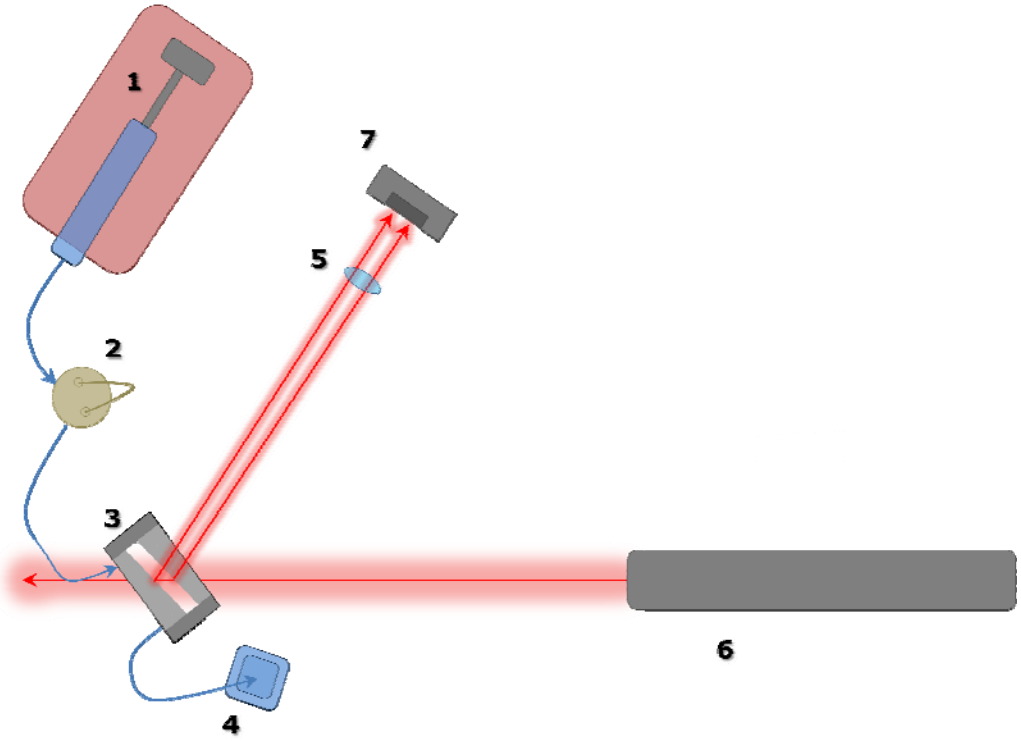

Figure 4.15 The double reflection biosensor. The principal components are: commercial motorized syringe pump (1) six-way valve (2) flow cell with two Hyflon AD surfaces (3) waste for analyzed buffer (4) lens to focalize the Laser baem (5) Laser (6) photodiode (7)

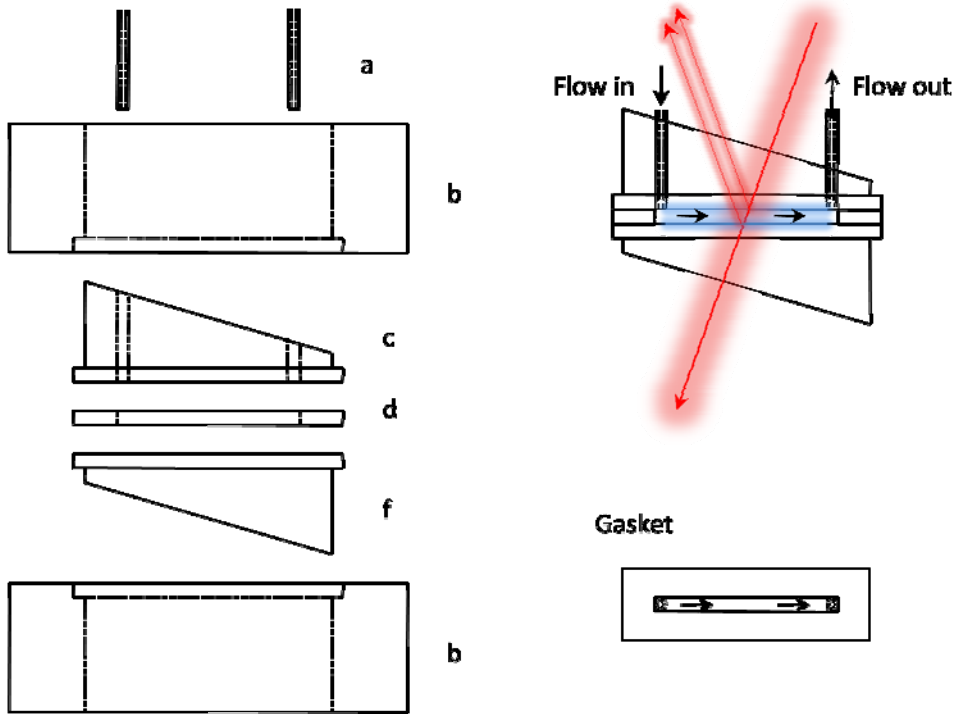

Figure 4.16 Measure cell schematic illustration (not in scale). The cell is composed of two wedges prism in Hyflon (c) and (f) The upper wedge (c) presents two bores for the tubing (a) insert.

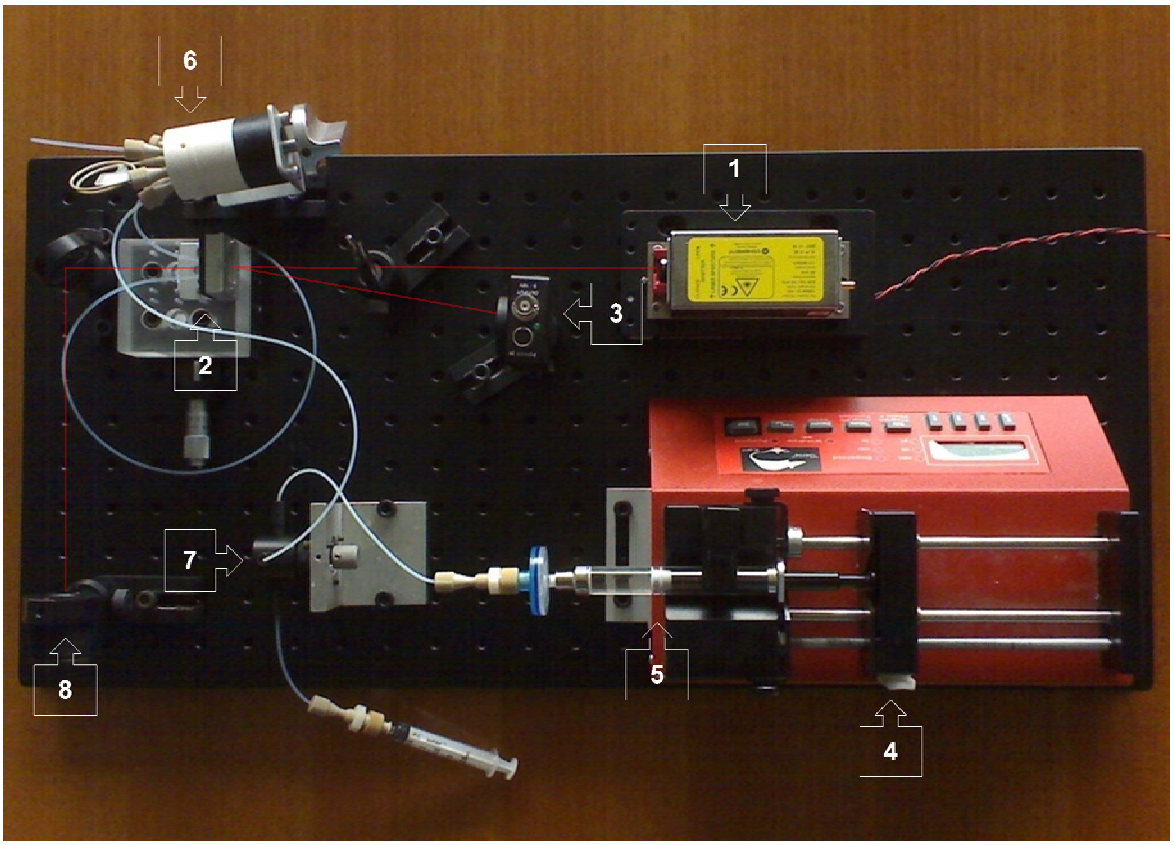

Figure 4.17 This biosensor is a low cost an transportable version, it has a final dimension of 30 x 60 x 25 cm,. The principal components are: solid state laser (1); flow cell (2); photodiode, the "low cost" detector (3); commercial motorized pump (4); buffer syringe flow cell (5); six-way valve (6); tre-way valve to facilitate the regeneration procedure (7); beam dumper (8). The red line is the laser beam artificially colored

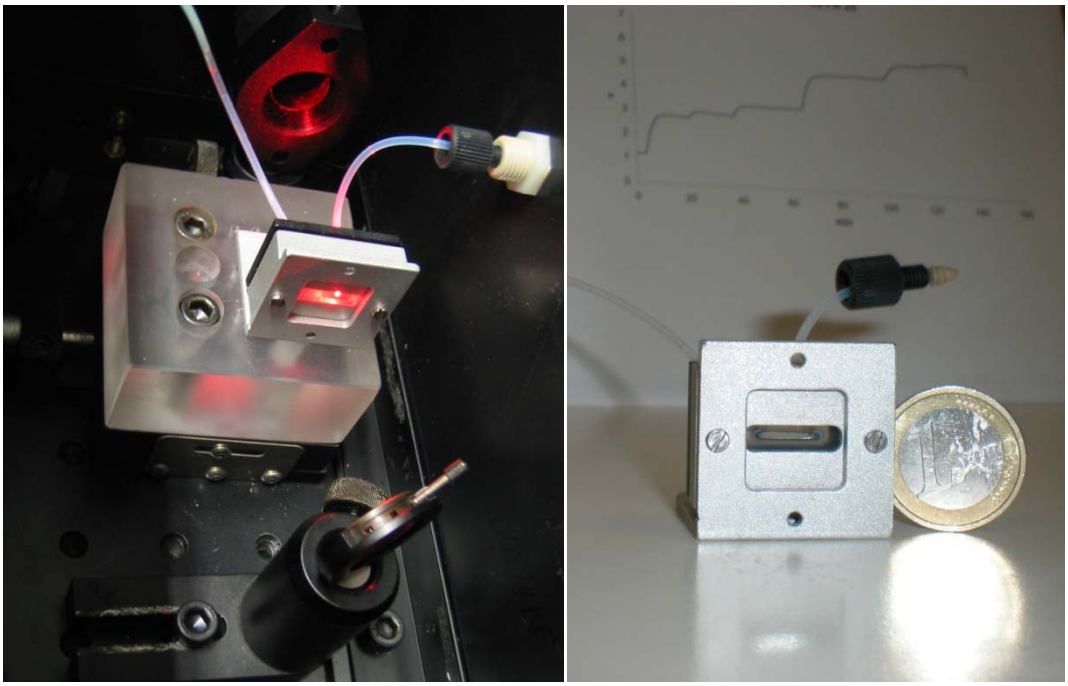

Figure 4.18 Two photos of the flow cell

With this device, we have performed some explicative concentration tests of a tumor marker (PSA). These experiments will be illustrated in the next chapter. To have a wide range of possibility for surface functionalization, we chose to employ different strategies of Hyflon AD interface treatments: we use a biotinylated anti-PSA antibody and two different antibody-binding proteins (Protein G and Protein A).
The correct biotinylation procedure is tested with the biosensor and the results will be shown in next chapter.

4.3.2 Biosensor Performance

Optical biosensors can be used to address a wide variety of applications ranging from high-precision detection of changes in biomolecular conformation, rapid measurement of the presence of a contaminant in a liquid, throughput measurement of kinetic binding constants of biomolecules. Our method has demonstrated to have the possibility to perform these tasks; now we want to compare it with the other technologies actually present to the market.
The suitability of an optical biosensor for a particular application depends upon its performance across a variety of metrics. In this section, we will define some of the methods used to compare optical biosensors.

Sensitivity and limit of detection

To understand the potentiality of our method we have the necessity to introduce the most common parameters used for the performance valuation; the following section can be applicable to the double reflection or the interferomentric biosensors.
The Sensitivity (χ) is defined as the amount of change in sensor signal (S) resulting from an unit change in mass density on the surface (σ). Therefore we can write:

$$dS = \chi \, d\sigma \qquad [4.3]$$

Often, the sensitivity is reported in terms of response per mass/area. The mass sensitivity represents characterization of the sensor structure at a basic

level that is not dependent upon the affinity between the analyte being detected and the immobilized ligand. It is independent to the assay and is a characteristic of the technique. For optical biosensors, the sensitivity is determined by how efficiently the electromagnetic waves associated with the optical transducer couples to biomolecules in contact with the sensor surface. Sensitivity is used to define the lowest value determined above zero concentration while the resolution describes the minimum resolvable difference between two measurements at any concentration.

Resolution or limit of detection (LOD) refers to the smallest change in mass density that can be measured. Resolution is an especially critical performance criteria for detection of analytes present at low concentration or detection of adsorbed molecules with low molecular weight. To determine the resolution of a sensor, one must characterize the noise of the sensor when operated with its detection instrument. Noise can be easily characterized at a basic level by allowing the sensor to reach a steady-state condition and recording the measured output many times in sequence without any intentional change to the sensor. The noise is thus defined as three times the standard deviation (3ε) of all the repeated measurements (Cooper et al. 2009); then the LOD is defined as the smallest measurable mass density change of the sensor therefore:

$$LOD = \frac{3\varepsilon}{\chi} \qquad [4.4]$$

In our technique, the optical transducer (the Hyflon AD surface) generates a very low signal and the detection is noisier if compared to the other optical label-free systems. Thus, to better appreciate the characteristic of our methods, we prefer to use the percentage variation sensitivity ($\chi_{\%}$). It can be described as:

$$\frac{dS}{S} = \chi_{\%}\, d\sigma \qquad [4.5]$$

A small variation of mass on the sensor surface in our method corresponds to an evident increment of signal: the formation of a monolayer of protein

generates a signal variation of many times. Typically, AVD (MW of 66-68 KDa) can generate a twofold or threefold increment of the reflectivity signal. SPR and other optical biosensors obtain their data from a fitting of a spectrum and interpolating the small variation. It is a efficient system (and more expensive) for the detection but the variation of $\chi_{\%}$ is very small. Then we can overcome the noisy detection with significative variation of signal and obtain a very competitive detection. The LOD can be rewritten as:

$$LOD = \frac{3\varepsilon}{\chi_{\%}} \qquad [4.6]$$

We calculate the performance of our optical transducer with a layer of AVD (our standard functionalization) and measuring for one hour (figure 4.19). We have reported a standard deviation of 0,3% from the mean value, so we can assume to detect a variation of 1% (3ε) that corresponds to a LOD of 30 pg/mm^2 whereas commercial Biacore and Genoptics instruments have a LOD of 10 pg/mm^2 (Sections 2.2). Our biosensor is only a prototype and could be further improved with a reduction of the signal noise.

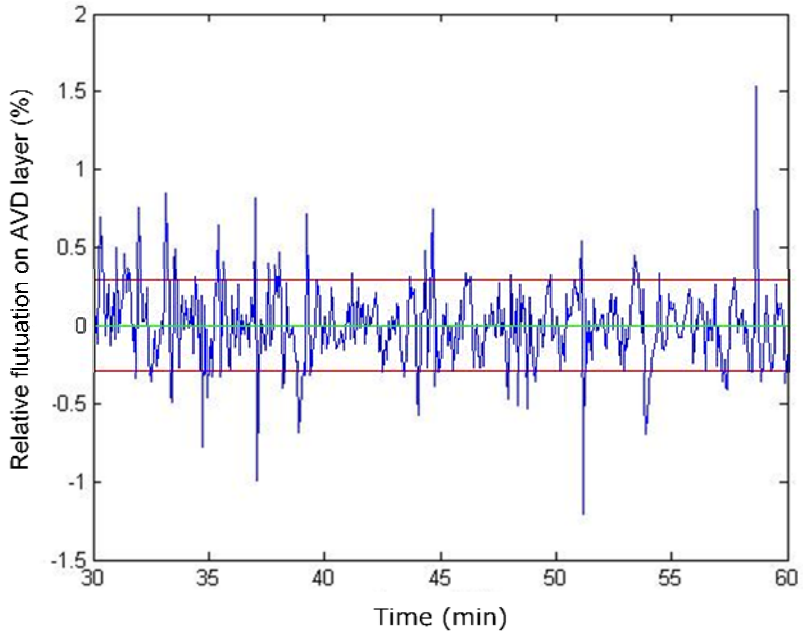

Figure 4.19 The LOD: this data are collected with a layer of AVD; the green line is the mean signal, the red lines represent the standard deviation of signal

4.3.3 The Taylor dispersion problem

This instrument has demonstrated the possibility both to have an efficient measure of concentration and, in some condition, of the kinetic constant. However, this cell design has shown some problems, illustrated in the following. The figure 4.20 illustrates the change of reflectivity caused by a sample injection of 500 µl of 0,5 M sodium chloride whose reflection index is different from that of water. Water is used as propulsion liquid. The frequency of data acquisition is increased respect to the standard experiment. Of course, the ions of the sodium chloride does not form a stable bond with the surface but its strong concentration changes the refection index of solution and it causes a temporary increment of signal: in other words, the graphic represents the real salt concentration into the cell.
We can observe that the signal has not an instantaneous increment. Moreover the fronts of entrance and exit do not present the same rate: the second is slower, because it has more time to diffuse during the flowing.

Figure 4.20 The signal obtained from a sample injection of 500 µl of 0,5 M sodium chloride

BIACore and other biosensor companies have an Integrated µ-Fluidic Cartridge (IFC). The IFC consists of a series of micro channels and membrane valves

and serves to control the delivery of liquid to the sensor chip surface. Besides, to prevent diffusion, the IFC introduces a number of air segments between buffer and sample. This air bubbles are removed near the cell. The implementation of this system in our prototype would require the use of a μ-fluidic chip.

The dispersion significantly reduces the resolution of kinetics studies performed using pressure-driven flow in the devices because the flow velocity between the center of the tubing and the wall are not the same. Although such dispersion is considered a well-understood phenomenon, nevertheless it remains difficult to quantify in practice for many configurations. This makes it difficult to define the real concentration for every shot of sample and also to quantify the real concentration in the cell. This dispersion is characteristic of flows that run smoothly and in regular paths, like a liquid into a tubing. This effect is named after the British fluid dynamicist G. I. Taylor.

When a fluid flows through a tube, a velocity profile develops. This profile is not uniform over the cross-section of the tube: at some radial positions, the fluid flows faster than at others. The laminar profile for fluids has a parabolic velocity distribution. Matter present in the fluid moves along with it and is therefore dispersed along the tube axis. Apart from this purely convective dispersion, diffusion can also be of influence.

Suppose that somewhere in the tube we have a small 'plug' of fluid with a composition different from an otherwise similar bulk of fluid (it occurs in our injection with the six-way valve). The flow of the fluid causes this plug to disperse, but it also induces radial composition gradients. This leads to diffusive fluxes at the front and back sides of the plug. This is the case when either the axial velocity is very low, or when the radial distances are very small. So, through the combined action of convection and diffusion, the plug will leave the tube as a broadened, but still more or less compact plug.

This convection-diffusion situation is known as Taylor dispersion. In many systems, concentration gradients exist and give rise to diffusion. This phenomenon is an effect of fluid mechanics in which a shear flow can increase the effective diffusivity of a species. Essentially, the shear acts to smear out the concentration distribution in the direction of the flow, enhancing the rate

at which it spreads in that direction. This effect is governed by the so-called convection-diffusion equation:

$$\frac{\partial [A]}{\partial t} = D\nabla^2 [A] - Q\nabla [A] \qquad [4.7]$$

where $[A]$ is the concentration, Q is the flow and D is a diffusion coefficient (for a medium size protein $D = 10^{-6}\, cm/s$). The two terms on the right side represent different physical processes. The first corresponds to normal diffusion (figure 4.21). The second describes convection. Through this we could assume that the profile of concentration in a tube has a parabolic and quasi-rectangular cross-section (figure 4.22) (Ajdari et al. 2006). This equation is also known as the convection–diffusion equation for the laminar flow.

Figure 4.21 The diagram represents the first term of Taylor dispersion of two fluids with a different concentration [A], in a tube with length=l and flow (φ)=0, at initial time (t=0) (on top) and after the start of the dispersion (on buttom); h is the region with a gradient of concentration.

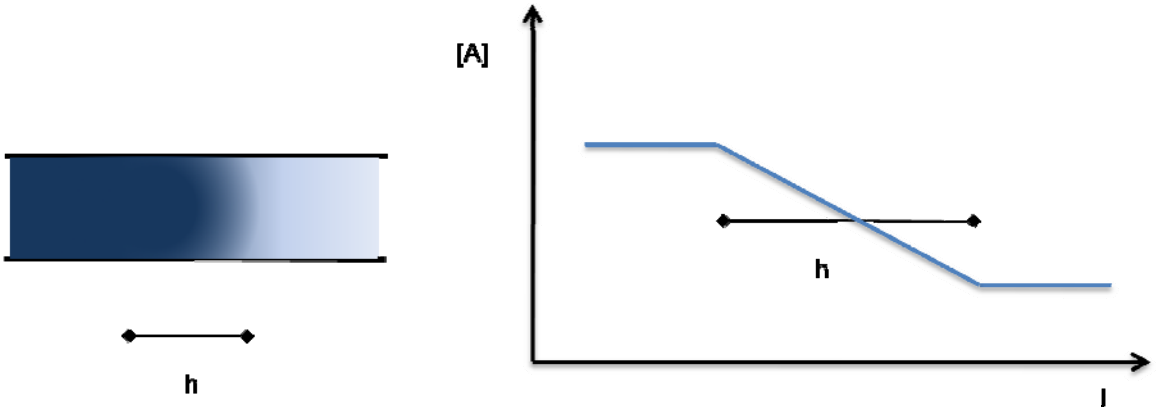

Figure 4.22 The profile concentration in a tube with φ>0: the dipersion is modifiedand improved.

The Taylor dispersion problem is especially evident in a millifluidic system, but it is also present in microfluidic system like the commercial SPR instrument even if the problem is more controlled with the IFC system. However the SensiQ instrument, made by ICx Nomadics (section 2.2.5), takes advantage of a systematic control of analytes concentration dispersion to achieve a fine gradient measure. The Taylor dispersion control allows a kinetic analysis without requiring multiple discrete injections of sample with a saving of analytes and time.

4.4 Interferometric Biosensor

We have studied an innovative system based on an interferometric technique. This method solves the problem of controlling the concentration dispersion, which represented a limitation of the previous version of the system. The figure 4.20 present a kind of modulation when the sample enter or exit the cell and this phenomenon is related to a interferometric effect generated from the reflection of two surface. To introduce the method, it is useful to explain the basic notion of the interference.

4.4.1 Interferometry

We can see the interference when two waves (for example two rays of a laser), with similar amplitudes, are combined. If we create an image of this

light we will observe a particular figure characterized by so-called fringes, a series of light bands (resulting from reinforcement) alternating with dark bands (caused by neutralization). Light wave must emanate from the same source; light from distinct sources has too many random differences to permit interference patterns. The relative positions of light and dark lines depend upon the wavelength of the light, among other factors. A very curios interference phenomenon is generate from soap film (soap bubble –figure 4.23b) or an oil film on water. It can be related to the thickness of the film by using the interference condition because there are two reflective surfaces (air-soap and soap-air). The generated interference patterns have different reinforcements or neutralizations depending on the different colors (wavelengths). The color seen depends also upon the angle of view.

The "thin layer interference" is important in thin films, in the design of anti-reflection coatings, interference filters, and thin film mirrors.

The interference is usually used in the instrument called interferometer. When the wavelength of the light is known, this device indicates the thickness or the index of refraction of the film by the interference patterns it forms. The reverse process, that is the measurement of the length of an unknown light wave, can also be carried out by the interferometer.

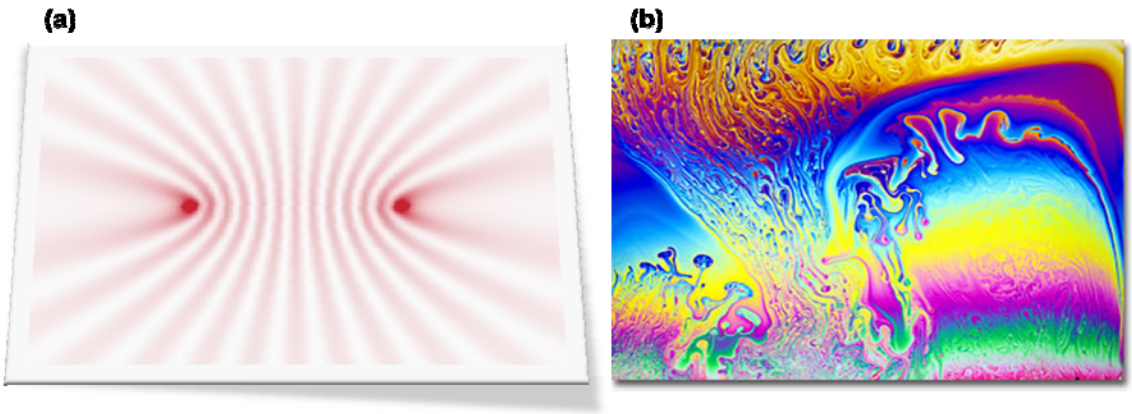

Figure 4.23 (A) An artistic interference image of two waves not in phase on a CCD camera (B) These interference colors are produced in a thin soap film established in a frame dipped in soap solution, like you would for making soap bubbles. They were made by Davidhazy Andrew .

4.4.2 Experimental set up

This version needs a CCD camera to acquire the interference images. The injection system, the light source and the buffer pump are the same as

previous versions (Figure 4.24). The structure of the cell is similar to that of the double reflection biosensor, while the active surface is larger to reduce the problems with the optical geometry (Figure 2.25).

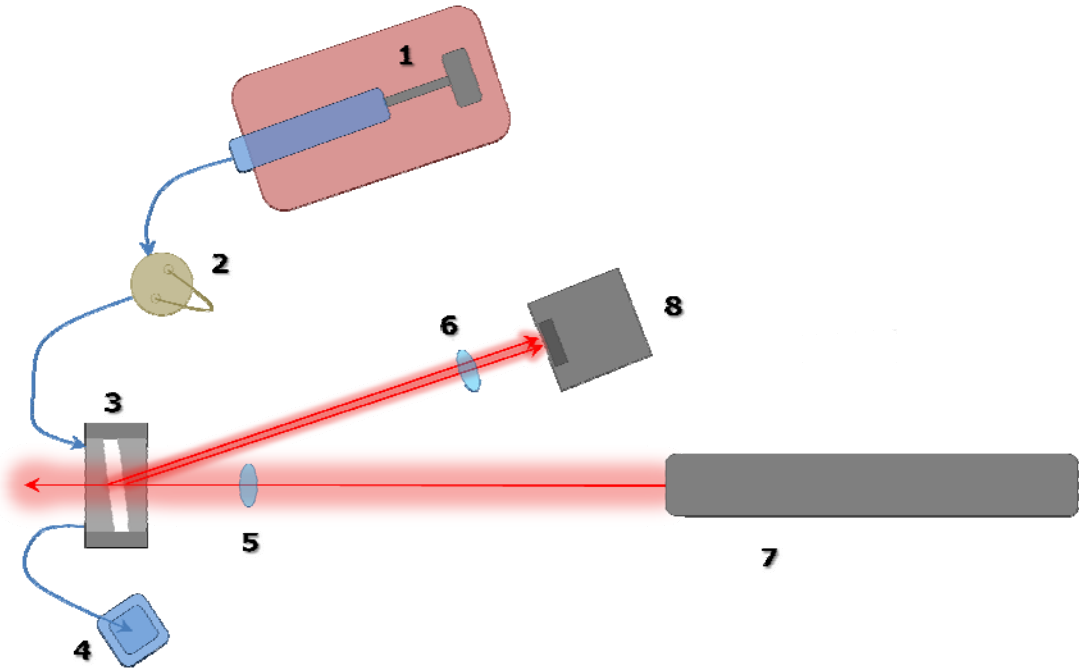

Figure 4.24 The interferometric biosensor version. The principal components are: commercial motorized syringe pump (1) six-way valve (2) flow cell with 2 Hyflon AD surface (3) waste for analyzed buffer (4) lens to focalize the Laser baem (5) lens to create the images (6) Laser (7) CCD camera (8)

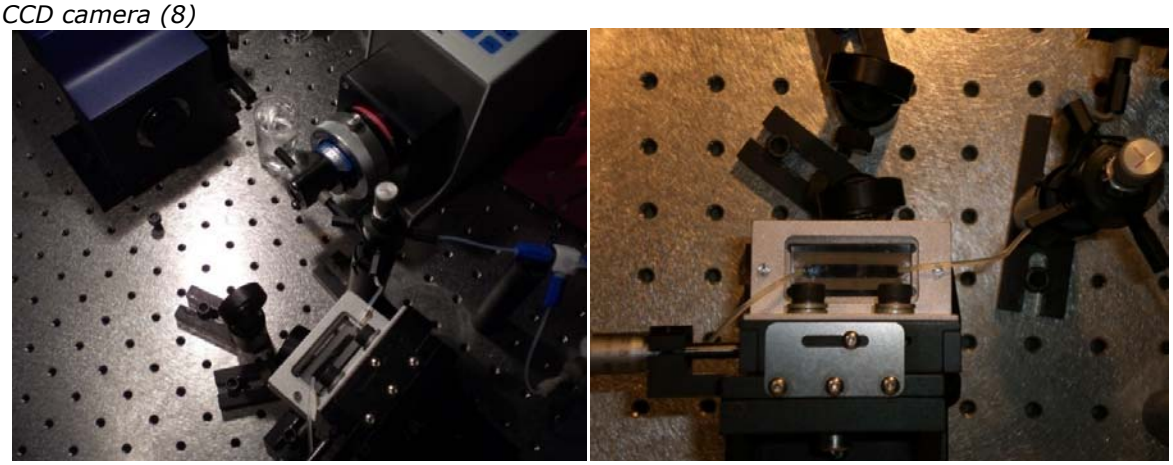

Figure 4.25 The photos of the flow cell

The Laser beam is focalizated some millimeters before the cell with a converging lens, in order to have a spread illumination. The light passes through the two "active" surfaces: Hyflon AD-sample and sample-Hyflon AD; part of the light is reflected by the interfaces. We collect the images of the two reflected beams on a CCD camera by using a second focusing lens (figure

4.23a). In a controlled condition, the figure observed is an interference pattern. An example of this image is represented in figure 4.23b. To create a good image with regular bands it is important to illuminate the cell with an incident angle distant to the normal; the inclination angle used in our set-up is near to 45°.

The external cell faces of the Hyflon AD prisms is inclined 5° to the inner faces. The interfaces air-Hyflon AD and Hyflon AD-air reflect in different directions and thus do not mix with the the interference pattern on the CCD camera.

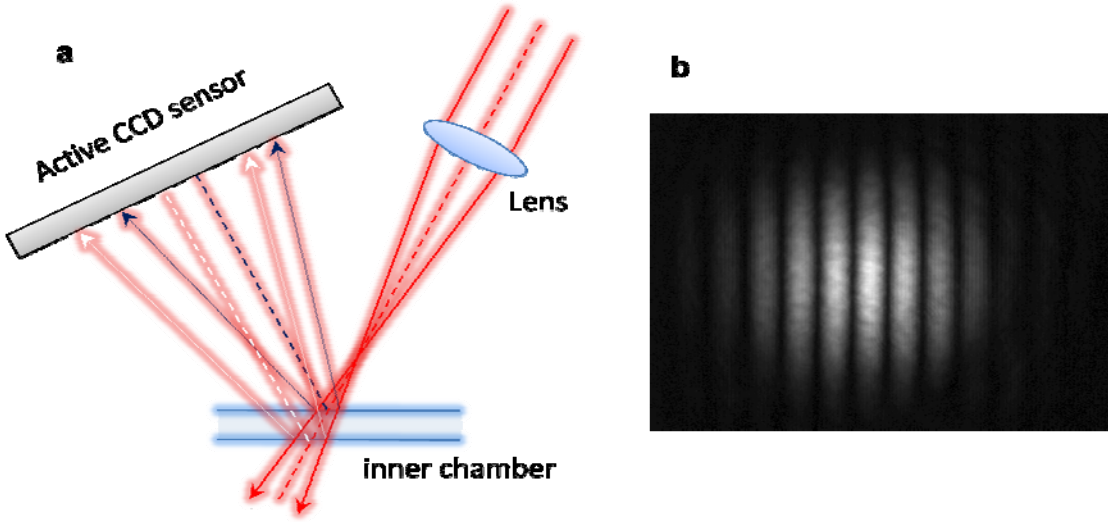

Figure 4.26 (a) A scheme of the interference image generate on the CCD camera (b) The pattern crated

4.4.3 Real-time sample concentration control

The image intensity, detected by the CCD, gives the same information of the photodiode used in the previous set-up, that is the mass adsorbed. The innovation of this prototype is the control of the instantaneous sample concentration as a function of time. If the solution into the cell changes we will observe a movement of the interference pattern (also called fringe shift). This change is linked to the variation of the refractive index of the solution. This correlation is explained by a simple equation.

The fringes position is determined by the phase difference φ between the light reflected from the first interface Hyflon-water and the second interface water-

Hyflon. This phase lag is due to the different optical paths travelled by the rays reflected from the two interfaces:

$$\varphi = \frac{2\,\pi\,L\cos\alpha\;n}{\lambda}$$

[4.7]

Here λ is the wavelength of the light, L is twice the cell thickness, α is the angle of incidence and n the average refractive index of the fluid portion crossed by the beam.

The variation of the fluid refractive index n with respect to initial value n_0 (running buffer) is proportional to the analyte concentration C present into the cell at given time:

$$n = n_0 + \frac{\partial n}{\partial C}\,C$$

[4.8]

Therefore, the phase difference is given by the initial difference φ_0 and the variation associated with the analyte concentration:

$$\varphi = \varphi_0 + \frac{2\,\pi\cos\alpha\;L}{\lambda}\frac{\partial n}{\partial C}\,C$$

[4.9]

When the cell is filled with buffer the phase difference is constant: $\varphi = \varphi_0$ and the fringes do not move. When the sample starts to flow in the cell a variation of the refractive index takes place and, as a consequence, a translation is observed in the interference pattern. When the sample begins to flow away from the cell the refractive index comes back to its initial value: the fringes move in the opposite direction until they return to their initial position when the sample is flown away completely.

To simplify, we can regroup the constant of equation 4.9:

$$\varphi = \varphi_0 + \beta\,C$$

[4.10]

The phase shift is:

$$\Delta\varphi = \varphi - \varphi_0$$

[4.11]

The phase shift is thus in a linear relation with the concentration:

$$C = \frac{1}{\beta}\,\Delta\varphi$$

[4.12]

β is a constant whose value can be not trivial to determine *a priori* . Anyway, the relation between C and $\Delta\varphi$ can be determined with the following self-consistent procedure. We can write the total mass of analyte M present into the sample (an experimentally controlled quantity) as:

$$M = \bar{C}\,V = \int C(t)dV$$

[4.13]

Here V and $\bar{C}$ are respectively, the total volume and the nominal concentration of the sample injected into the cell. In general the pumping rate $Q = dV/dt$ in an experiment is constant, so:

$$M = Q\int C(t)dt = \frac{Q}{\beta}\int \Delta\varphi\, dt$$

[4.14]

or:

$$\beta = \frac{Q\ \int \Delta\varphi\, dt}{\bar{C}\,V}$$

[4.15]

We can therefore restate the relation between instantaneous concentration and phase shift as:

$$C(t) = \frac{\bar{C}\,V}{Q}\,\frac{\Delta\varphi\,(t)}{\int \Delta\varphi\, dt}$$

[4.16]

Figure 4.27 The calculation of fringes intensity operated with Matlab.

Data analysis

During a measurement the interference pattern recorded by the camera is saved with a fixed frame rate (typically 0.2-1 images/second).
From each image a twofold information is obtained:

- The total intensity $I(t)$;
- The lateral position $\Delta x(t)$ of the interference fringes.

These quantity are extracted from the image sequence with the help of a dedicated software developed in a Matlab environment.
In the following it is detailed how, through a suitable processing of the acquired images, one can determine, time by time, the evolution of the concentration profile.
The total intensity $I(t)$, being the sum of the intensity reflected from the two interfaces, is proportional to the reflectivity of the interfaces. The latter is determined by both the thickness of molecular layer present on the surface and the bulk refractive index.
Let us consider an experiment where the binding between an immobilized receptor and a ligand in solution is studied. Let us suppose that initially the cell is filled with a running buffer and let R_0 be the reflectivity of the surfaces. Small variations in the thickness of the molecular layer present on the surface

and/or in the refractive index of the medium within the cell lead to a reflectivity change (dR):

$$dR = \frac{dR}{dh}\, dh + \frac{dR}{dn}\, dn$$

[4.17]

We can define the signal S associated to this variation as:

$$S \equiv \frac{dI}{I_o} = \frac{dR}{R_0}$$

[4.18]

Taking into account the linear relation holding between the fringes position Δx and phase shift $\Delta\varphi$, equation 4.16 can be rewritten as:

$$C(t) = \frac{\overline{C}\, V}{Q}\, \frac{\Delta x(t)}{\int dt \Delta x(t)}$$

[4.19]

The integral $\int dt \Delta x(t)$ is numerically evaluated from the data. The detailed knowledge of ligand concentration in solution as a function of time is relevant for the quantitative study of the binding kinetic.

Let us suppose that the binding we are considering is governed by a first order kinetic equation:

$$\psi(t) = -\left[\, C(t)\, k_{on} + k_{off} \,\right] \psi(t) + C(t)\, k_{on}$$

[4.20]

where ψ is the fraction of occupied binding sites.

$C(t)$ is a known function so, for every choice for the kinetic parameters, the kinetic equation can be numerically integrated, leading to a prediction ψ^* for the time evolution of the fraction of occupied binding sites (and thus of the average thickness of the layer of bound ligand):

$$\psi^*(\mathrm{t}|\, k_{on} + k_{off}) \propto dh\, (\mathrm{t}|\, k_{on} + k_{off})$$

[4.21]

This behavior is to be compared with the experimental signal. The latter, taken into account a (generally small) corrective term due to the refractive index variation, which is in turn proportional to C, is expected to be proportional to ψ:

$$S(t) = a_1 C(t) + a_2 \psi(t)$$

[4.22]

An indicator of the agreement between prediction and experimental data is given by the mean square difference:

$$\Delta(a_1, a_2, k_{on}, k_{off}) = \int dt \left[S(t) - a_1 C(t) - a_2 \psi^*(t|k_{on}, k_{off})\right]^2$$

[4.23]

The minimization of Δ gives a criterion to determine iteratively the kinetic constants and the auxiliary parameters a_1 and a_2.

In the successive sections some experiments, made with this set-up, will be shown. The data will be illustrated in two graphics: one reporting the intensity and the other reporting the fringes shift.

Interferometry test

In this section, I want to introduce the experiments conducted with the interferometric prototype and an innovative control of flux. The experiments with this biosensor are monitored with a CCD camera so we obtain an image sequence.

The figure 4.28 shows the result obtained in the first experiment. In this experiment we use water as the propulsion fluid. With the six-way valve we inject 20 µl of the specified analyte with a constant flow rate of 20 µl/min. The injections are:

- 100 mM potassium phosphate buffer, pH 7;
- 5 µM AVD in 10 mM potassium phosphate buffer, pH 7;
- 0.1 µM bBSA in 10 mM potassium phosphate buffer, pH 7.

The first graph (in blue) illustrates the number of fringe shift as a function of the time. The first boost is caused by the concentration of the first buffer (100 mM); the two following rises describe the injections of the proteins (AVD,

bBSA) with the same buffer concentration (10 mM). In all case we can measure the precise time course of the samples injection.

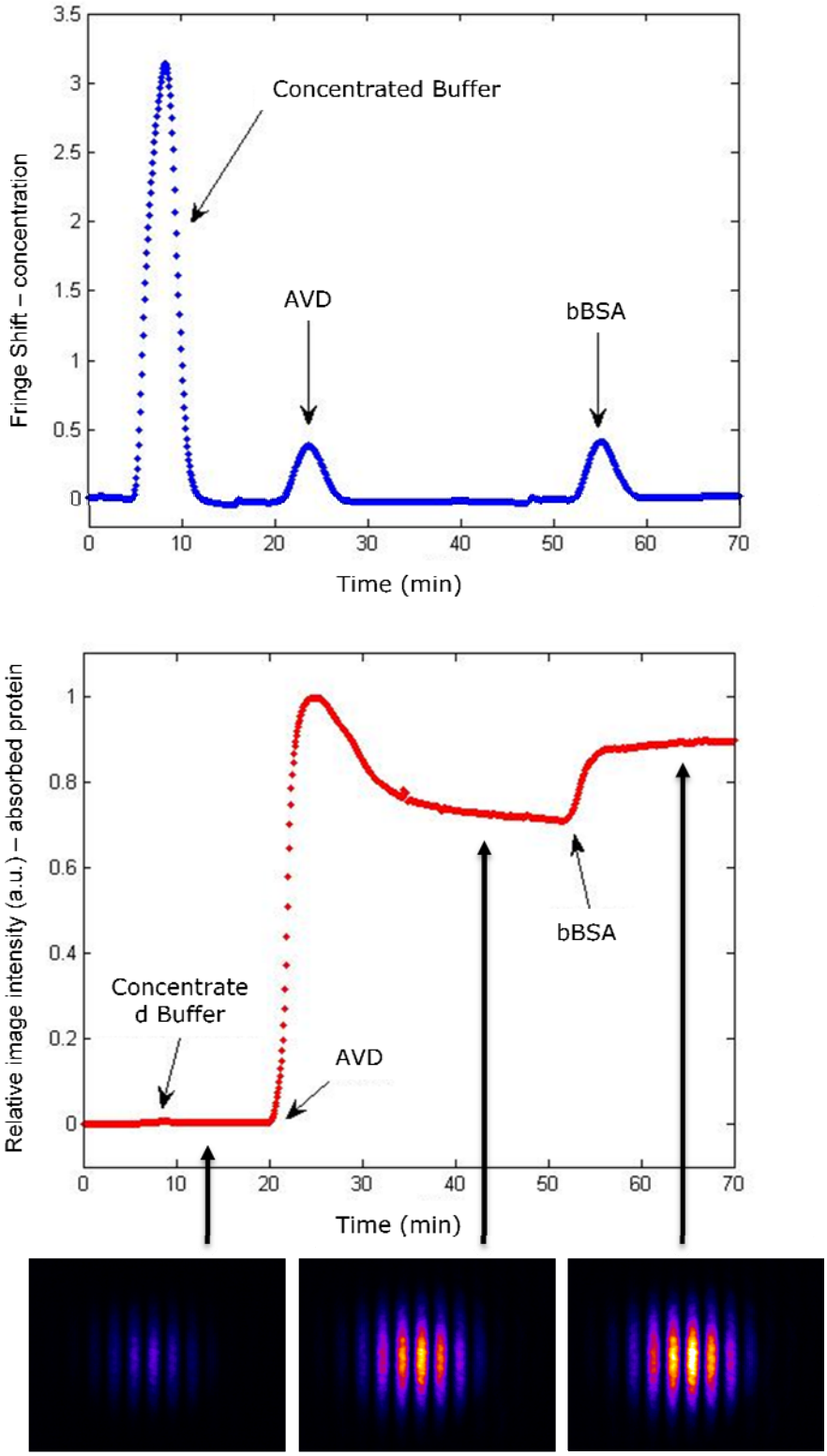

Figure 4.28 the test conducted with the interferometric prototype

In the second graph (in red) we show the variation of the intensity signal. We observe no increment with the concentrated buffer, followed by a significant AVD adhesion and a bBSA binding. This result is similar to the data collected with a photodiode. BIACore and other commercial biosensor have the IFC to control and reduce the Taylor dispersion. So their increment of concentration can be considered instantaneous and for the calculation of the kinetic parameter this approximation can be used.
The fluidic of our prototypes cannot guarantee the efficiencies of the IFC. Anyway with the interferometric control we can correct our problem. The intensity data (corresponding to the binding mass as a function of the time) can be adjusted for the real concentration in the cell. We can use the equation 4.19.
In the successive chapter we show an experiment of immune- recognition and test this methods for the determination of the association constant.

4.5 Imaging biosensor

The importance of HTS has been demonstrated by the success of gene array (Wang 2000). This success has further provided impetus for the proposal that protein–protein arrays could achieve similar utility for the analysis of multiple binding events. An array is a system of ligand-binding assays, in which every single interaction occurs separately, on a spot area of a solid support. To monitor this active surface, we need to acquire some images and to study the variation in the time.
Our technique is favored to be transformed in an array, because our principle is based on the monitoring of the intensity variation from a surface. Of course, the optical set-up must be adjusted to image acquisition.

4.5.1 Biosensor set-up

Our imaging cell does not need two faces in Hyflon AD (like in interferometry). The structure is similar to the single reflection biosensor; the main improvement is to transform our device in a chip with multiple spots. To do that, we enlarge the dimension of the surface and modify the gasket shaped in silicon (figure 4.29).

The optical configuration setup is shown in figure 4.26. The measurement technique requires a temporally incoherent light source (as a LED- Agilent HLMP-ED18-UXT00: 630nm, intensity 5000 mcd with a stabilized power supply), because a spatial coherence illumination (as a Laser) causes unwanted artifacts due to diffraction and speckle. However, we utilize a LED with a low-divergence beam not to disperse the light produced. A collimation lens conjugated to a diaphragm is used andthe focalization is near to the cell. With this set-up, a changing of diaphragm aperture can be used to regulate the angular spread and the illumination on the cell. A second lens is used to create the image on the CCD camera (figure 4.30).

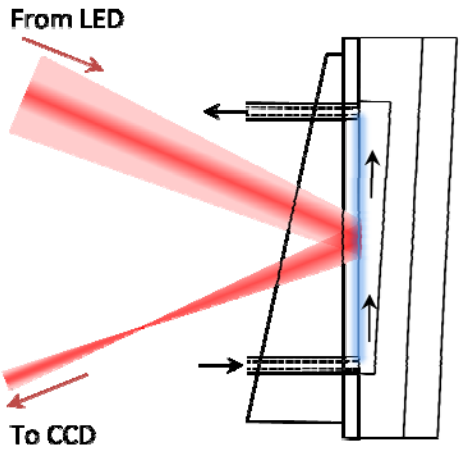

Figure 4.29 the of the imaging flow cell

The experiments are performed by depositing a drop (0.5 µl) of an AVD solution (3 µM) on the inner Hyflon AD face. This operation is carried on by a "home-made" spotter, so the drops generated are not fully regular. After 20 minutes from the deposition (a time sufficient to allow the binding of AVD on Hyflon AD) the cell is assembled and abundant water is flowed on the surface. Subsequently, the biotinylated substrates are flowed with a standard injection by using the six-way valve. We observe the reflectivity change on the image and measure (by acquisition of image sequence) the difference of signal between the protein spot and the uncoated surface. The image analysis has been performed with the software Imagej.

For the fluidic system we use the same devices: a motorized syringe pump and the six way valve. The Hyflon AD interface is regenerated using the regeneration procedure previously described.

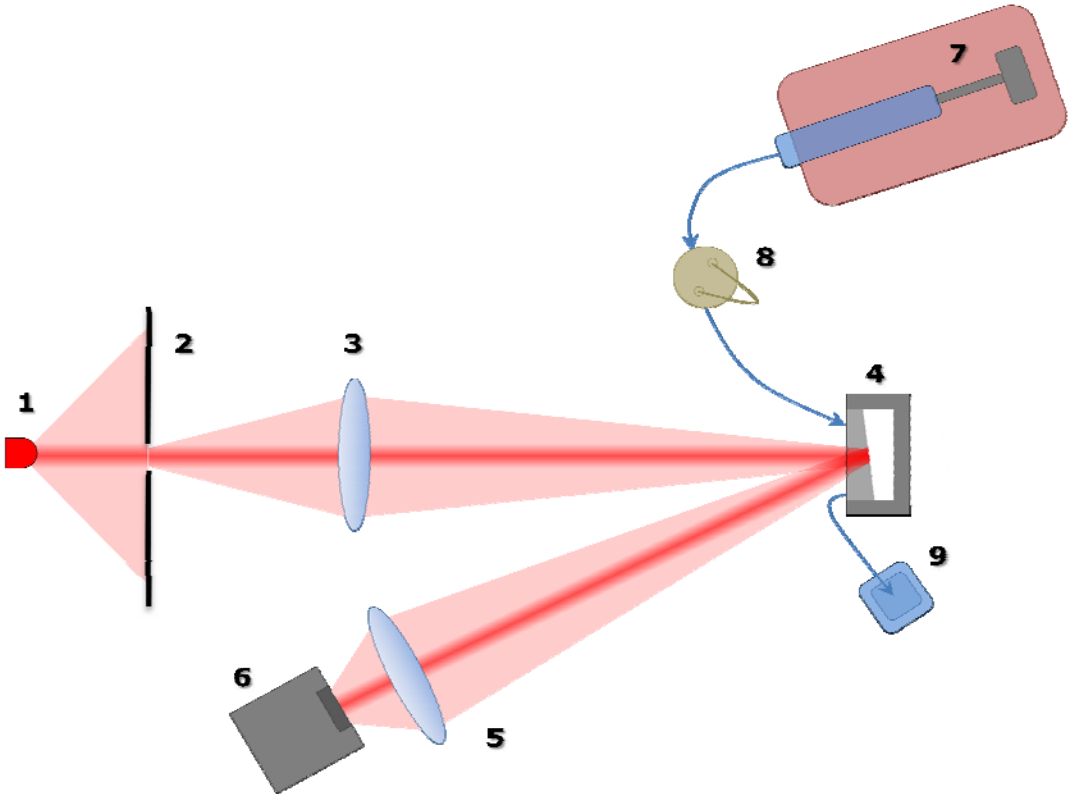

Figure 4.30 In our system, a LED is used (1), the incoherence eliminates image artifacts; the other systems are: collimation lens (3), collimation lens conjugated to a diaphragm plain (2),the flow cell with a Hyflon AD surface (4), a second lens to create the images (5) on a CCD camera (6), a commercial motorized syringe pump (7), a six-way valve (8) and a waste collector (9)

4.5.2 Spot experiment

The figure 4.31 illustrates the image of the cell surface after this device has been assembled in the prototype. The drop of the AVD solution (3μM) is shown.

When the propulsion buffer has been loaded into the cell, we cannot see any traces of the AVD spot. Afterwards, when the bBSA solution (2 μM) reaches the surface of the cell, it is evident the increase of image intensity on the region of the AVD drop (figure 4.32). The effect can be improved by a simple operation. On the image sequence we operate a subtraction of the first image: we can remove the background noise and improve the signal contrast (figure 4.33 and 4.34).

At the same way we have performed a double spot experiment. Beside the standard AVD solution we have put a drop of 3 μM AVD solution with 15 μM biotin (we have saturated the protein, since it binds four molecules of biotin). The procedure is the same as the precedent. After the flow of the bBSA, the

difference of intensity between the two spot. is evident In the image 4.35 we can see the result: the AVD spot behaves as the precedent experiment; on the contrary, the second one does not increase the intensity signal.

From this data it is evident the possibility to expand our methods in a HTS with a surface able to monitor numerous interactions.

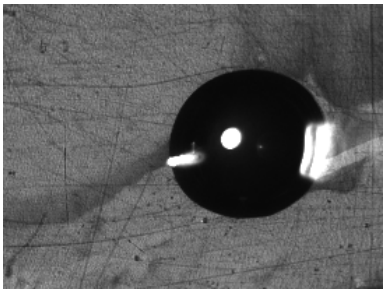

Figure 4.31 The image of a drop of AVD on surface

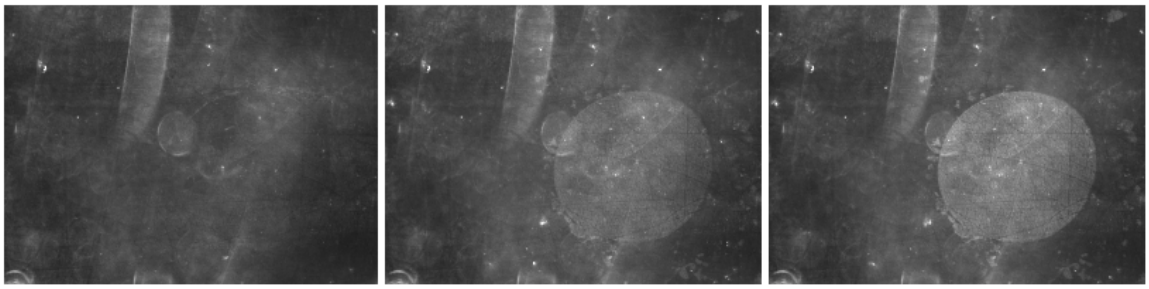

Figure 4.32 The intensity of the surface while flow bBSA. signal increases coinciding drops of AVD

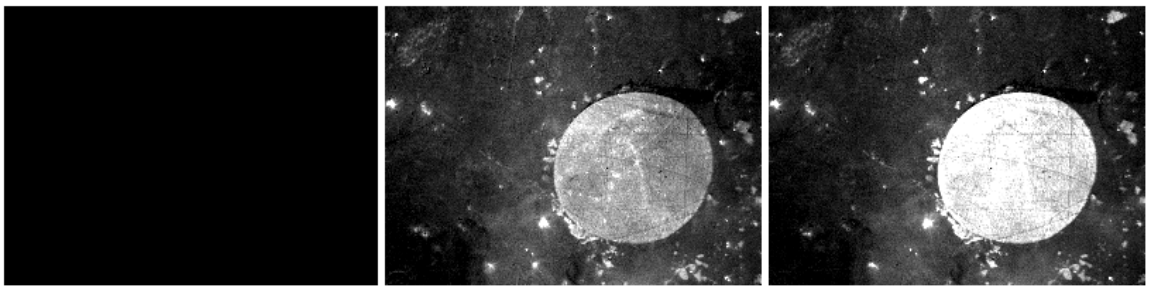

Figure 4.33 the signal after subtraction of background

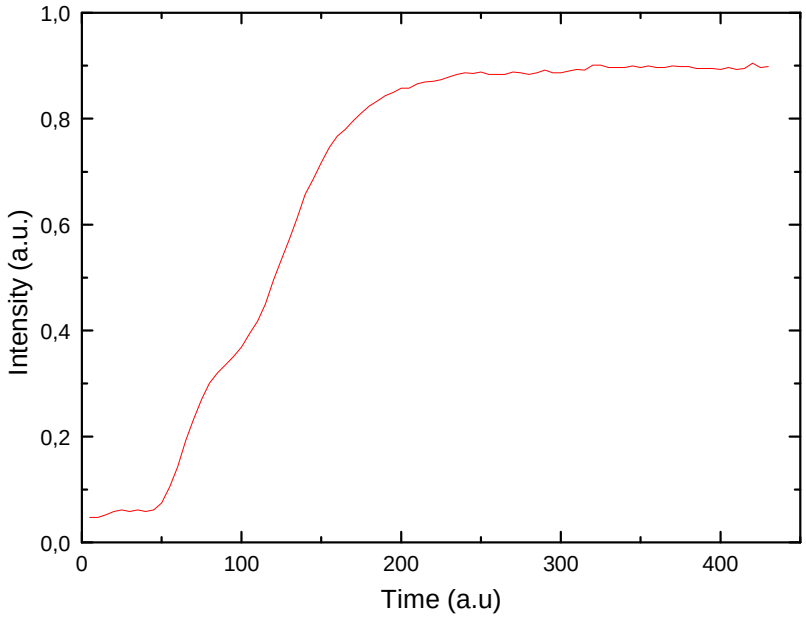

Figure 4.34 The intensity of the surface with the AVD

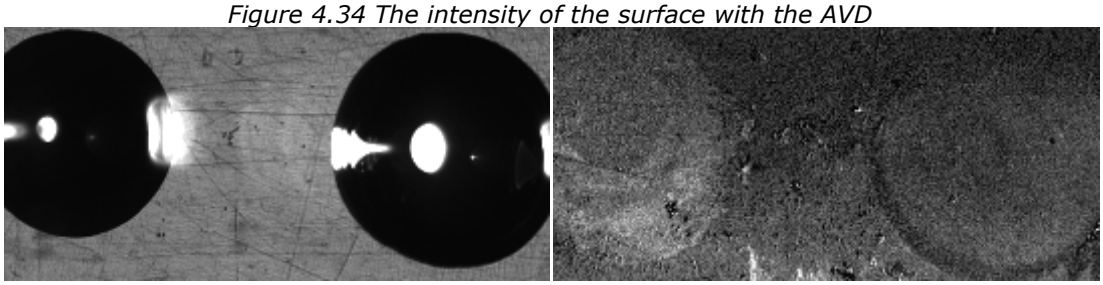

Figure 4.35 The experiment with two drops on the right the AVD saturated with the biotin.

5 INTERACTIONS ANALYZED

5.1 Single Reflection Experiment

The experiments described in this section have been carried out with the set-up "single reflection" by using the silicone cell end the other device illustrated in previous chapter.

5.1.1 Antigen and antibody recognition

The experiment presented here (specific binding between BSA and Antibody anti-BSA) consists in four sequential steps, each one accomplished by loading and flowing 20 µl of the specified analyte, with a constant flow rate of 30 µl/min, on the sensor surface.
These steps are:

- Surface preparation with 3 µM AVD (as described in section 4.2.3)
- Receptor immobilization (1 µM bBSA)
- Saturation of the unspecific binding sites (as a common Western blotting experiment, we use 1 g/l nonfat dry milk)
- Ligand binding (0,1 mg/ml Ab/BSA anti-bovine Serum albumin produced in rabbit purchased from Sigma-Aldrich)

All the analytes are resuspended in a sodium phosphate buffer (10 mM, pH 7.4) which is also used as running buffer. Raw data are collected by the photodiode (which measures the intensity of the light reflected by the sensor surface). The signal intensity is converted in adsorbed mass per unit area, using the Fresnel thin layers model implemented in the software of the sensor (section 4.1.1). To simplify, our signal can be transformed in mass per unit surface, σ, expressed in ng/mm^2, with this equation:

$$\sigma = \sqrt{I/I_0 - 1} \qquad [5.1]$$

where I/I_0 is the ratio between the measured intensity and initial intensity.

We can observe that the thickness of AVD is completely compatible with a monolayer of protein (Pugliese et al. 1993 - Section 4.2.3).

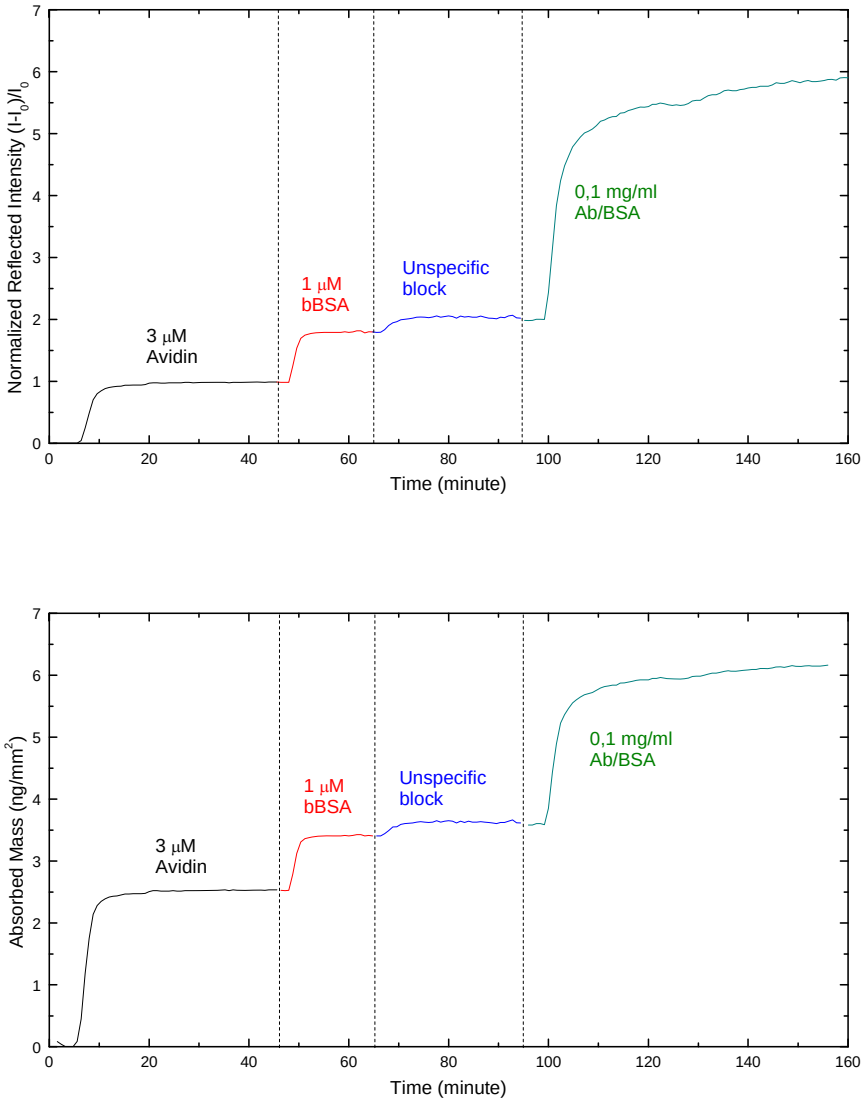

Figure 5.1 Two plots of the BSA and Antibody recognition; the first shows the obtained data and the second illustrates the conversion in absorbed mass.

As outlined in the figure, the increment of the adsorbed mass, due to the bBSA, ($\Delta\sigma_{bBSA}$) is:

$$\Delta\sigma_{bBSA} = 0{,}85\ ng/mm^2 \qquad [5.2]$$

This value allows to estimate the number density of the bounded bBSA molecules and thus the effective biotin binding site density N_{biot} on the surface:

$$N_{biot} = \frac{\Delta\sigma_{bBSA}}{M_{bBSA}} = 5.4\ 10^{9} mm^{-2} \quad [5.3]$$

where M_{bBSA} is the mass of a single bBSA molecule, corresponding to 68 kDa.
Repeated tests have shown that this value of N_{biot} is nearly optimal, in the sense that greater bBSA concentrations do not lead to a higher surface coverage. The reproducibility is found to be quite good.
The injection of the antibody leads to an adsorbed mass increment $\Delta\sigma_{ab} = 2{,}6\ \mathrm{ng/mm^2}$. The number density N_{ab} of the ligand on the surface can be thus determined as:

$$N_{biot} = \frac{\Delta\sigma_{ab}}{M_{ab}} = 6.7\ 10^{9} mm^{-2} \quad [5.4]$$

Where the antibody mass M_{ab} corresponds to 180 kDa. Each immobilized BSA binds, on average, $N_{lig} / N_{biot} \approx 1{,}2$ polyclonal antibodies.
This value can be explained in this way: a bBSA can be bound by more than one polyclonal antibodies, since they recognize different epitopes; anyway in a 2D system (as a surface) the steric hindrance limits the recognition (Lassen et al. 2008), giving a ratio close to 1:1.

5.1.2 Protein / peptide interaction

To test our methods in an experiment of protein/peptide interaction, we use a biotinylated peptide with a phosphorilated tyrosine (purchased from Biomol) and a SH2 domain present in SRC (purchased from Marligen Biosciences). As introduced in the section 3.4.2, Src homology 2 domains provide phosphorylation-dependent and sequence-specific contacts for assembly of receptor signaling complexes during signal transduction. The peptide used includes the sequence pTyr-Glu-Glu-Ile.

The experiment shown in figure 5.2 is carried out using water as propulsion buffer; the pumping rate is of 4 µl/min and the experimental steps are:

- Surface preparation with 3 µM AVD ;
- Peptide immobilization: 110 µM of biotinylated peptide in 150 mM NaCl, 10 mM potassium phosphate buffer, pH 7;
- Protein binding: 0,69 µM SH2 domain in 150 mM NaCl, 10 mM potassium phosphate buffer, pH 7.

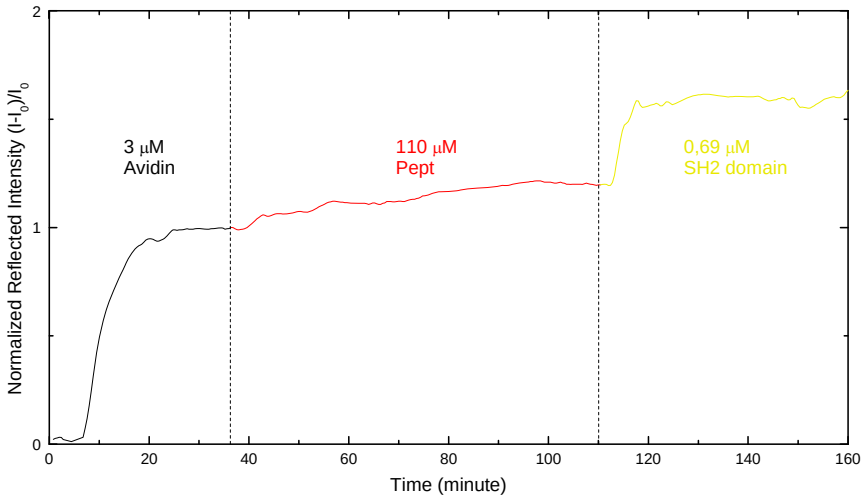

Figure 5.2 Protein/peptide interaction

Using the same conditions, we perform a negative control experiment to evaluate the formation of possible unspecific interactions (figure 5.3). To do that, we inject the SH2 domain directly on a layer of AVD. Thus, the steps are:

- Surface preparation with 3 µM AVD;
- Protein binding: 0,69 µM SH2 domain in 150 mM NaCl, 10 mM potassium phosphate buffer, pH 7.

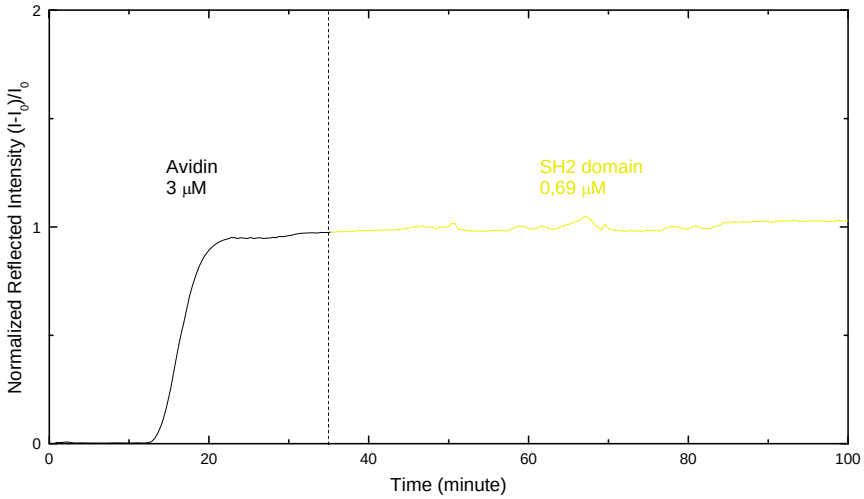

Figure 5.3 Negative control of Protein/peptide experiment

It is interesting to underline the ratio of the mass of the two macromolecules used: AVD has a MW of 66 kDa, the SH2 domain has a MW of 23 kDa; these values are approximately observed in our biosensor as the difference of mass/surface adsorbed. However, the SH2 domain does not present the typical fast kinetic of dissociation from the biotinylated peptide (de Mol et al. 2005); this phenomenon can be explained by two different effects. The first is the formation of some possible unspecific bonds between SH2 domains and other structures present on surface (like the AVD), which can occur after the specific bond with the biotinylated peptide. The second factor is an uncontrolled concentration into the cell, problem that has been addressed in the successive experimental set-up.

5.2 Double Reflection Biosensor

The following experiment has been carried out with the advanced set-up by using the cell with two Hyflon AD faces.

5.2.1 Antigen-antibody recognition

We show another experiment of specific binding between BSA and Antibody anti-BSA. The test consists in sequential steps, each one accomplished by

loading and flowing 50 µl of the specified analyte, with a constant flow rate of 15 µl/min, on the sensor surface.

These steps are:

- Surface preparation with 3 µM AVD in 10 mM potassium phosphate buffer, pH 7
- Receptor immobilization (1 µM bBSA in potassium phosphate buffer, pH 7)
- Ligand binding diluted in potassium phosphate buffer, pH 7 (Ab/BSA anti-bovine Serum albumin produced in rabbit with the commercial serum – Sigma Aldrich); it is performed with a increasing concentration.

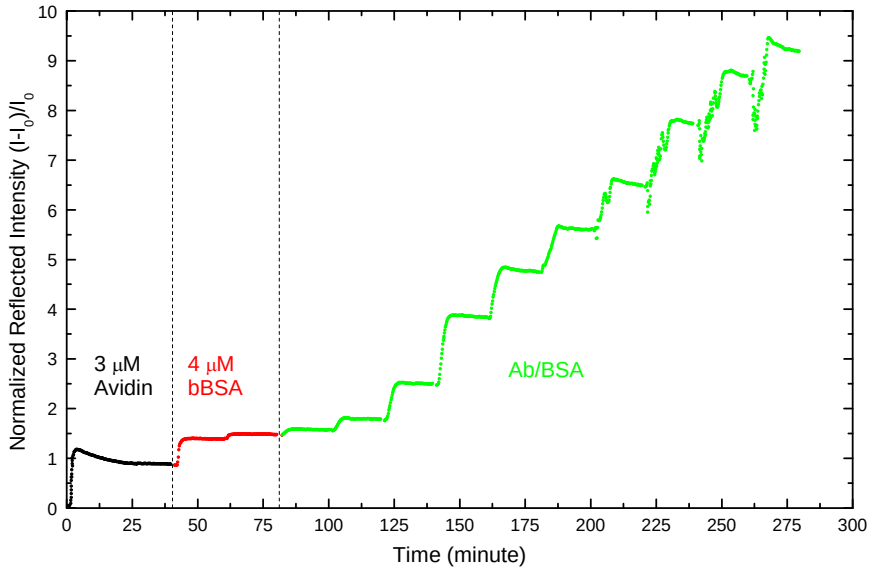

Figure 5.4 Antigen and antibody recognition

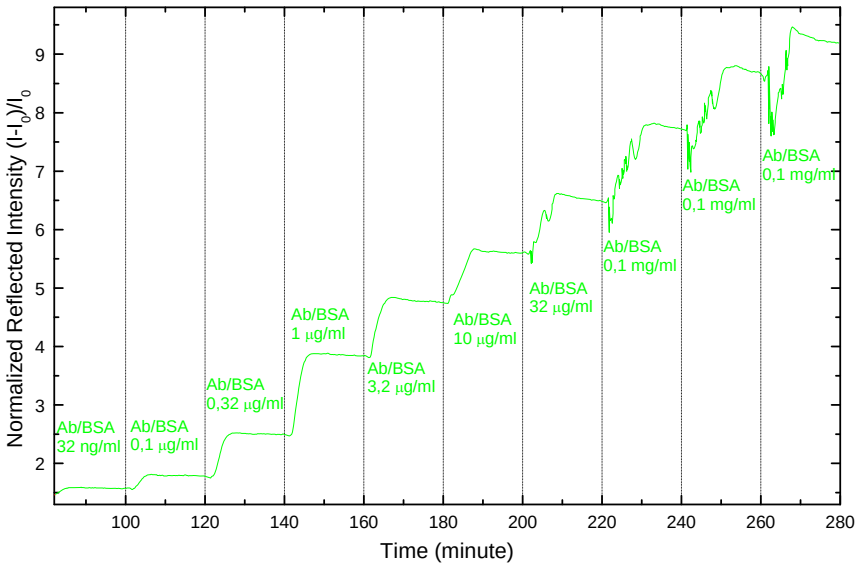

Figure 5.5 Antigen-antibody recognition: the signal increases in proportion to the concentration up to the fourth injection (1 µg/ml)

The data are collected by the photodiode and illustrated in figures 5.5 and 5.4. The signal and the equilibrium values depend on the antibodies concentration, as expected : the signal increases in proportion to the concentration up to the fourth injection. At this point the recognition is limited by the unbound BSA molecules. Therefore, it is fundamental to use a flow cell with a correct fluidic and the analytes must be addressed on the active surface; this measure cannot be performed with the single reflection biosensor. The final ratio of the mass absorbed between Ab and bBSA is higher than 1:1, compatible with the binding of more than one polyclonal antibody. In the last injections we can observe a typical modulation on the slope, it is due to the intensive change of index of refraction (the samples is less diluted an less similar to the propulsion buffer).

5.2.2 PSA Measures

The biomarker discovery and the PoC are very attractive applications for a biosensor. The possibility to accurately measure the PSA concentration could prove the real effectiveness of our method for both these applications. In other words, our goal consists in detecting a low level of PSA.

These experiments use three different antibody immobilization strategy: in the first one we use a anti-PSA antibody biotinylated in the laboratory, while in the other two we utilize commercial biotinylated proteins able to link the antibody anti-PSA (protein A and the protein G). To allow a direct bond with AVD, we need to perform a chemical modification of this protein with activated biotins.

PSA antibody Biotinylation

NHS esters of biotin are the most popular type of biotinylation reagents. NHS-activated biotins react efficiently with primary amino groups (-NH_2) in pH 7-9 buffers to form stable amide bonds (Section 3.3.1). Proteins, including antibodies, generally have several primary amines in the side chain of lysine (K) residues and the N-terminus of each polypeptide that are available as targets for labeling with NHS-activated biotin reagents. We use a NHS-biotine with a spacer to reduce the steric hindrance: NHS-LC-Biotin, (succinimidyl-6-(biotinamido)hexanoate) (Pierce).

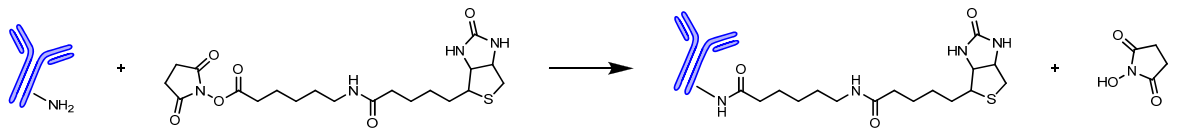

Figure 5.6 The biotinylation reaction of antibody

The amount of biotin reagent to use for each reaction depends on the amount of protein to be labeled and its concentration. By using the appropriate molar ratio of biotin to protein, the extent of labeling can be controlled.

We use 20-fold molar excess of biotin with a 2 mg/ml protein solution. The antibody is dissolved in PBS (an amine-free buffer) , pH 7.4 The sample is incubated on ice for two hours.

Protein labeling is complete at this point, and although excess non-reacted and hydrolyzed biotin reagent remains in the solution, the labeled protein may be purified for optimal performance and stability using desalting.

The Zeba Desalt Spin Columns (Pierce) contain a high-performance resin that offers desalting and protein recovery characteristics. We use this procedure to remove the remained reagents and the NHS leaving groups. This procedure requires no chromatography system or cumbersome column preparation or equilibration. Additionally, the spin-column method eliminates the need to wait

for samples to emerge by gravity flow, allowing multiple sample processing in about 6 minutes.

PSA Test

The test has been performed by using a proper functionalization of the surface, followed by a successive injection with increasing concentrations of PSA (purchased from Calbiochem) in a physiologic solution. The experiment consist of sequential steps, each one accomplished by loading a 20 µl injection loop and flowing the specified analyte with a constant flow rate of 10 µl/min. The used cell has an active area of about 5 mm^2. The detection of the reflected intensity is performed by a low cost photodiode.

To enhance the binding of Avidin on Hyflon surface, a low ionic strength buffer is used at the beginning of the experiment (10 mM potassium phosphate pH 7.4). After the coating with Avidin the buffer is gradually changed with buffer (10 mM potassium phosphate, 150 mM NaCl, pH 7.4).

The first experiment is performed both to test the cross reactivity of the protein used and to verify the biotinylation protocol efficacy of the anti-PSA mAb (purchased from Biodesign Internaional).

The figure 5.7 illustrates our positive control. We assemble a protein multilayer and we measure the reflection increment. The flow rate is set at 50 µl/min. The steps are:

- Surface preparation with 50 µl of 3 µM AVD in 10 mM potassium phosphate buffer, pH 7;
- Antibody binding: 50 µl of 1 µM biotinylated anti-PSA mAb in 150 mM NaCl, 10 mM potassium phosphate buffer, pH 7;
- Ligand binding: 50 µl of 30 mg/ml PSA in 150 mM NaCl, 10 mM potassium phosphate buffer, pH 7.

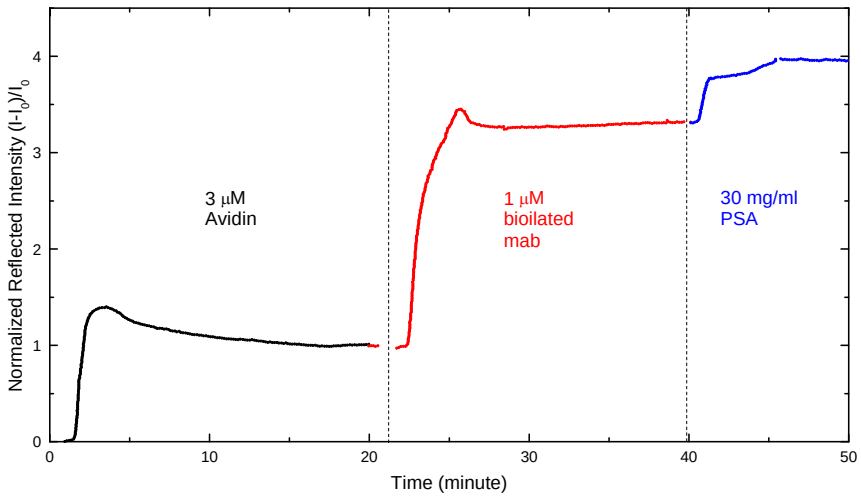

Figure 5.7 The positive control

Two negative controls are carried out. The first is performed to exclude the formation of unspecific bonds with AVD. Thus, we use non-biotinylated anti-PSA mAb. The steps are:

- Surface preparation with 50 µl of 3 µM AVD in, 10 mM potassium phosphate buffer, pH 7;
- Antibody binding: 50 µl of 1 µM non-biotinylated anti-PSA mAb in 150 mM NaCl, 10 mM potassium phosphate buffer, pH 7.

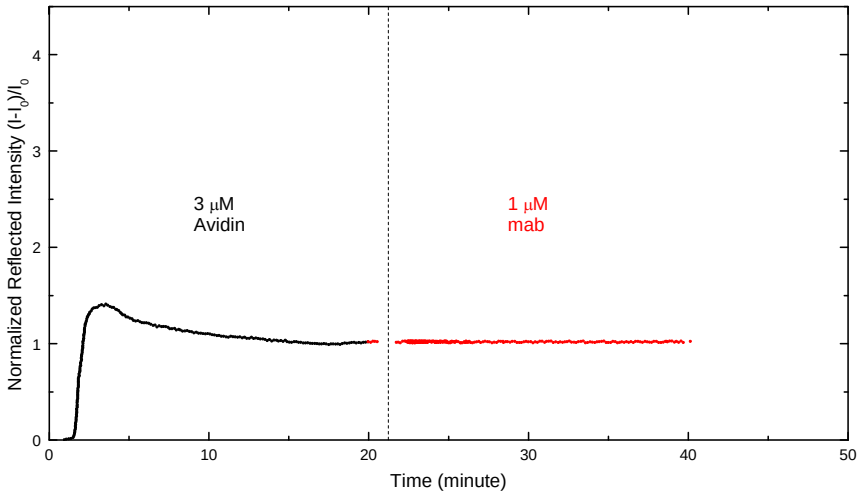

Figure 5.8 This experiment excludes the formation of unspecific bonds between AVD and Antibody

The second negative control is performed to verify the specificity of the interaction between PSA and its antibody. Thus, we use biotinylated anti-PSA mAb and human serum albumin (HSA), the most common protein in blood. The steps are:

- Surface preparation with 50 µl of 3 µM AVD in 10 mM potassium phosphate buffer, pH 7;
- Receptor immobilization: 50 µl of 1 µM biotinylated anti-PSA mAb in 150 mM NaCl, 10 mM potassium phosphate buffer, pH 7;
- Unspecific check: 50 µl of 300 mg/ml HSA in 150 mM NaCl, 10 mM potassium phosphate buffer, pH 7.

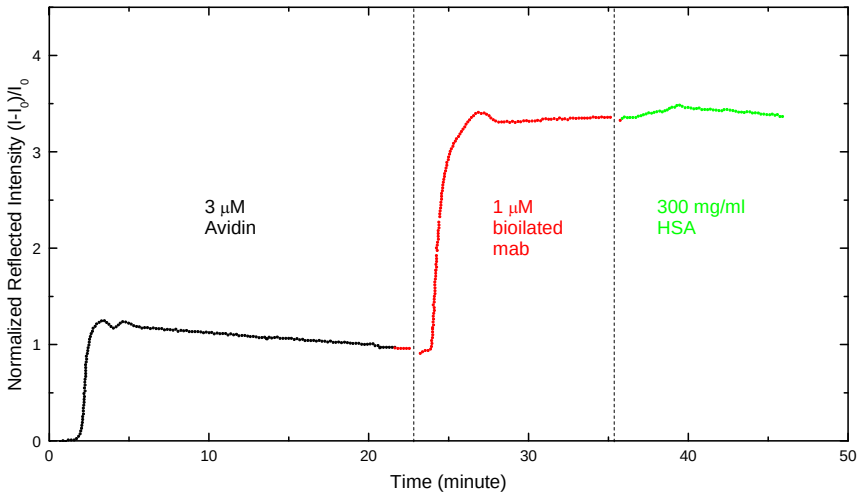

Figure 5.9 This experiment excludes the formation of unspecific bonds between HSA and Antibody

As shown in the figures 5.8 and 5.9, the results of the negative controls confirm that our procedure is not observing an unrelated effect and that all the interactions occur according their correct specificity. The following plots 5.10 5.11 5.12 represent the immune recognitions with the three different strategies of Hyflon AD interface treatments . The flow rate is set at 50 µl/min.

Biotinylated antibody:

- Surface preparation with 50 µl of 3 µM AVD in 10 mM potassium phosphate buffer, pH 7;
- Antibody binding: 50 µl of 1 µM biotinylated anti-PSA mAb in 150 mM NaCl, 10 mM potassium phosphate buffer, pH 7;
- A sequence of increasing concentration of PSA in 150 mM NaCl, 10 mM potassium phosphate buffer, pH 7.

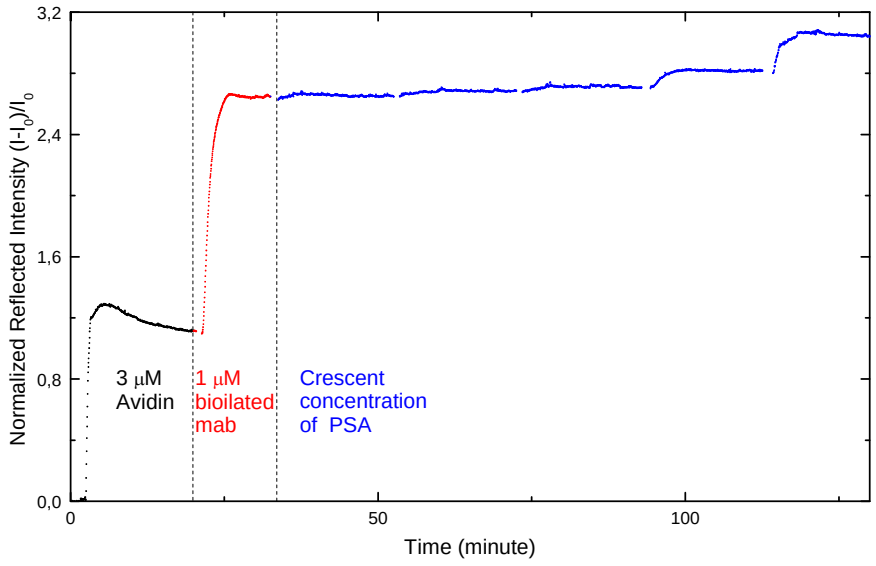

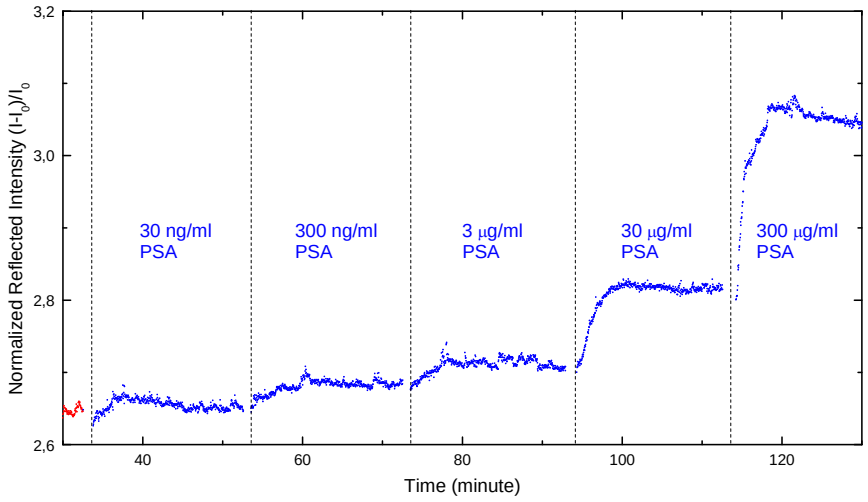

Figures 5.10 PSA test with a biotinylated antibody

Protein A and antibody:

- Surface preparation with 50 µl of 3 µM AVD in 10 mM potassium phosphate buffer, pH 7;
- Receptor immobilization: 50 µl of 4 µM biotinylated Protein A in 150 mM NaCl, 10 mM potassium phosphate buffer, pH 7;
- Antibody binding: 50 µl of 3 µM anti-PSA mAb in 150 mM NaCl, 10 mM potassium phosphate buffer, pH 7;
- A sequence with increasing concentration of PSA in 150 mM NaCl, 10 mM potassium phosphate buffer, pH 7.

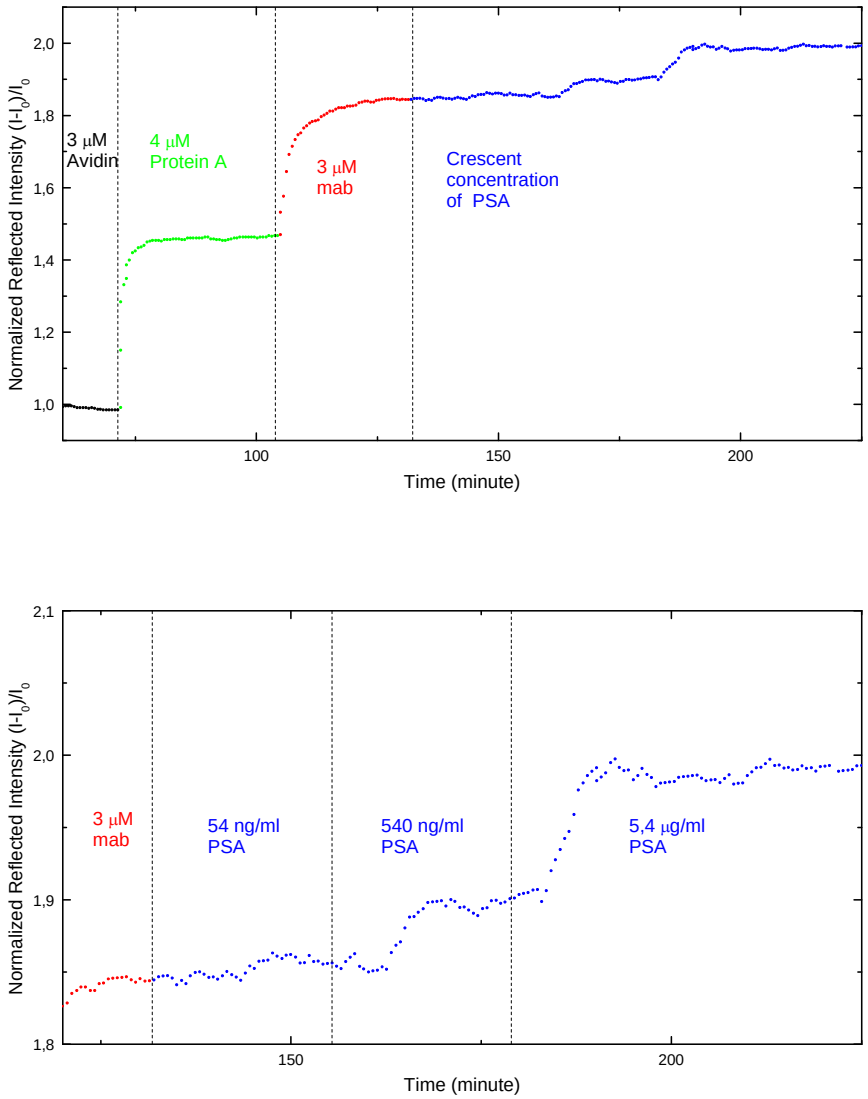

Figures 5.11 PSA test with protein A and antibody

Protein G and antibody:

- Surface preparation with 50 µl of 3 µM AVD in 10 mM potassium phosphate buffer, pH 7;
- Receptor immobilization: 50 µl of 4 µM biotinylated Protein G in 150 mM NaCl, 10 mM potassium phosphate buffer, pH 7;
- Antibody binding: 50 µl of 3 µM anti-PSA mAb in 150 mM NaCl, 10 mM potassium phosphate buffer, pH 7;
- A sequence with increasing concentration of PSA in 150 mM NaCl, 10 mM potassium phosphate buffer, pH 7.

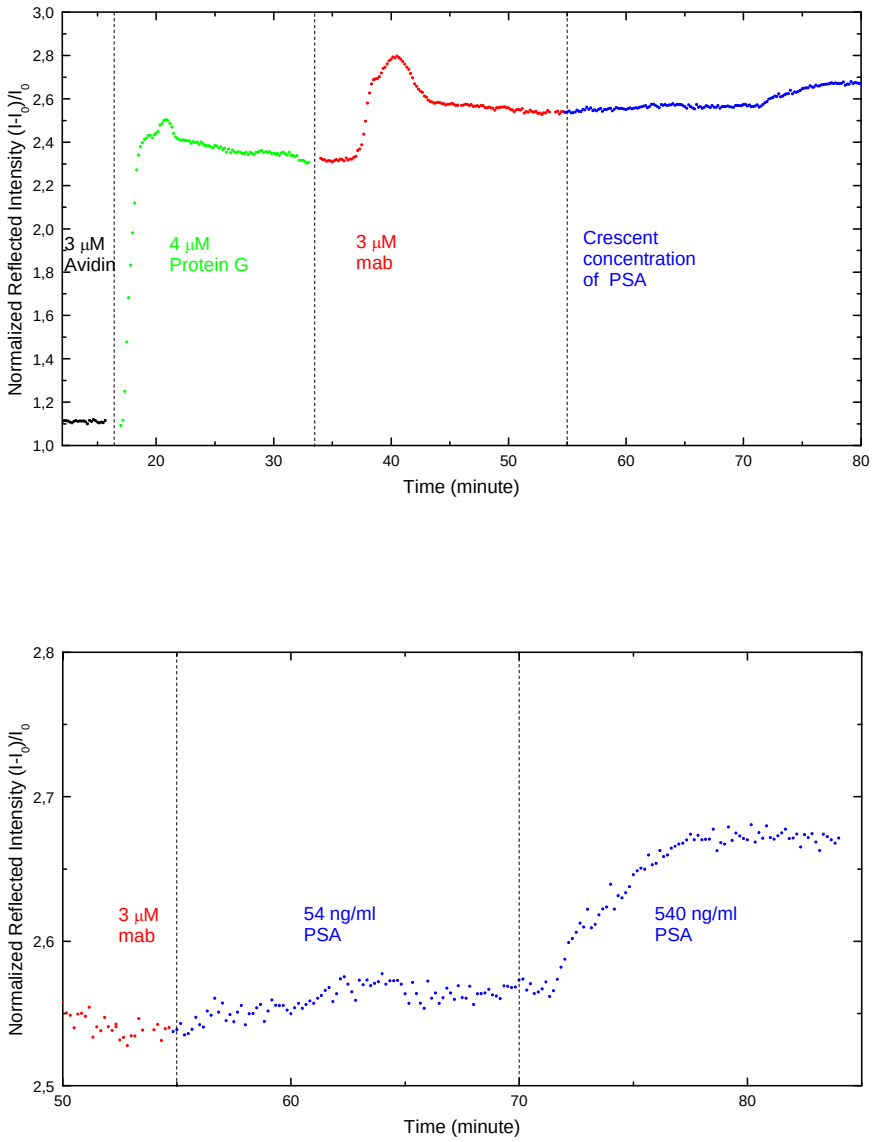

Figures 5.12 PSA test with protein g and antibody

The direct binding of the biotinylated antibody shows the best performance. Therefore, with this procedure the ratio of antibody/AVD is close to 1:1 and, in addition, it is possible to detect the lowest PSA concentration.

The minimum relievable concentration is 30-300 ng/ml, whereas the pathologic levels are of 4-10 ng/ml. In the proposed system, the response to low PSA concentration is limited by mass transport and by antibody affinity. Current studies aim at overcoming mass transport limitations by using injection loop with larger volume, decreased flow rate and smaller active areas on the Hyflon AD surface (theoretical limit ~ 0.01 mm^2).

5.2.3 Kinetic measure

With this set-up we can perform measures to analyze the kinetic constant between ligands and receptors. We want to illustrate an experiment which has shown the binding of human IgG with the protein A. The flow rate is set at 50 µl/min. The injections are:

- Surface preparation with 50 µl of 3 µM AVD in buffer 10 mM potassium phosphate, pH 7.4;
- Receptor immobilization: 50 µl of 10 µM biotinylated Protein A in 150 mM NaCl, 10 mM potassium phosphate buffer, pH 7;
- A sequence of increasing concentration of Human IgG in 150 mM NaCl, 10 mM potassium phosphate buffer, pH 7.

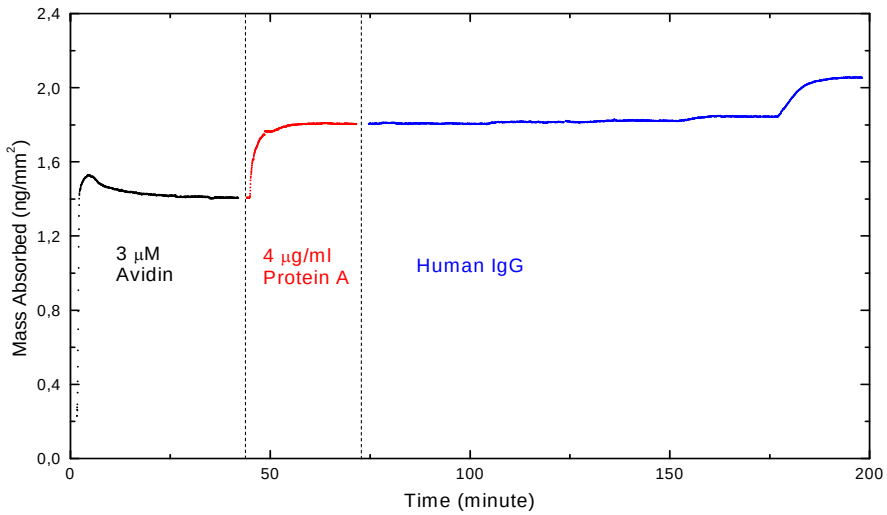

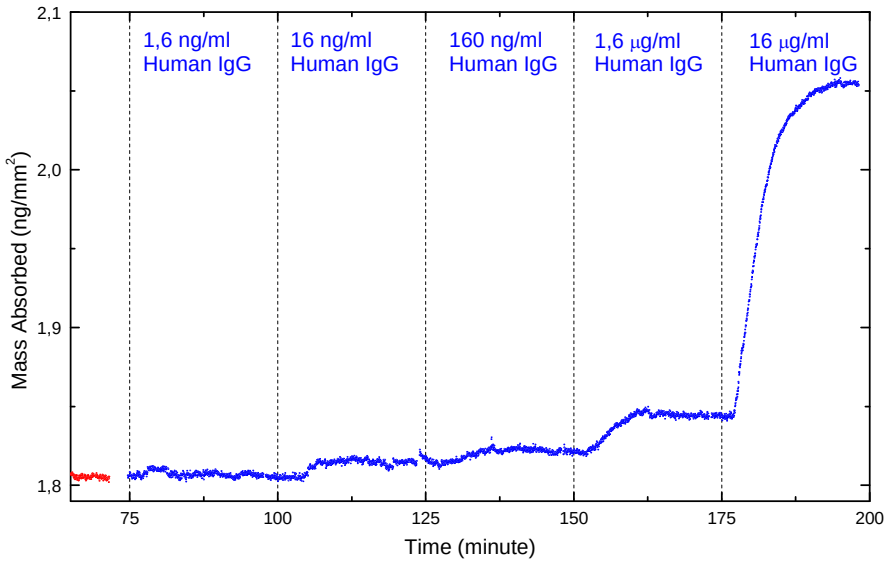

Figure5.13 The binding of human IgG with the protein A

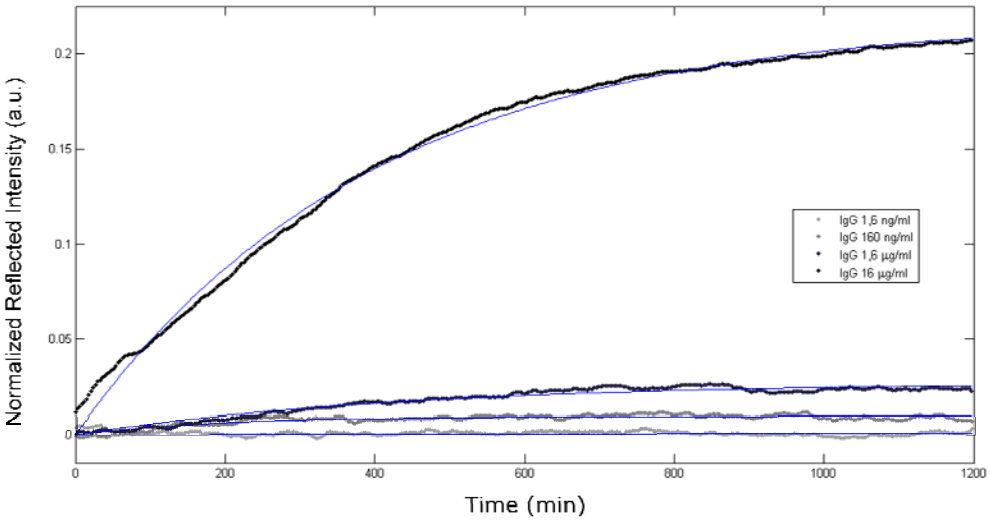

Figure 5.14 The sensorgram of the diverse IgG association at different concentration

The data obtained are plotted in a sensorgram that shows the diverse association kinetics at different concentration (figure 5.14). We have analyzed IgG samples, spanning 1.6 to 16000 ng/ml in concentration.

Kinetic analysis is performed on data in a concentration series by applying a 1:1 interaction model by using a software specifically created in Matlab; with this we can perform the fitting of the curves with a exponential function; the calculation takes care of the estimated time of interaction (about 12 minutes)

and the number of occupied receptors (that is the successive injections of sample) . From this data we can calculate the association constant between protein A and IgG. Our result is 1,2 * 10^5 $M^{-1}s^{-1}$. The literature reported 1,1-1,5 * 10^5 $M^{-1}s^{-1}$, measured by using BIACore instrument (Andersson et al 1999).

5.3 Interferometric experiment

A typical experiment of immune-recognition are performed with this methods. it is shown in figures 5.15 and 5.16. As precedent described, with this set up we obtain two data one is the "standard" intensity signal (as the precedent experiment) an the second information is the real concentration of sample into the cell (it is performed by the analysis of the fringes-shift).

With the six-way valve we inject 20 µl of the specified analyte with a constant flow rate of 20 µl/min. We use 10 mM potassium phosphate buffer, pH 7 as propulsion fluid. The injections are:

- 20 µl of 5 µM AVD, 10 mM potassium phosphate buffer, pH 7;
- 20 µl of bBSA 0.1 µM, 20 mM potassium phosphate buffer, pH 7;
- 20 µl of anti-BSA antibody in commercial serum.

Since the propulsion buffer has the same concentration (10 mM) of the buffer used to inject AVD, we do not observe a fringe shift; on the contrary, the slight difference of the concentration (20 mM) of the buffer used to inject bBSA can detected. Obviously, the serum is very different from 10 mM potassium phosphate buffer, so it is well detected.

The anti-BSA antibody injection gives an intensive signal and saturate the signal.

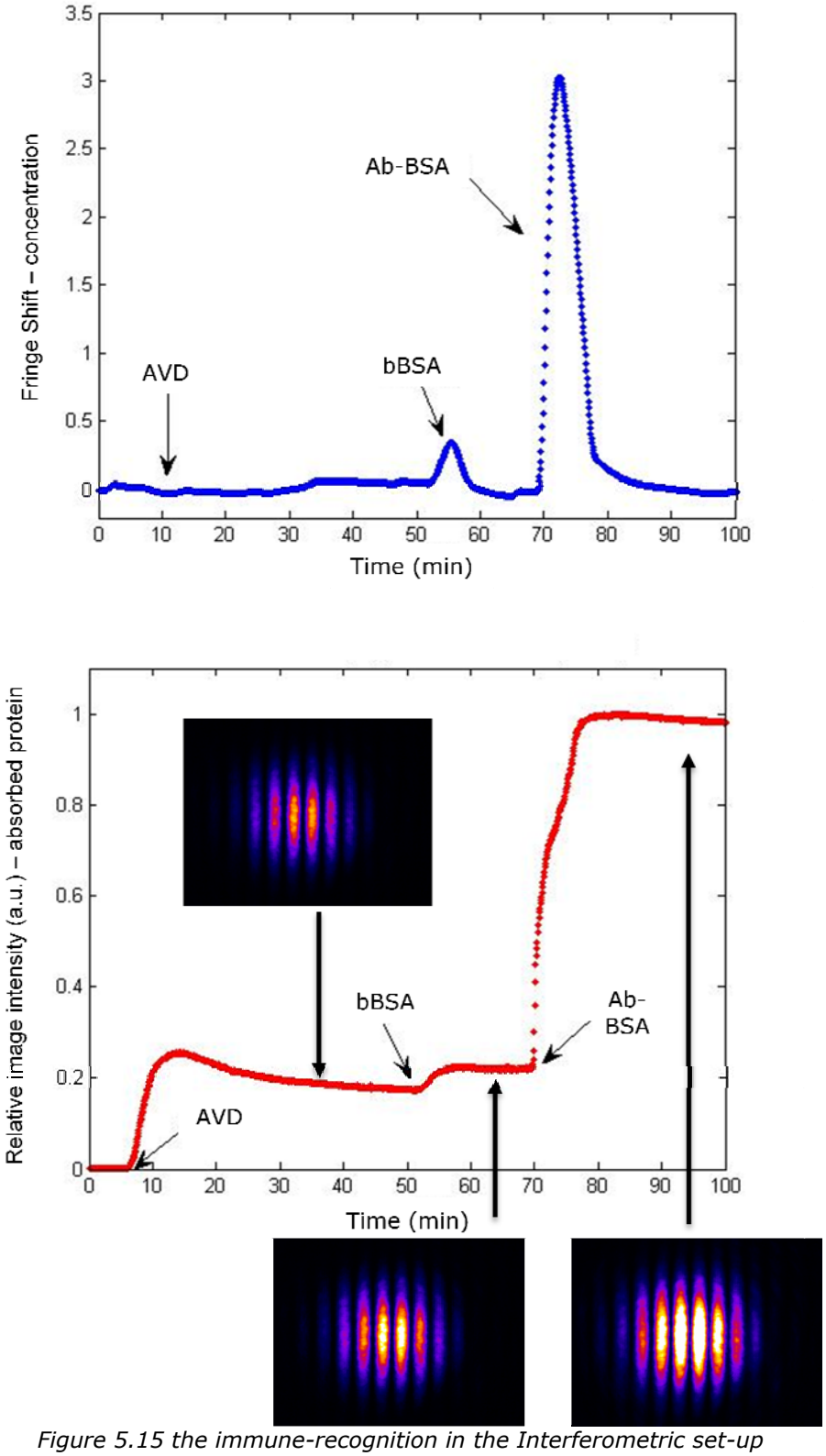

Figure 5.15 the immune-recognition in the Interferometric set-up

We have used the formula 4.19 to correct the concentration into the cell and by using the real-time sample concentration control procedure (section 4.1.3)

we have made a correction of the signal. The figure 5.16 illustrates this operation on an AVD-bBSA interaction. The blue line is the intensity data, while the red curve is the concentration and the black is the correction of the data considering the variation of concentration. We have calculated a $K_{on} = 2{,}74 * 10^4\ M^{-1}s^{-1}$.

This is a functional and innovative method to solve the Taylor dispersion problem present in all the precedent versions of our biosensor and in many other fluidic systems.

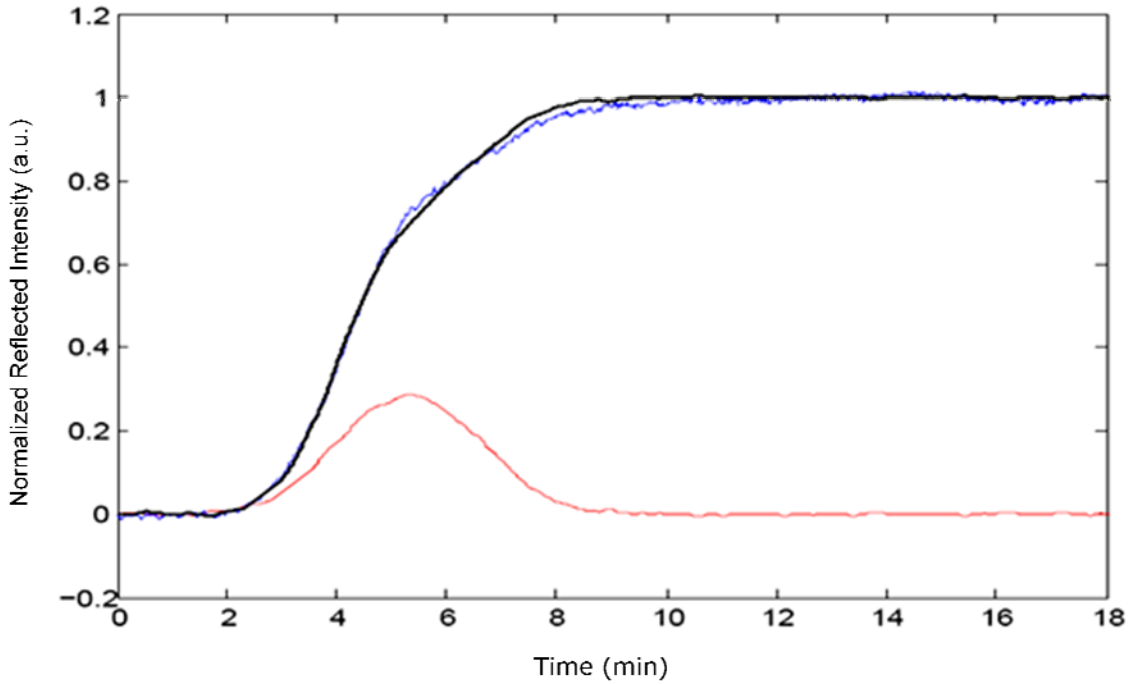

Figure 5.16 correction of concentration into the cell and by using the real-time sample concentration control procedure

ABBREVIATIONS

Ab	Antibody
AcOH	Acetone
AVD	Avidin
bBSA	biotinylated BSA
BLI	BioLayer Interferometry
BSA	Bovine Serum Albumin
CCD	Charge-Coupled Device
EtOH	Ethanol
FRET	Fluorescence Resonance Energy Transfer
HTS	Highthroughput Screening
iSPR	imaging SPR
ITC	Isothermal Titration Calorimetry
IUPAC	International Union of Pure and Applied Chemistry
LASER	Light amplification by stimulated emission of radiation)
LED	Light Emitting Diode
LOD	Limit Of Determination
mAb	Monoclonal Antibody
PEEK	Polyetheretherketone
pI	Isoelectric point
PTFE	polytetrafluoroethylene (Teflon)
pYEEI	pTyr-Glu-Glu-Ile
RU	Resonant Unit
LOD	Limit of detectionn
HSA	Human serum albumin
PoC	Point of care
IFC	Integrated µ-Fluidic Cartridge
SH2	Src homology 2
SPR	Surface Plasmon Resonance

REFERENCES

Ajdari A. et al. *Hydrodynamic Dispersion in Shallow Microchannels: the Effect of Cross-Sectional Shape* Analytical Chemistry **2006** 78, 387-392

Andersson K et al. *Kinetic Characterization of the Interaction of the Z-Fragment of Protein A with Mouse-IgG3 in a Volume in Chemical Space* Proteins **1999** 37, 494–498

Ankerst D. P et al. *Understanding Mixed Messages About Prostate Specific Antigen: Biases in the Evaluation of Cancer Biomarkers* The Journal of urology **2007** 177, 426-427

Bjork I. et al. *Some physiochemical properties of protein A from Staphylococcus Aureus* European Journal Biochemistry **1972**, 29, 579-584.

Cherif B. *Clinically Related Protein–Peptide Interactions Monitored in Real Time on Novel Peptide Chipsby Surface Plasmon Resonance Imaging* Clinical Chemistry **2006,** 52, 255–262.

Clark L.C. Jr et al. *Electrode systems for continuous monitoring in cardiovascular surgery* Annals of the New York Academy of Sciences **1962**, 102, 29–45.

Comley J. *Label-Free Detection New biosensors facilitate broader range of drug discovery applications* Drug Discovery **2005,** 63

Comley, J. *Label Free Detection Trends* **2004** HTStec

Cooper M.A. *Label-Free Biosensors tecnique and applications* **2009** Cambridge University Press

Fan X. et al. *Sensitive optical biosensors for unlabeled targets: A review analytica* chimica Acta **2008,** 620, 8–26.

Goding J.W. *Use of staphylococcal protein A as an immunological reagent*

Journal of Immunology Method **1978**, 20, 241-253.

Green N.M. *Avidin: stability at extremes of pH dissociation into sub-units by guanidine hydrochloride* Biochemical Journal **1965** 89, 609

Green N.M. *Avidin: the nature of the binding-biotine site* Biochemical Journal **1964** 89, 599.

Green N.M. *Avidin: the use of [14C] biotin for kinetic studies and for assay* Biochemical Journal **1963** 89, 585

Green N.M. *Thermodynamics of the Binding of Biotin and some Analogues by Avidin* Biochemical Journal **1966** 101, 774

Guss B. et al. *Structure of the IgG-binding regions of streptococcal protein G* EMBO J. **1986**, 5, 1567-1575.

Hermanson G.T. *Bioconjugate Techniques*, 2nd Edition **2008** Published by Academic Press, Inc.

Jemal A. et al. *Cancer Statistics 2008* Cancer Journal Clinic **2008**, 58,71–96.

Joseph W. *Survey and summary: from DNA biosensors to gene chips* Nucl. Acids Res. **2000**, 28, 3011-3016.

Klaus S.L. *Microscale characterization of the binding specificity and affinity of a monoclonal antisulfotyrosyl IgG antibody* Electrophoresis 2008, 12, 2557-2564

Kudin K.N. et al. *Why Are Water-Hydrophobic Interfaces Charged?* Journal of the American Chemistry Society **2008**, 130, 3915-3919

Liedberg B. *Biosensing with surface plasmon resonance how it all started* Sensors Actuators, **1983**, 4,299–304.

Ligler F.S. *Perspective on Optical Biosensors and Integrated Sensor Systems* Anal. Chem. **2009**, 81, 519–526.

Lindmark R. et al. *Quantification of specific IgG Antibodies in Rabbit by a Solid-phase Radioimmunoassy with 125I-Protein A from Staphylococcus*

aureus Journal of Immunology **1981,** 14, 409-420.

Matthew A. *Optical biosensors: where next and how soon?* Drug Discovery Today **2006** 11, 23-24,

Mol N.J. *Surface Plasmon Resonance Thermodynamic and Kinetic Analysis as a Strategic Tool in Drug Design. Distinct Ways for Phosphopeptides to Plug into Src- and Grb2 SH2 Domains* Journal of Medicinal Chemistry **2005** 48, 753-763.

Myers F. B. et al. *Innovations in optical microfluidic technologies for point-of-care diagnostics* Lab Chip. **2008**, 8, 2015–2031.

Nam N. *Design of tetrapeptide ligands as inhibitors of the Src SH2 domain* Bioorganic & Medicinal Chemistry **2004** 12, 779–787

Nguyen-Hai N. et al. *Design of tetrapeptide ligands as inhibitors of the Src SH2 domain* Bioorganic & Medicinal Chemistry **2004**, 12, 779–787

O'Brien T. et al. *Isothermal titration calorimetry of biomolecules.* Chapter 10 **2000** Protein-Ligand interactions: hydrodynamics and calorimetry Oxford University Press.

Pedrotti F.L. *Introduction to Optics* **1993** Benjamin Cummings.

Pugliese L. *Three-dimensional structure of the tetragonal crystal form of egg-white avidin in its functional complex with biotin at 2.7 A resolution* Journal of Molecular Biology **1993** 231, 698-710.

Schubert M. *Infrared Ellipsometry on Semiconductor Layer Structures: Phonons, Plasmons, and Polaritons*. **2004** Springer,Heidelberg

Sia K.S. et al. *Microfluidics and point-of-care testing* Lab Chip **2008**, 8, 1982–1983.

Singh B.K. et al. *Surface plasmon resonance imaging of biomolecular interactions on a grating-based sensor array* Analytical Chemistry **2006** 78,

2009–2018.

Songyang Z. et al. *SH2 Domains Recognize Specific Phosphopeptide Sequences* Cell **1993** 72, 767–778.

Szostak J.W. *Invitro selection of RNA molecules that bind specific ligands* Nature **1990** 346, 818–822.

Voros J. *The Density and Refractive Index of Adsorbing Protein Layers* Biophysical Journal **2004,** 87, 553-561.

Wilchek M.A. et al. *Essentials of biorecognition: The (strept)avidin–biotin system as a model for protein–protein and protein–ligand interaction* Immunology Letters **2006** 103, 27–32,

Wood R.W. *A suspected case of the Electrical Resonance of Minute Metal Particles for Liqht-wares. A New Type of Absorption* Philos. Mag **1902,** 4, 396–402.

Xiaobo Y. et al. *Label-free detection methods for protein microarrays.* Proteomics **2006**, 6, 5493–5503

Yager P. et al. *Point-of-Care Diagnostics for Global Health* Biomedical Enginering **2008,** 10, 107-144.

Ye G. *Solid-phase binding assays of peptides using EGFP-Src SH2 domain fusion protein and biotinylated Src SH2 domain* Bioorganic & Medicinal Chemistry Letters **2005** 15, 4994–4997.

Yuen P.K. *Self-referencing a single waveguide grating sensor in a micron-sized deep flow chamber for label-free biomolecular binding assays* Lab Chip **2005,** 5, 959-65.

SUPPLEMENTARY INFORMATION

4.4 Interferometric Biosensor: to see page 82 for details.

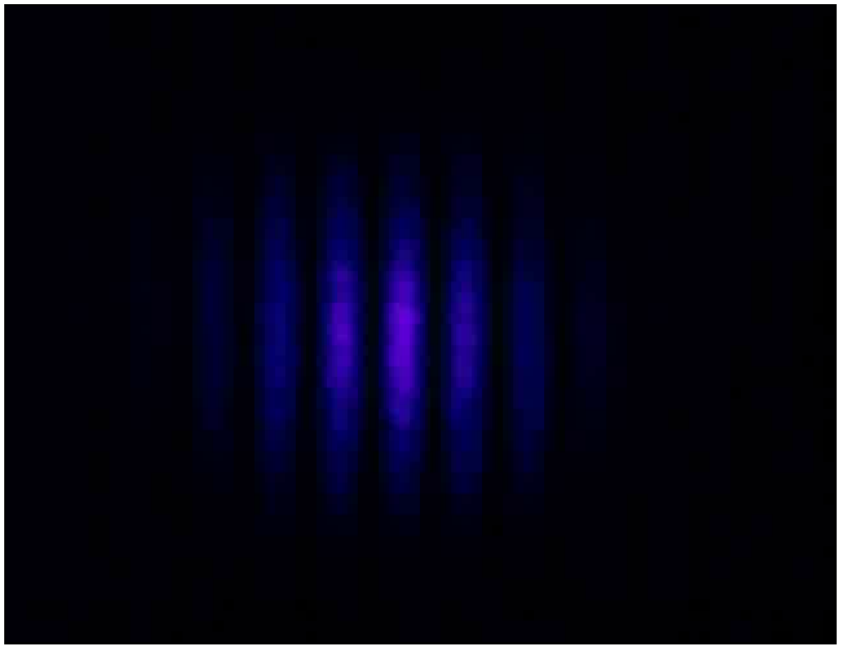

4.5.2 Spot experiment: to see page 86 for details.

5.3 Interferometric experiment: to see page 105 for details.